CHAPTER ONE

INTRODUCTION

1.1 Background of the study

Earth system involves a complicated cycle, naturally covered by different land cover types which are mainly distributed based on climate patterns (United Nations, 2015). Man's presence on the earth and his use of land has had a profound effect upon the natural environment thus resulting into an observable pattern in the land-use/land-cover change over time (Opeyemi, 2014). Land-use/land-cover change contributes significantly to earth-atmosphere interactions, forest fragmentation, and biodiversity loss. It has become one of the major issues for environmental change monitoring and natural resource management (Wang, Berardi and Akbari, 2015; Allegrini, Dorer and Carmeliet, 2015).

United Nation (2015) has presented series of well written articles that elaborate on the meaning of land use and land cover. According to United Nation (2015) Land-use is the term used to describe what goes on in the land (the ways in which, and the purposes for which human beings employ the land and its resources). United Nations (2012) has distinguished between the natural and social scientists' view of what land is; Natural scientists define land use in terms of patterns' of human activities such as agriculture, forestry and building construction that alter the land surface while social scientists and land managers define land use to include social and economic purposes and contexts for and within which land is managed. Land-cover on the other hand, describes the physical or natural and biological cover over

the earth surface including water, vegetation, bare land or artificial structure. It also refers to the kind of vegetation (forest or grass cover), but includes structures such as building or pavement and other aspects of the natural environment such as soil, biodiversity, surface and ground water.

Bayan, Alhawiti, Diana, (2016) and Weng, (2014) highlighted the role of land use / land cover change on urban heat island. They reckon that, the conversion of land from its natural form into buildings, roads, and other impervious surfaces in urban areas generally have higher absorption of solar radiation and greater thermal capacity and conductivity which leads to changes in the local weather and climate, with one of the most familiar products being the urban heat island (UHI) phenomenon.

The UHI is a climatic phenomenon where urban areas have higher air temperatures than the peripheries due to anthropogenic modification of land surfaces. A combination of factors such as building materials, thermal properties, urban design geometry (urban canyons) anthropogenic factors, urban development leads to the development of UHI (EPA, 2014). Some building materials such as tar, asphalt, brick and concrete store solar energy during the day and release it at night, so UHI intensity is reported to be stronger at nighttime. Urban design geometry is one of the leading factors where urban canyons are created by narrow streets and tall buildings. These decrease wind speeds and increase reflective surfaces that trap heat. Anthropogenic factors such as waste heat from vehicles and buildings alter land surface cover in a way that porous vegetation is replaced with non- porous materials thus restricting evaporation cooling city (Wang, Berardi, and Akbari, 2015).

The UHI effect magnitude can vary depending on the LU/LC pattern, city structure, city size, seasonal variations, ecological context, urban geometry, topography and location of the study area (Effat and Hassan, 2014; Imhoff, Zhang, Woife, and Bounoya, 2010; Lo and Quattrochi, 2003; Oke, Yap and Maxwell, 1972). Economic development, population increase, urban growth and evolving industry can be considered as the main reasons of urban climate change (Bayan, Alhawiti and Diana, 2016; Hu and Jia, 2010). UHI effect increases when the city's size increases. Besides, UHI effect varies seasonally and it is more apparent in summer (Aslan and Koc-San, 2016; Imhoff, Zhang, Woife and Bounoyan, 2010).

Urban Heat Island studies are important for urban climate, urban planning and the health and comfort of population living in the area and can be studied by means of Land surface temperature (LST) and air temperature difference between urban centre and rural area (Brandsma and Walters, 2012; Kantzioura and Kosmopoulos, 2012, Wang, Qin, Song, Tu, Karnieli, and Zhao, 2015).

Previous studies have demonstrated that the LST product retrieved from thermal infrared (TIR) sensors can be used to monitor the UHI Effect ((Lin, Moore, Messina, Devisser and Wu, 2016; Voogt, 2004; He, Liu, Zhang and Liu, 2007; IPCC, 2007; Adinna, Enete and Okoli, 2009; Rafferty, 2011; Weng, 2015). Land Surface Temperature (LST) provides an accurate measure for indicating energy exchange balance between the Earth and the atmosphere (Liu and Zhang, 2011). LST, which is controlled by the surface energy balance, atmospheric state and thermal properties of the surface/subsurface rocks, is one of the important parameters in several envi-

ronmental models (Becker and Li, 1990). LST is important for environmental studies and management of the Earth's resources because it determines the effective radiating temperature of the Earth's surface. It is also a major factor in determining the partition of the available energy into sensible and latent heat fluxes. For example, the rate of change of LST is sensitive to the characteristics of the land surface such as soil moisture, land use and vegetation (Fabrizi, Bonafoni and Biondi, 2010).

With the advent of thermal remote sensing technology, observation of UHI has become possible using Satellite and Aircraft platforms (Ema, Nengah and Widiatmaka, 2016). This has provided new direction for the observations of UHI and the study of their effects through the combination of thermal remote sensing and urban micrometeorology (Voogt, 2003). Various satellites and methods are available that can be used to examine the LST and to determine the UHI effects. Landsat TM Bands are the data that are most widely used for these studies (Jimenez-Munoz et al., 2014; Jin et al., 2015; Sekertekin et al., 2016; Wang, Berardi and Akbari, 2015; Yu et al., 2014). Several studies have estimated air temperatures using Landsat TM Imageries to estimate land surface temperature values (Wang, Berardi and Akbari, 2015; Allegrini, Dorer and Carmeliet, 2015, Bernard et al., 2015; Lays, 2013; Qin, Karnieli and Berline 2001). Calabar   which comprised of Calabar South and Calabar Municipality has been chosen   as the focus for this study and the justification is provided in the next section and the justification is provided in the next section.

1.2 Statement of the Research Problem

Calabar, the Capital of Cross River State of Nigeria which comprises of Calabar South Local Government Area and Calabar Municipality is assuming an important role as a tourist destination in West Africa. It has witnessed unprecedented influx of people which has necessitated the building of services, thus resulting into changes in the land use and land cover patterns. Since there is a fixed amount of land, increase or decrease in one will affect the others. One common consequence of shifting from natural to built-up surfaces is higher thermal inertia of urban surfaces.

Common land conversion in Calabar in the past mostly came from the biophysical conditions like soil type and landform limitations, while recent land use conversion is from Agriculture to built-up as a result of industries such as the Tinapa Business and Leisure Resort, the Export processing Zone (EPZ), Dangote Mills, Unicem Factory, Niger Mills as well as a host of businesses and commercial activities such as Banks, Hotels and Fast Food Joints with most of the land being covered with reflective surfaces, which according to Bayan, Alhawiti and Diana (2016) leads to higher temperature which encourages the formation of Urban Heat Island.

The development of UHI potentially affects the health of individuals living in localities that continue to experience it (Awuh and Amawa, 2017; Enete, Awuh and Amawa, 2014). Despite this concern, UHI has continue to develop in many areas of the town. Areas that were cold islands in the past are gradually turning to hot island. Several authors (Brandsma and Walters, 2012; Kantzioura and Kosmopoulos, 2012; Awuh and Amawa, 2017; Wang, Qin, Song, Tu, Karnieli, and Zhao, 2015) have acknowledged that the type of land

use and land cover in a town might have contributed significantly to this problem. In response, this research seeks to quantify the impacts of land use / land cover Change on LST in Calabar metropolis from 2002 to 2016.

1.3 Aim and objectives of the Study

The aim of this study is to assess the impact of LULC change on UHI pattern in Calabar Metropolis between 2002 and 2016.

Objectives of the Study

The objectives of this study include:

i. to determine land-use and land-cover changes in Calabar between 2000- 2016.

ii. to determine LST over Calabar from 2000 -2016.

iii. to determine LST for different LULC for the years 2000-2016.

iv. to determine UHI magnitude

v. to map out UHI zones within Calabar metropolis

vi. to project future land use change

1.4 Research Questions

i. What is the land-use and land-cover status for Calabar?

ii. To what degree does land-use control temperature difference within Calabar Metropolis?

iii. How do we determine points of Temperature Island in Calabar Metropolis?

iv. What is the urban heat island magnitude for Calabar?

v. What will be the future status of land-cover and LST status in Calabar Metropolis?

1.5 **Research Hypothesis**

1. There is no significant increase in the annual temperature trend of Calabar Metropolis?
2. There is no significant relationship between land-use /land-cover change   and urban heat island in the Calabar Metropolis.

1.6 **Significance of the Study**

1. Land use and land cover change has become a fundamental constituent in recent strategies for managing natural resources and monitoring environmental change. Hence information on land use / land cover and possibility for their optimal use is essential for selection, planning and implementation of land use schemes to meet the increasing demands for basic human needs and welfare and will also assist in monitoring the dynamics of land use resulting out of changing demands of increasing population. Thus, it will be of immense benefit to   urban development ,

2. Qualitative and quantitative studies on the relationship between land use/land-cover pattern and LST are imperative for effective urban land-use planning. Thus, information produced from this analysis will go a long way in adding value to the database of   planners when issues

regarding human comfort, health and city geometry need to be addressed and if adequately updated, the result may be a baseline data to them for monitoring temperature variation, pollution and impact of development.

3. This research will act as a catalyst in rekindling an already existing research in urban climatology in Nigeria higher institutions and research centres. Thus, it will be significant to students on academic findings in relation to the topic. Also, the findings of this research will be of great significance to international organisations since it addresses one of the millennium development goals.

4. Maps of UHIs depicting urban locations that produce "hot spots" within the city can provide useful information to stakeholders in city management (Architects, Builders, policy makers and city Administrators) regarding new measures that may reduce the undesirable impact on the urban thermal environment and at the same time contribute to the microclimatic rehabilitation of Calabar.

5. Discovering a temporal relationship between land use change and land surface temperature can be an important input to predict future land warming. This study may provide practical information for urban planners, natural resources managers and environmental experts to manage natural landscapes to be sustainable and healthy

An understanding of how land use changes occur and what are the impacts of these changes are important in different aspects of environmental management issues such as microclimate changes.

1.7 Justification of the Study

Urban heat Islands are of interest primarily because they affect so many people. According to estimates by the United Nations (2015), nearly half of the world's population currently live in urban areas. Within western nations, this number can approach 75percent. The impact of urban heat Islands on the world's population is far-reaching.

Urban heat Islands directly influence the health and welfare of urban residents. Within the United States alone, an average of 1000 people die each year of extreme heat. This is higher than death due to all other weather events combined (Enete, Awuh and Amawa, 2014). As urban heat Islands are characterized by increased temperature, they can potentially increase the magnitude and duration of heat waves within cities.

Research shows that the mortality rate during a heat wave increases exponentially with the maximum temperature, an effect that is exacerbated by the urban heat Island. The nighttime effect of urban heat Island can be particularly harmful during a heat wave, as it deprives urban residents of the cool relief found in rural areas during the night (Clarke, 1972).

Another consequence of urban heat Island is the increased energy required for air conditioning and refrigeration in cities that are in comparatively hot climates. Aside from the obvious effect of temperature, urban heat Islands can produce secondary effects on local meteorology, including the altering of local wind patterns, the development of clouds, and fog, the number of lightning strikes, and the rates of precipitation.

1.8 Scope of the Study

This study is limited to Calabar Metropolis, which comprises of Calabar Municipality and Calabar South Local Government Area. It focuses on the changes that have occurred on land-use/land cover and Land surface temperature (LST) over Calabar Metropolis from 2002 to 2016.

REVIEW OF RELATED LITERATURE /CONCEPTUAL FRAME-WORK

2.1. Conceptual Framework/Models

2.1.1. The Concept of Land Use transition

Transitions in land use has been denoted to account for a stylised vision of sequential alteration of land use from presettlement natural vegetation to frontier clearing, then to subsistence agriculture and small – scale farms, and finally to intensive agriculture, urban areas, and protect recreational lands (Figure 2.1). Different parts of the world are in different transition stages, depending on their history, social and economic conditions, and ecological context. Furthermore, not all parts of the world move linearly through these transitions. Rather, some places remain in one stage for a long period of time, while others move rapidly between stages.
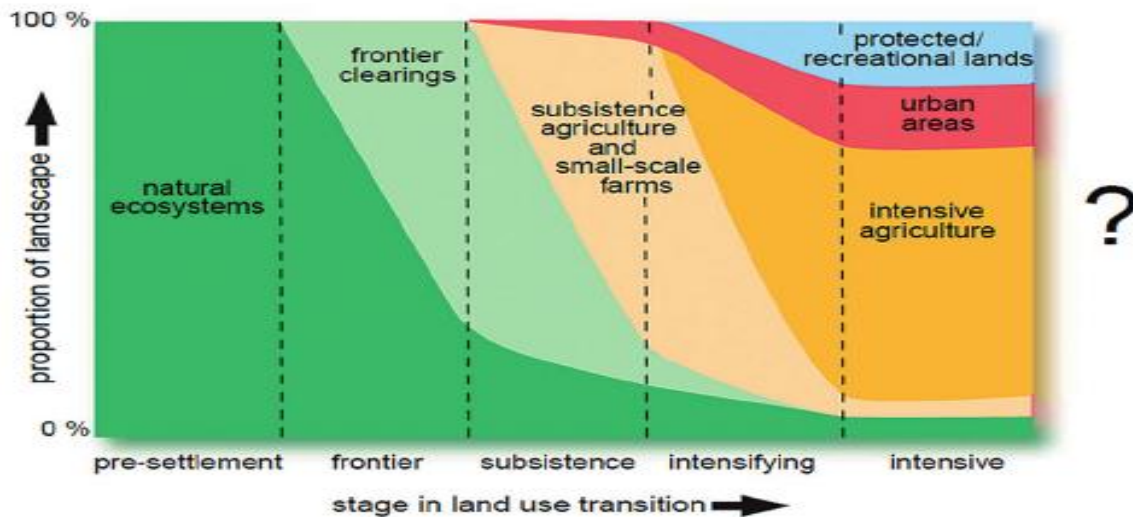

Figure 1: Stages in land use transition
Source: (Foley *et al.,* 2005)

The land use change notion has been useful in pointing out the various stages of land use transformations that regions are expected to go through in the development from predominantly agrarian to an industrial or even post-industrial society. As such, land use transitions are linked to both historical and ongoing biophysical and societal changes. These changes have been convincingly captured by the "social metabolism" concept, denoting the "entire flow of material and energy that are required to sustain all human economic activities". This transition has also been conceived in terms of regime shifts, a notion adopted from systems ecology, to describe the occurrence of sudden transitions between distinctly different states of socio-ecological systems in response to unforeseeable events, threshold and tipping points.

2.1.2. The Concept of Urban Heat Island

The Urban Heat Island (UHI) is a climate modification phenomenon that is generated unintentionally by humans, mainly in urban and suburban environments. UHI manifests itself as relatively warmer air and surface temperatures inside towns and cities when compared to the temperatures of their rural surroundings (Oke, 1982; Enete, Awuh and Ikekpeazu, 2014). The main reason for the occurrence of UHI is that as urbanisation progresses inside a region, radical changes are carried out on the surface and consequently the terrestrial and atmospheric properties of the area change accordingly (Bayan, Alhawiti and Diana, 2016). Luke Howard, a British meteorologist, is attributed to be the first to record an "excess of heat" back in 1818 when he compared the temperatures inside the city of London with those of the surrounding countryside (Oke, 1982). However, he did not use the term "heat island" in his work, as the phrase was coined later by meteorologists who noted the

resemblance between urban isotherm maps and the topographic map of an island. UHI zones within cities usually feature high thermal gradients that resemble 'cliffs' surrounded by an 'ocean' of lower values. Moving 'inland' towards the city centre, these transform into 'plateaus' with weak thermal gradients. In some spots within the city, the temperature tends to rise again forming 'peaks' (2000; Oke, 2004; American Meteorological Society, 2015). This has been summarized in Figure 2.2.
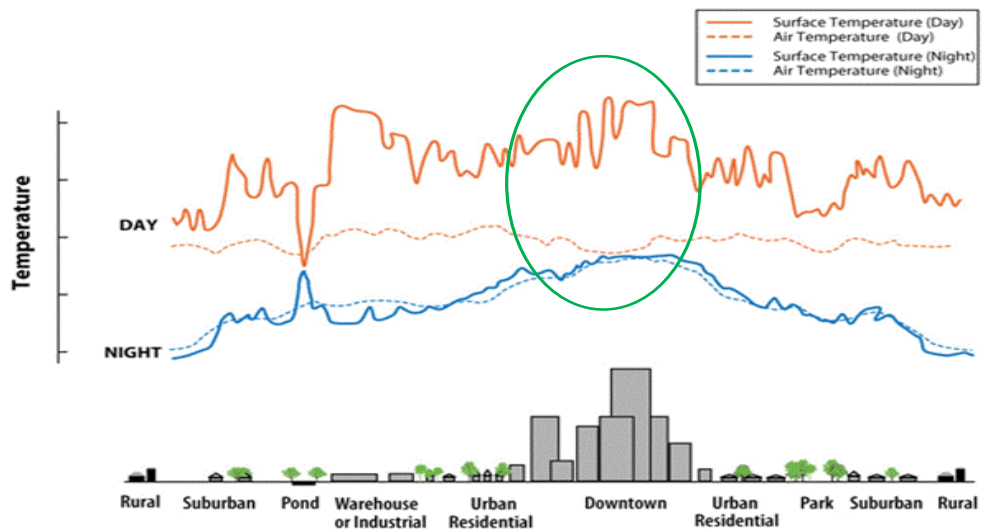

Figure 2: An idealized crossed profile of urban heat island
Source: EPA, (2009).

2.1.4. The Normalized Difference Vegetation Index Model

The Normalized difference vegetation index (NDVI) is a vegetation index used in remote sensing analysis to assess whether or not a target contains live green vegetation. Healthy vegetation is highly absorbent of visible light (0.4 to 0.7 μm) and reflects most near-infrared light (0.7 to 1.1 μm). Unhealthy or sparse vegetation, on the other hand, will generally reflect more visible light and less near-infrared light (FSNAU, 2010). Therefore, greater reflected radiation in the near-infrared wavelengths than in the visible wavelengths generally -indicates the presence of green vegetation, whereas little difference in the intensity between the two 10 wavelengths is generally an indicator of sparse vegetation or non-vegetated surfaces (Weirer and Herring, 2010).Figure 2.3.
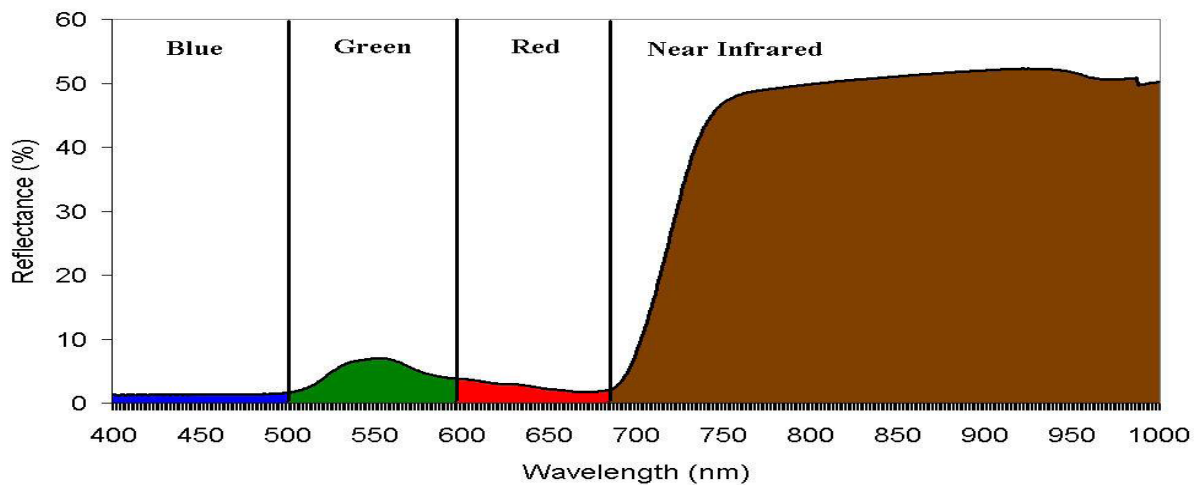

Figure 3: The spectral curve of vegetation.
   Source: SEOS, (2010).

As near- infrared and red bands of satellites are those most sensitive to vegetation information, these bands can be employed to quantify the density of plant growth in a given pixel (FSNAU, 2010; Weirer and Herring, 2010).

14

NDVI values will typically range between -1 and 1 where the higher the value, the healthier and denser the vegetation. Moreover, values greater than 0.2 usually indicate vegetation, whereas values below 0.2 generally indicate soil, rock, or man-made materials. Water bodies typically give negative NDVI values (Liao et al., 2005; Tam et al., 2010).

As stated earlier, LSTs correspond closely with near surface temperatures and can therefore be considered a reliable indicator of the UHI. Vegetation abundance is also known to influence LSTs and UHI conditions through the process of evapotranspiration. Therefore, investigation into the relationship between NDVI and LST becomes informative and meaningful, especially with regards to areas where the UHI phenomenon is more pronounced and where mitigation measures are needed.

Given that vegetation abundance is known to reduce LSTs through the transfer of latent heat from the surface to atmosphere through evapotranspiration, NDVI can be used to investigate this relationship and thereby, provide insight into how this natural cooling mechanism of vegetation might be employed to help improve urban thermal environments. In general, areas with high NDVI will typically have lower LSTs, however, this correlation may be influenced by soil moisture conditions and evapotranspiration of the surface (Su *et al.,* 2010).

2.1.5 Markov Chain Model

Markov chain modelling is a good example of a stochastic model. Markov chains was named after and developed by a Russian mathematician — Andrei Andreyevich Markov. The basic premise of the Markov chain model is

that land use at some point in the future *(t + 1)* can be determined as a function of current land use (t), or mathematically,

$$X_{t+1=}f(X_t)$$ (1)

Where $X_{(t)}$ represents the land use at time *t + 1* and X_t represents land use at time t. The structure of the Markov chain model as applied to land use change involves a vector $\mathbf{n_t}$ with dimension *m x 1* (where m represents the number of states, in this case land use classes) describing the distribution of land use among current states and an

m x m matrix of transition probabilities **(p)** that governs the probability of transition between each pair of land uses, *i* and *j*. The model can then be written as a difference equation in matrix form Baker (Baker, 1989)

$$n_{t+1=}Pn_t$$ (2)

Where n_{t+1} is another *m x 1* column vector describing the distribution of land use at time. Since the transitions are probabilities, it follows that:

$$\sum_j^m =_1 p_{ij} =1i =1, 2...m$$ (3)

Meaning simply that the rows of the transition matrix must sum to 1. Maximum likelihood estimates of the transition probabilities can be obtained as (Anderson and Goodman, 1957):

$$p_{ij=}n_{ij}/\sum_j^n =1\,n_{ji}$$ (4)

Where p_{ij} is the probability of transition between i and n_{ji} and denotes the number of transitions from *i to j*. These values can all be obtained empirically. To test the validity of the Markov chain model, a useful first step is to

test the null hypothesis that land use at one point in time ,$t + i$, is statistically independent of land use at the preceding time period ,t . This test can be conducted using standard contingency table techniques for cross-classified categorical data. The expected values for each cell indicating the number of transitions between i and j can be compared with the actual number of transitions to compute the test statistic, Pearson's chi-square, which is distributed x^2 with$(m-1)^2$ degrees of freedom, where m indicates the number of land use classes. Under the hypothesis of independence, the expected number of transitions in each cell of the transition matrix $\hat{m}ij$ can be calculated by:

$$\hat{m}_{ij} = n_i + n_{+j}$$ (5)

Where n_i + denotes the marginal total of transitions for the ith row of the transition matrix and n_{+j} denotes the marginal total for the jth column of the transition matrix.

Using these expected values, the test statistic (k^2) then takes the form:

$$k^{2=}\sum_j^i =1 \sum_j^J \frac{(ij +\hat{m}_{ij})^2}{\hat{m}_{ij}}$$ (6)

The test statistic is typically given the notation k^2 instead of x^2 to differentiate it from its distribution, which is chi square. The null hypothesis of independence is almost universally rejected, indicating some level of dependency between successive land use states. Another important property of Markov chains, as identified in an earlier section, is the property of stationarity, particularly as it applies to the transition probability matrix. This property is critical for applications in which a Markov chain model is to be

17

used for forecasting. The transition probability matrix *(p)* is assumed to remain constant in successive periods *t + k*, meaning that at any future period, the matrix of cell transitions can be obtained by multiplying the vector of current land uses, *nt* by the transition probability matrix *p*, raised to the *kth* power. In most forecasting applications, the transition probability matrix is assumed to remain constant through successive time periods, and is seldom tested empirically. This study follows the work of Bourne (1971), who compared transition matrices for successive periods using simple correlations between cells of the matrix. By expressing the elements of one matrix *(p $_{t + 1; t + 2)}$* as a function of another *(p $_{t; t + 2)}$*, one can provide a rough check for stationarity by determining whether the correlation between matrix elements is significantly different from a value of one. In order to use the Markov chain model for prediction, an additional stochastic element is added. Since the transition probabilities represent estimates of the likelihood of conversion from one land use state at time to one of 10 other states at time *t + 1*, a mechanism is added to introduce randomness to the model and its predictions of future states. Since each row of the transition probability matrix sums to one, predictions of future land use states are obtained by drawing a pseudorandom number between zero and one, rounded to four digits. If the number falls within the probability space allocated to a particular land use state according to the transition matrix, then that state is chosen for conversion. This process is repeated for each land use cell in the data set. Predicted land uses can then be compared to actual observed land uses to summarize the accuracy of the model's predictions.

From the review, a lot of scholars applied different concepts and models in studying the relationship between land use /land cover change and urban

heat island effect. The following models will be relevant to this study; Change Detection Model, Normalized Difference Vegetation Index Model (NDVI), and Markov Chain Probability Model. Change detection model will be used to establish the changes that have taken place in Calabar south and Calabar municipality based on simulating the current and the previous land uses; NDVI Model will be used to correlate LULC/LST (UHI); whereas the Markov chain probability model will be used to forecast future trend in Land cover and land surface temperature in Calabar.

2.2   Review of Related Literature

2.2.0 Introduction

This section reviews literature on: the trend in land-use / cover-change., simulation studies on land cover changes. Over-view of the physical properties that create urban heat, Urban Heat Island Phenomenon the LST component of UHI effect, its character, and key measures.

2.2.1 Trends in Land Use/Land-cover Change

Historically, the driving force for most land use changes is population growth(Ramankutty et al., 2002b) although there are several other interacting factors , but rates of deforestation and population growth are not linear (Lambin et al., 2003). During the 20th century, the world population increased from about 1.5 billion in 1900 to 5.2 billion in 1990. Currently, the world population is growing by 1.3 percent per year compared to two percent growth in the late 1960s. More than 90 percent of the population growth takes place in tropical regions. About 80 percent   of the population lives in developing regions; Asia accounts for 61 percent of the world total. The rate of population growth is declining and population will reach around 8.9 billion in 2050 (*Lutz et al.*, 2001).

Land in tropical regions is being used for the same reasons as in temperate regions, namely to grow trees, raise crops, and rear animals for food., as well as, providing building sites for houses and roads, or for recreational purposes. Part of the land in the tropics is being used by smallholders who

farm for subsistence. Small holder agriculture is differently practiced in different parts of the world but it has the following characteristics: small scale, subsistence or semi-subsistence with little or no external inputs, low level of mechanization, and relatively low yields. Farm sizes largely depend on the intensity of the farming system which, amongst others, is determined by both population pressure and agro-ecological conditions. With rapid population growth and in the absence of agricultural intensification, smallholders require more land to grow crops and earn a living; it results in deforestation and land use conversions from grassland to cropland (*Lutz et al*., 2001).

According to Verheye (2004), demographic pressure and competition for land in modern societies have modified not only the rural/urban equilibrium, but also the existing land use patterns. Despite migration to the cities, population pressures are still on the rise in many rural areas, especially where good quality soils are present. Four major trends can be recognized in modern land use changes: first, the continuous expansion of arable land in order to meet the increasing food demands of a growing population; second, the rapid development of urban and suburban areas; third, the ongoing deforestation and loss of pasture lands in favor of (mainly) agricultural and urban areas; and, fourth, the increasing concern for protection of the environment, resulting in the creation of nature reserves. Such conversions also take place because of the expansion of the area under cash crops (for example, oil palm and soybean) in the Amazon basin, the Argentinean pampas and in several countries in SE Asia. There is an increase in the area under forestry plantation in the tropics although accurate data on reforestation are scarce (Lepers et al, 2005). Forestry statistics show that in 1965 there was about 6.7 million hectares of forest plantations, in 1980 it increas-

es to 20.9 million ha, and the total area for 1990 was estimated to be 42.6 million ha (Evans, 1992). Brown et al., (1997) estimated the total plantation area in the tropics to be 44 million in 1990. In China, 1.1 million ha and in India 1.5 million ha of new forest plantations were established in 2000 according to FAO data (Lepers *et al.,* 2005).

It has been estimated that already more than 8 million km^2 of the virgin tropical rain-forest mainly in Central and South America, Central Africa and Indonesia, have been cleared for agro industrial projects and extensive cattle farming (Haitemink , Veldkamp,Zhang and Lui 2008). Elsewhere in the tropics, large agro-industrial complexes for the production of palm oil, coffee, or rubber are replacing the smallholders' settlements in tropical forest areas, while similar estates for sugar cane, pineapple, and other tropical export products have been established in former Savana regions. In Guinea, Liberia, Ivory Coast, and Nigeria, more than 80 percent of the original forest canopy have already been affected. Extensive deforestation for timber exploitation is taking place in many tropical countries, as well as in Canada and Russia, especially in areas where population densities are low, and large forest reserves still exist. In many African countries such as Sierra Leone, Benin, Togo, and many others, forest exploitation is not only focusing on economic gains, such as, timber production, but also on the collection of fuel wood and charcoal, which are the main energy source for the local population.

In recent years however, there has been growing concern about nature protection and the preservation of special biotypes, viz-a-viz, the maintenance of biodiversity. This attitude has been reflected in the introduction of recent

legislation to regulate the use of land, even including land that is privately owned. In many countries, especially in the developed world, this policy has been implemented in part through physical planning and zoning (Lambin, Geist, Lepers, 2003). The underlying principle of this zoning strategy is to create the conditions for governments, in the medium and long term, either to acquire nature protection reserves in direct ownership and management, or to impose strict exploitation rules in existing rural areas. In this respect, a number of recent EU directives have imposed very stringent environmental rules in selected, biologically valuable, agricultural areas in Belgium, the Netherlands, and Germany, restricting the use of mineral fertilizers, the transfer of livestock waste products to the open fields during part of the year. In many of those cases, zoning is taking agricultural land out of exploitation, while designating it an exclusive objective of nature protection (Verheye, 2004; Lambin, Geists, Lepers, 2003).

The loss of pasture land in favor of arable farming is a well-known phenomenon in the Sahel region, and is to some extent, directly or indirectly, encouraged by government policies. It is a direct threat to traditional extensive livestock raising. In Nigeria, Senegal and Niger river floodplains and grazing areas that were traditionally used by pastoralists have substantially decreased, and access to watering places for the cattle has seriously been hampered, due to the continuous expansion of irrigation schemes (commercial) and rain fed cultivation, such as the so-called "groundnut and rice schemes". In those areas where land and water rights are traditionally shared between agriculturalists and pastoralists, the changes in land use pattern often end up in open or latent conflicts between farmers and pastoralists as evident in the northern part of Nigeria.

Due to urbanization and industrialization, ever increasing amounts of arable and forest lands, in and around suburban areas, are being transformed into building plots, industrial zones, infrastructure projects, and recreational areas (Hartemink et al., 2008), At present, and for the first time in history, the urban population in the world is overtaking the number of rural settlers. Urbanization and industrialization are closely linked to economic growth, and is therefore a typical feature of the developed world. However, urban development is also rapidly taking place in developing countries, and it is estimated that in those countries as a whole some 14 million ha were converted into urban land between 1990 and 2000. In Indonesia for example, to mention only one of those countries, with 22 percent of the population already living in urban areas in 1980, major cities have almost doubled in size over the past twenty years, and it is believed that, at present, 50,000 ha of good arable lands are lost annually to city expansion in Java alone (Verheye, 2004).

2.2.2 Urban Heat Island Phenomenon and its Key Characteristics

UHI is a warming of the UCL and UBL relative to adjacent cooler locations. UHIs are produced by: (1) urban land covers, (2) neighborhood building configuration, and (3) adjacent heat sources and sinks (Oke, 1987; Oke, 2006; Stone, 2012; Stewart et al., 2014). UHIs are measured using either land surface temperatures or air temperatures between two or more locations.

Typically, the UHI intensity (ΔT) is measured as the difference in surface or air temperatures between an urban and a rural location (Stewart et al., 2014). Past researches have shown that UHIs increased air temperatures by

5^0C in Rome, Italy, 6.5 ^{o}C in Shanghi, China (Djen *et al.,* 1994), 7 ^{o}C in London, United Kingdom (Wilby, 2003), and as much as 12 $^\circ$C in Lodz, Poland (Klyysik and Fortuniak, 1999) Based on these studies, it is evident that these differences are associated with the influence of an area's urban physical characteristics.

UHI are not unique to the urban downtown (Jenerette *et al.,* 2007). For example, Memon and Leung (2010) reported that Hong Kong's mean temperature difference between urban and rural areas is 2^0C in winter and 0.5^0C in summer, but they have measured maximum air temperatures differences as high as 10^0C. In addition, UHI patterns vary by region (Imhoff *et al.,* 2010), occur in more dispersed pattern than once thought and may increase or decrease over time (Stone, 2012; Akbari et al., 2001). Imhoff et al. (2010) investigated UHI patterns in eight different biomes in the U.S. and found that the largest UHIs (on average 8^0C) were in cities located in temperate broadleaf and mixed forest regions where evapotranspiration played a key role in cooling. Akbari et al. (2001) also reported that since 1940, urban air temperatures in U.S. cities have increased between $0.5–3.0^0$C on average. They found that most of this warming was the result of intensifying urban heat island.

Understanding UHIs requires isolating the urban warming effects from other warming influences such as weather, regional air patterns, water bodies, or topographic effects (Stewart et al., 2014; Oke, 2006; Stone, 2012). Researchers and planners are most concerned about UHIs in hot weather. UHIs are not as problematic in cool weather and may even have the benefit of reducing heating bills and cold-related mortality in cold weather (Oke,

1988; Santamouris et al., 2007). However, during hot weather, UHIs enhance heat waves and produce a host of negative societal impacts. Stone (2012) found that, a July 1999 heat wave enhanced Chicago's UHI by 3-4^0 F. Not only were urban centers hotter on average, but during heat waves the difference or UHI intensity was amplified (Stone, 2012). Planners address the physical characteristics that influence UHIs because of their concern for the negative impacts of increased heat (Gartland, 2008; Memon et al. 2010; O'Neill *et al,* 2007; Stone, 2012; EPAb, 2012). High air temperatures associated with UHIs directly increase heat related illnesses and deaths, decrease air and water quality, decrease urban soil quality and tree health by drying soils, and lead to failures in infrastructure. In addition, high air temperatures indirectly increased energy and water demand as residents use air conditioning and additional irrigation to cope with the heat, which also contributed to even higher air temperatures. Finally, high heat indirectly increases energy use and leads to the release of more waste heat. Elevated temperatures make neighborhoods not only uncomfortable but they cause potentially deadly consequences for vulnerable residents. Deaths from heat surpass all other natural disasters combined in terms of mortality (NWS, 2009, Enete, Awuh and Amawa*,* 2014).

Mechanical buffers such as air conditioning can be a buffering resource to cope with hot temperatures and poor air quality (O'Neill *et al.,* 2007). Yet, not all residents are able to afford air conditioning (Santamouris *et al.,* 2007). In some hot regions, residents have little choice but to use air conditioning to stay cool (Awuh and Amawa, 2017).

2.2.3 . Relationship between Land Use Land Cover and Urban Heat Island (LST).

Typical urban materials include concrete, asphalt, metals, glass, and other artificial materials (Aslan and Kok-San, 2016. These urban materials change the reflectivity and energy balance of land covers in several important ways; the first class of the physical factors that influence urban Heat island is the conversion of land cover from rural to urban covers. UHI formation is triggered by the relative proportion of the urban impervious surface to natural vegetation covers. The surface temperature of urban area has a close relationship with surface structure and texture. Urban anthropogenic areas have the potential to accumulate heat which influences air temperature (Aslan and Koc-san 2016). Bayan and Diana, 2016, Bhang and Park, 2009; Pitman *et al.,* 2011, reckons that a change in LST is related not only to land use/land cover type conversion, but also in the existence and increase of greenhouse effect.

According to EPA (2008), Paving and building materials used in urban areas generally have a lower albedo than areas with vegetation. The materials used in urban areas reflect less and absorb more sunlight, which naturally results in higher surface and air temperatures. Most building materials, with the exception of metals, have high emissivity coefficients, meaning that those materials start radiating heat if the temperature rises even slightly Metals do not start radiating heat until they reach much higher temperatures; compared with stony materials, for example, metals heat up to higher temperatures. Emissivity is determined by the material's surface (or finishing). Impervious materials change the reflectivity and energy balance of surface resulting in locally higher air temperature or UHIS (Gartland, 2008; Stone, 2012; Coseo, 2013).

The built environment impacts the albedo (reflectivity) and emissivity (energy) of solar radiation Painted metal has the emissivity value of the paint.

Table 1. Radiation properties of surface materials

Material surface	Solar Reflectance*	Emittance	SRI*
Black acrylic paint	0.05	0.9	0
New asphalt	0.05	0.9	0
Aged asphalt	0.1	0.9	6
"White" asphalt shingle	0.21	0.91	21
Aged concrete	0.2 to 0.3	0.9	19 to 32
New concrete (ordinary)	0.35 to 0.45	0.9	38 to 52
New white portland cement concrete	0.7 to 0.8	0.9	86 to 100
White acrylic paint	0.8	0.9	100

Source. EPA, 2008.

Numerous studies are dealing with relating LST to other factors and indexes. Some, Bayan and Diana, (2016) and Suzana et al. (2016) opin that LST is related to different types of human activities, but so far, only the relationship between LST and LULC types distribution have been documented and proven. Especially well documented is the relation of LST with vegetation cover and NDVI. Others also say that LST is sensitive not only to vegetation type, but also to soil moisture and density (Aslan *et al.,* 2016; Aakriti *et al.,* 2015;   Mallick et al., 2013).

2.2.4 Studies on the Relationship between Land Use and Land Cover Change and the Urban Heat Island.

Chaobin et al. (2017), employed both qualitative and quantitative models to explore the effect of LULC on UHI in Changchun, China. UHI and LULC maps were retrieved from Landsat data acquired from 1984, 1992, 2000, 2007, and 2014 to show their spatio-temporal patterns. The results showed that: (1) both the patterns of LULC and UHI have had dramatic changes in

the past 30 years. The urban area of Changchun increased more than four times, from 143.15 km^2 in 1984 to 577.45 km^2 in 2014, and the proportion of UHI regions has increased from 15.27 percent in 1984 to 29 percent in 2014; (2) the spatiotemporal changes in thermal environment were consistent with the process of urbanization. The average LST of the study area has been continuously increasing as many other land use types have been transformed to urban regions. The mean temperatures were higher in urban regions than rural areas over all of the periods, but the UHI intensity varied based on different measurements; and (3) the thermal environment inside the city varied widely even within a small area. The LST possesses a very strong positive relationship with impervious surface area (ISA), and the relationship has become stronger in recent years. The UHI we employed, specifically in this study, is SUHI (surface urban heat island).

Gaylan Rasul and Faqe Ibrahim(2017) investigated the effect of land use changes on LST in Dohuk City in the Kurdistan Region of Iraq ; they made use of data from three Landsat images (two Landsat 5-TM and Landsat OLI_TIRS-8) from 1990, 2000 and 2016. Supervised classification was used to compute land use/cover categories, and to generate the land surface temperature (LST) maps the Mono-window algorithm was used. Images were also used to create the normalized difference vegetation index (NDVI), normalized difference built-up index (NDBI), normalized difference bareness index (NDBAI) and normalized difference water index (NDWI) maps. Linear regression analysis was used to generate relationships between LST with NDVI, NDBI, NDBAI and NDWI. The study outcome proves that the changes in land use/cover have a significant role in the escalation of land surface temperatures. The highest temperatures are

associated with barren land and built-up areas, ranging from 47°C, 50°C, 56°C while lower temperatures are related to water bodies and forests, ranging from 25^{0}C, 26^{0}C, 29^{0}C respectively, in 1990, 2000 and 2016. This study also proves that NDVI and NDWI correlate negatively with low temperatures while NDBI and NDBAI correlate positively with high temperatures.

Juliana et al. (2016), quantify and identify the spatial patterns of the daytime and night-time UHI in Brimingham, UK. The analysis was performed under a range of atmospheric stability classes. They investigated the relationship between surface and canopy UHI. The findings of their study revealed that the distribution of UHI within the city could be linked to land use, whereas for canopy UHI, advective processes appear to play an increasing important role. Furthermore, strong relationships were found between air temperatures and LST during both the day and night at a neighborhood scale.

In addition, Suzana et al. (2016) findings based on the relationship between land surface temperature/ land cover in Lanwawi island using normalized difference vegetation index(NDVI), NDBI,NDWI ,proved that as the impervious surface (built –up) increases, the surface temperature of the area increases . Also, based on the linear regression between LST and NDVI, NDBI and NDWI, these indices can be used as an indicator to monitor the impact of land use on land surface temperature.

Aslan and Koc-san (2016) carried out a research in order to understand the relationship that exists between urban heart island and land cover type in the central district of Antalya. Using landsat 7 ETM+ and Landsat 8OLI

Images, they observed that, during a 13year time interval, urban and industrial areas were increased significantly and maximum LST Values were detected for dry agricultural, urban and bareland classes, while minimum LST values were detected for vegetation and irrigated agricultural classes. The validity of the result using MODIS Terra and emissivity data revealed a strong correlation between landsat LST and MODIS for 2001-2014.

Similar study was carried out by Bayan and Diana (2016) for the city of Fort Lauderdale, Florica using LST data derived from Landsat 8 data captured on March 23rd, April 24th, October 18th and November 2nd, 2014. Their aim was to analyse the relationship between urban thermal environment and urban heat island. Lansat 8 TIRS and operational land imager (OLI) band data were converted to top of atmosphere spectral radiance using radiance recalling factors. The results indicated that the highest maximum and surface temperature was observed in high density residential and commercial areas near city downtown, while coastal and areas near water bodies were found to have lower surface temperature.

Yasuyo and colleagues (2016) on their part investigated the variation of Daytime urban heat island in Doha. Using three statistical approaches, (Ordinary least squares (OLS), Regression Tree Analysis (RTA), and Random Forest (RF) to help explain near –surface air temperature using land cover variable. The predictions of the statistical models were validated by computing the root mean squares error (RmsE). They observed that, the temporal variations in urban heat were mediated by different factors throughout the day. They suggested RF to be the best model for predicting near-surface air temperature.

Aakriti and Ram (2015) carried out a study in 2010 which compared the UHI in the two largest metropolitan cities of India (Delhi and Mumbai), making used of landsat 5Tm image. The validation of the urban heat island was done in relation to the normalized difference vegetation index patterns. The study revealed that, in Delhi, being and inland, built –up and fallow lands recorded higher temperatures, whereas the vegetated areas and water bodies excited lower temperatures , which according to them attributed to the presence of mixed land use and substantial tree cover along roads . The results further revealed a strong negative correlation between NDVI and UHI in Mumbai.

Brandsma and Wolter (2012) analyzed high-resolution measurements of temperature and humidity taken on a bicycle in the morning and afternoon. The sampling was done along a 14 km transect through the city of Utrecht to describe and model the UHI intensity between 2006 and 2009. Representative route was determined with fixed points every 10 m for both the early morning and afternoon transect. Two multiple linear regression models have been proposed to describe the mean and maximum night-time UHI intensity profiles with area-averaged sky-view factors and land use (build-up, vegetation and open water) of the city Utrecht. Land use was expressed as fractions summing up to 1. The fractions are denoted as FB (fraction build-up), FV (fraction vegetated), and FW (fraction open water).

Furthermore a non-linear model is constructed that relates the temperature difference between the warmest and coldest part along the profiles to wind speed and cloudiness. Their results showed that the difference between the warmest and coolest temperatures along the transects is about 1.5 for the

mean night-time profiles and 0.6C for the daytime profiles. Also their results showed less UHI in more windy and cloudy weather situation. They relate UHI with wind speed which can be used in this study. Xiong *et al. (2012)* found that, high temperature anomalies were closely associated with built-up land, densely populated zones, and heavily industrialized districts. They analysed Landsat TM/ETM+ images, NDVI and NDBI indices for UHI analysis of Guangzhou in South Chinan. Jiang et al. (2010) examined the effect of land use/land cover change on LST for Beijing city in China. This city is surrounded by mountains in 3 sides and plain in the other side. Three Landsat images of Beijing with clear weather condition acquired on April 9, 1995 and April 30, 2000 were selected to this research. The land surface temperature (LST) and land use and land cover (LULC) classes were retrieved. To find the pure effect of LULC change on LST and reduce the effect of seasonal variation, images were selected in the same season. To this end temperature/vegetation index (TVX) approach were used. TVX space is a plot of normalized NDVI and LST. The cross point of LST and NDVI was indicated for some LULC type pixels in 1995 and for correspond pixels which was converted to urban in 2000. The pixel trajectory was performed to relate cross points shifts with LST temporal behaviour of the results which is useful for the current research.

Keramitsoglou et al. (2011) analyzed urban heat island phenomenon. They investigate 9-year temporal LST behavior got from daily LST retrievals of MODIS 3000 images in 1 km resolution and Coordination of Information on the Environment (CORINE) land cover data set. The study area is in Greater Athens, Greece which is a coastal city in central basin bounded by mountains and Saronic Gulf in the south west; it is bisected by small hills

and under the effect of see-breeze. Thermal pattern analysis was done to select three hot spots to be analyzed about spatial-temporal trends. They masked out cloudy and obliquely land pixels and then for dealing with missing cells they applied averaging techniques on invalid pixels. Then they used smoothing pixel to remove extreme LST values. All pixels with LST higher than sub-urban LST plus 6 C were introduced as potential hot spots. Using object-based analysis, they grouped hot pixels and selected 4 hot spots (objects). Then they did spatial thermal analysis in hot spots and over a decade, they extracted thermal information like temporal min and max LST. Some of their interesting results were finding cooler pixels along the coastline, or observing lower LST in higher altitudes. They also found that during day time bare soil and sparse vegetation showed faster heating rate than urban areas, inversely later in the day and mostly at nights city center of Athens showed UHI (urban heat island) phenomenon. Finding cooler pixels near the sea or masking out cloudy pixels would be interesting points which can be used in further analysis.

Zhou et al. (2011) examined how LST responded to urban growth, they retrieved spatial patterns of LST and land use for 1992 and 2006 from Landsat images dated 16 August 1992 and 19 May 2006. They classified TM images into five Land-use types, including built-up land, water, barren land, forest, and agriculture land. Then they characterized the land use types with Remote sensing indices, The NDBI (normalized difference built-up index) is an indicator of urban area, NDVI (Normalized Difference Vegetation Index) as greenness indicator and The MNDWI (Modified Normalized Difference Water Index) is selected to represent water areas. They overlay classified land-use maps and the derived LST layers to recognize their spa-

tial patterns and to sample 5929 points distributed evenly in study area to do correlation analysis. To examine the effect of LUCC on LST pattern, land use change detection was performed. Changed areas were then overlaid with LST layers to calculate the LST differences between 1992 and 2006. They did correlation analysis between LST and three mentioned indices separately and then they used two global and local multivariate regression to model LST based on indices. Some of their results showed that LST increased about 3.4 °C and 1.9 °C, respectively, for forest and agricultural land that were converted into built-up areas. Among the three indices, NDBI had the strongest relation with LST.

Steeneveld et al. (2011) studied the urban heat island phenomenon. The aim of this study was to quantify the canopy layer urban heat island which is done in the Netherlands based on observations by a network of hobby meteorologists and three weather stations. They related the UHI to the amount of green cover, presence of water bodies, and population densities. The majority of the largest cities in the western part like Rotterdam, Delft, The Hague, Leiden, and Haarlem have been included in this study. They also quantified the sensitivity of the recorded UHI to mean wind speed and daily solar radiation. Some of their results showed that average maximum UHI during a diurnal cycle is 2.3 Kelvin, while the average 95 percentile over all cities is 5.3 K. They relate UHI to wind and population density.

Neteler (2010) focused on estimating daily land surface temperatures in mountainous environments by reconstructed MODIS LST data from a total of 11,179 MODIS LST maps between 2000 and 2008. Study area was Northern Italy including the provinces of Trento, Bolzano and Belluno, and also parts

of the regions of Friuli-Venezia Giulia, Lombardia and Veneto. They provided a new self-contained algorithm to reconstruct incomplete MODIS LST maps. Since the amount of available data was huge, reconstruction required to be automated. Their procedure included re-projection to UTM, filter out invalid pixels using quality assessment layer with applying the bit patterns of interest to LST maps, Nearest Neighbor (NN) resampling using MRT software, spatial oversampling to 200 m × 200 m resolution, applying several outlier detector filter, filling holes in the original LST maps, volumetric splines interpolation and checking the results with weather station data. Some of their results showed that between 32% and 41.5% of each altitudinal zone has good pixel coverage between 2000 and 2008 for the study region. The way of managing MODIS time series in this study will be useful for further researches.

Xiao et al. (2007) studied the impact of land use and land cover changes on land surface temperature in Guizhou Province in Southwest China including four counties. It is a mountainous agricultural province and about 73% of it is karst formation, including poljes, cockpits, towers and dolines. Three cloud-free Landsat TM scenes, acquired on November 7, 1991, December 5, 1994, and December 19, 2001, were obtained for this study. The satellite images were corrected to remove atmospheric effects and georectified with control points. Then all the data were projected to a common UTM coordinate system. Using hybrid image classification system, five land use/land cover (LULC) types were selected, including natural vegetation, water, agriculture, urban, and barren land. In the next step LST and NDVI were computed for each image and in each land use type and the correlation coefficient between NDVI and LST were found around 0.78. Their results

showed that urban/built-up land increased by almost three times from 1991 to 2001, while agricultural land decreased at a similar rate of about 4% per year. Of all the LULC categories, urban and built-up had the highest average temperature, followed by forest, agriculture, and barren land. The conversion of forest and agricultural land into urban/built-up land increased the amount of LST. The average LSTs for urban and built-up land increased by 1.1, 1.5, 1.4, and 1.2 K from 1991 to 2001 and in four counties.

Cao et al. (2008) analyzed Land surface temperature changes in response to land use/cover change in Sangong River basin in China. The study area is oasis located in the edge of desert. To achieve their objective, they selected two images of Landsat TM/ETM+ which belong to 1990 and 1999 respectively and analyzed them for retrieving Land Use/Cover Change (LUCC) and land surface temperature (LST) data. They used mono-window algorithm to get LST values. Then changes of LST from 1990 to 1999 were got from the LST of 1990 and 1999 by Using Arc/Info 9.0 (ESRI, ArcGIS Desktop: Release 9. Redlands, CA: Environmental Systems Research Institute). Besides, using Matrix in ArcGIS they got land use change map. They also got the average LST through the weight sum and standard deviation of pixel by pixel in each land use and in 1990 and 1999. Based on mean LST values they calculate LST Change rate per land use and between 1990 and 1999. They have found that LST is in remarkable response to LUCC. On the whole, because of rapid growth of cities in 1990-1999, more farm land was needed so that land Use/cover changed remarkably and the average of LST rose about 10 °C within this period. What we can use from this study is the way they got average LST through the weight sum in each land use.

Neteler (2005) analyzed time series of MODIS LST and NDVI/EVI satellite data in Province of Trento, Italian Alps with GRASS GIS software (Geographic Resources Analysis Support System) to do an epidemiological study about the exposure risk to Lyme and tick-borne encephalitis (TBE) diseases. They did Pre-Processing analysis of MODIS Data for GIS Usage. At first they used "MODIS Reprojection Tool" (MRT) to re-project images to UTM; moreover using MRT output images will be in standard data formats such as Geo TIFF. Then they did the pixel-wise application of the quality maps (QA) with re-projected LST maps to limit low quality cells. Then they applied one more quality filter due to removing thin cloud and high aerosol presence effects. To do so they applied outlier detection method to remove the minimum temperatures cells. In the next step they provide monthly LST values. Then to validate LST data they investigate mean monthly LST data with monthly mean temperatures of selected meteorological stations. And finally they tried to relate LST with mentioned diseases. Some of their results showed that just in months with nearly continuous cloud cover the mean temperatures deviate significantly from corresponded LST values. Using MRT software they re-project MODIS images to UTM and Geo TIFF format which can be considered in the current research.

Dimoudi and Nikolopoulou (2003) in their findings reveal that in dense Attens neigbouhoods that for every 10 percent increase in percentage of vegetation to highly impervious areas resulted in a decreasing in air temperature by $0.8^{o}C$. Impervious surface limit the presence of moisture; which plays a key role in moderating local air temperature. Large areas of impervious surfaces intensify at least three environmental problems related to (UHI) dry

urban environments, storm water flooding and reduction in water quality and more intense UHI (Alberti, 2009; Stone,2012; Gartland, 2008; Coseo, 2013; Weng et al., 2015; Apama et al 2015). When an area is mostly made up of impervious surfaces, there is less planting area for healthy vegetation resulting to less moisture from plants (Hough, 2004).

Taha (1997) estimated that, unlike natural areas, urban areas reflect only 15-20 percent of the incoming shortwave while absorbing 80-85 percent of the energy. Emissivity measures a materials a materials ability to store heat energy and release it back into the atmosphere. Most concretes and asphalts have emissivity around 0.90 (on a scale of 0to 1.0), thus effectively storing and slowly releasing heat energy (Golden and Kaloush, 2006). In addition to generally being low albedo and high emissivity environments, urban areas have less available moisture pavement and buildings that replace natural vegetation and 'seals' soils. This undesirable sealing means that urban environments are drier and thus have a lower percentage of latent heat relative to sensible heart (Stone, 2012). For this reason, vegetation and permeable soils play a critical role in moderating and dampening the warming effects of impervious land covers in urban environment. Zhang et al., 2011) observed that impervious of 17 Detroit area sites explained 59(%) of the variance in average daily minimum area temperature. Xiao *et al.,* (2007) reported that impervious surface is positively correlated with LST in Beijing, China. They used Landsat TM and QuickBird images to analyze the correlations (Xiao et al., 2007).

Weng and Yang (2004) argued that low vegetation coverage is one of the main reasons for UHI effect in Guangzhou city, China. They generated land

cover and LST maps from Landsat TM images.Haven applied remote sensing and GIS methods, examined the urban expansion and its impact on surface temperature. He found out, that urban development caused the rise of LST by 13.01 K. However, Pitman et al., (2011) concludes that LULC conversion affects LST in different directions, by increasing the impact on its extremes. Ali-Toudert & Mayer (2007) found that models of Ghardaia, Algeria east-west oriented streets had higher temperatures than north-south due to the lack of shading over the course of the day. The same study found that simulating a 5 m/s breeze parallel to the urban canyon reduced the apparent temperature by 12^{0}C (Ali-Toudert&Mayer, 2007).

2.2.5 Urban Heat Island Studies in Nigeria

In Nigeria, the earliest documented research in the field was done by Oguntoyinbo (1970) in which he studied the albedo and reflection fluxes of urban and rural surfaces in Ibadan. His findings indicated a mean albedo of (12%) for urban surfaces and (6%) for rural surfaces. Oguntoyinbo (1973) further examined the impact of urbanization on the climate of Ibadan; he used thermo- hygrographs and whirling hygrometer to measure temperature and relative humidity data across the city. Since the pioneer works of Oguntoyinbo, other urban climate studies were undertaken largely on the issue of the urban heat island phenomenon using ground based measuring instruments for example, Ojo, 1981; Adebayo, 1985; and Omogbai, 1985 have a common feature of being empirical in nature. Other works in urban climate studies in Nigeria include those by Adegoke (2002) who checked the variations of carbon monoxide

with thermal comfort in Ibadan; Efe (2002) examined the effect of the urban landscape on precipitation and rainwater quality in Warri. Nduka and Abdul-hamed (2011) both conducted similar studies; the first in Kano where they assessed the spatio-temporal variation of urban canopy heat island, while the latter assessed the urban canopy heat island variation and land use/land cover in Onitsha metropolis, they both used digital temperature loggers (i-buttons) in assessing the spatial and temporal distribution of the urban canopy layer heat island in the study areas of interest.

Ademiluyi, Okude and Akanni (2008) reviewed some of the foremost works in this area from Nigeria which included NIRAD Project (1976/79), Areola (1977), FORMECU (1996) and Omojola (1997). While the NIRAD Project, Areola's work and FORMECU Project were more of land use classification, Omojola extended his work to cover change detection. Ekpenyong (2008) used the GIS database to model the land use/cover change between 1984 and 2003 for Akwa Ibom State. The result showed that some urban centres had expanded into farmlands/fallow lands and the surrounding secondary forest. Within that period, mangrove forest had reduced by 50 per cent. Other forest covers in the area also changed, threatening food security and climate among others.

While examining the process of land use conversion and rate in common and public lands in South-Eastern Nigeria between 1972 and 2001, Bisong (2007) showed that deforestation was higher in publicly controlled lands than in communal lands. Agricultural land use characteristics, such as farm types and

the nature of croplands/fallows, correlated strongly and significantly with deforestation rates. Similarly, Idoko, Bisong, and Okon (2008) analyzed satellite imageries of 1987 and 2004 for the Federal Capital Territory, Abuja for land use change. The imageries were characterized into five classes using maximum likelihood algorithm. The classes were vegetation, built-up, rock outcrop, and water body and farm land. The two classified imageries were compared to identify any changes. Also, a spatio-temporal change in land use type was obtained in quantitative terms. The analysis revealed that vegetation cover reduced by 85.22 per cent between 1987 and 2004. Again, the built-up area increased by 21.99 per cent and farm land increased by 0.14 per cent.

Also, Enete (2009) evaluated the microclimate of Enugu at several sites using paired measurement program (PMP) and landsat /ETM Satellite Imagery. The results indicate that urban climate modification at day and night was very different. A down-town centred heat island was observed at night in both dry and rainy seasons. The day   time variation was strongly correlated to Sky – View factors and thermal properties in the city. The thermal comfort classification for the city range between $25.4^{o}c$ and $27^{o}c$ which is a class where over 50(%) of the population suffers discomfort.

In their study on participatory land use planning for community based forest management in south-eastern Nigeria, Bisong, Animashaun and Andrew-Essien (2007) presented an empirical classification of current land uses in their study area. They include those under high forest, secondary forest, savanna/grasslands, swamplands and farm/fallow lands. About 51 per cent of the overall land uses was classified under tropical high forest from a total land area of 665.72km2. The values ranged between 38 per cent in Agoi-

Ekpo community to 91 per cent in Etara/Ekuri-Eyeyeng Communities. They concluded that high forest was the dominant land use type followed by secondary forest and farm/fallow lands in all the three communities studied.

Umar and Satish (2016), investigates the spatial and temporal pattern and changes of urban heat island (UHI) in Kano metropolis, Kano State Nigeria. Land surface temperature (LST) values were extracted from Landsat TM image (1986), ETM+ (2000) and OLI (2014). Built-up area and road system were derived from 1:50,000 scale topographic maps. A Normalized Difference Vegetation Index (NDVI) map was extracted from the same image. Multiple correlation analyses were used to examine the relationship between UHI pattern and land use/land cover parameters (NDVI, built-up density and road density). Results show that, multiple heat islands emerged over central part of the city and along the major road that linked the city with other states. These areas coincide with the densely build-up area of the metropolis. Likewise, heat island emerges around the international airport of the state. The statistical analysis indicates that the UHI intensities had a negative relationship with NDVI, but a positive correlation with built-up. Interestingly, the temporal analysis indicate that, areas observe with lower land Surface Temperature In 1986 Have Been Recorded With Higher Temperature In 2000 And 2014.

Lays (2013), in assessing the dynamic of Abuja city's land cover, Federal Capital Territory Abuja Nigeria made used of Landsat TM and ETM+ images (path and row 189/54 respectively) with a 30m spatial resolutions; for the periods 1986,1990,2001,2006 and 2011; and sourced from glovis and glcf

NASA. The satellite images selected for the land cover classification were bands 543. Artificial Neural Network algorithm was used for the urban Land cover classification. Land cover categories were analyzed by regression techniques. The results of the analysis showed that the built up area was more prominent in the urbanized areas with (207%) change from 1986 to 2011. There is inverse relationship between vegetation and built-up area and direct relationship also exist between the built-up and the years. The study concluded that the green vegetation area has weaken the effects on urban heat island, while, built-up area has the capability of strengthening the effects of urban heat island in the Abuja city. Owing to the constraints posed by availability and quality of data; to study the dynamics of city land cover; satellite based sensors with very high spatial resolution were recommended to enable highly detailed land use/cover, and ecological characterization of the urban environment of the city.

Bernard and Raymond (2015), utilizes remote sensing, in conjunction with geographic information system (GIS), to explore the effect of LULC change on land surface temperature (ST) over 15-year period in Makurdi, North central Nigeria. A total of twelve (12) Landsat TM/ETM+ images acquired for April, June and January of 1991, 1996, 2001 and 2006 for the study. The Landsat TM/ETM+ images were analyzed using Integrated Land and Water Information System (ILWIS) 3.3, ERDAS Imagine 8.6 and ArcGIS 9.3 software. The Normalized Difference Vegetation Index (NDVI), Normalized Difference Wetness Index (NDWI) and Normalized Difference Built-up Index (NDBI) were used to represent the dominant land use/land cover (LULC) types in the study area. The effect of NDVI, NDWI and NDBI on ST was investigated using pixel-by pixel correlation analysis. The results show that

areas of water, forest, undergrowth/wetland and cultivated land have decreased by 4km2, 37km2, 119km2 and 19km2 from 1991-2006. The ST is negatively correlated with NDVI and NDWI but positively correlated with NDBI for all the months/seasons and years. The results suggest that change in land use/land cover, driven by urbanization, is the primary driver of surface and atmospheric temperatures in Makurdi.

Julius and Oyewole (2016), presents the analysis of Akure urban land use change detection from remote imagery perspective. Efforts were made to examine the direction that the continuous expansion of the city tends towards since its inception as a state capital in 1976. Using Aerial Imagery Overlay (AIO), the pattern of land use changes in Akure and its environs were determined. This involves imageries interpolation and overlaying to determine the land use changes, direction, and extent of the expansion. Findings revealed unguided expansion in the growth of the city which affects the pattern of land uses within the city and, by extension, into the adjoining settlements. There were incompatible conversions in land uses and undue encroachment into green areas in the adjoining communities. The study suggests effective zoning strategy on unguided nature of urban development whose effects on land use are very prominent in the study area. Adequate monitoring by the Development Control Department and other stakeholders in urban planning is equally suggested to mitigate the incompatible land use changes in the area.

Adeoluwa (2015) examined the effect of changing land use on land surface temperature (urban heat island) in Onitsha, Anambra state. He employed Landsat imageries of 1989, 2002 and 2014 covering Onitsha in Anambra State to examine the dynamics of Landcover, daytime LST and SUHI. The

result showed a temporal variation in land cover pattern. However, between 1989 and 2014, the study area had lost a proportion of natural land cover [forest (-519.59 ha) and bare soil (-1427.34 ha)] to built-up areas (+1189.45 ha), vegetation (+235.09 ha) and water bodies (+522.38 ha)]. LST across the study area varied between 23.7-36.7 ± 2.3 °C; 21.7-36.5 ± 3.0 °C and 22.5-32.5 ± 2.1 °C in 1989, 2002 and 2014 respectively. The visual pattern of LST showed that most areas at the centre of Onitsha, where built-up areas are densely present, appeared warmer than areas North and South of study area where built-up areas are sparsely present. Small hotspots indicating SUHIs were noticed in the three periods. The study therefore concluded that the dynamics of land cover categories resulted in a variation in the LST, which as well altered the pattern of SUHI in the three periods cons Nduka, 2011 used thermochron i-Button data-loggers to assess the urban canopy heat island variation and land use/land cover in Onitsha metropolis in the hot and dry season. His work was able to establish a significant variation in both spatial and temporal distribution of UHI in the metropolis. Abdulhameed, 2011 also conducted a similar study but in a different location (Kano) and over a different time frame (one year period). He used the same method and obtained similar results, which is significant spatio-temporal UHI variation for the location under study. Other works include those by Efe, 2004, which checked the impact of the urban landscape on rain water quality in Warri using thermo-hygrographs. The same instruments were used in the study by Adegoke, 2002, Aina, 1989 and ojo, 1981.

Abegunde and Adedeji (2015) carried out a research on the impact of land use change on surface temperature knowing that the built-up environment absorb and store solar energy, resulting into the Urban Heat Island (UHI) effect.

The Landsat imagery was used to examine the land use change for a period of 42 years (1972-2014). Land Surface Temperature (LST) was obtained by converting the thermal band to a surface temperature map and zonal statistic analyses was used to examine the relationship between land use and temperature emission. The results showed that the settlement area increased to a large extent while the area covered by vegetation reduced during the study period. The spatial and temporal trends of surface temperature are related to the gradual change in urban land use/land cover and the settlement area has the highest emission.

2.2.6 Measurement of land Cover changes

Some popular packages include: Geomod (Pontius, 2005), SLEUTH (2003), Land Use Scanner (1999), Environment Explorer (Verburg, 2004), SAMBA (2005), Land Transformation Model (Pijanowski, 2002), and CLUE (2000). These tools, again, utilize a number of methods in order to model land cover change such as Markov Chain (Balzter, 2013), Cellular Automata (Santé, Garcia, Miranda, Crecents, 2010), Logistic Regression (McConnell et al., 2004), and Artificial Neural Network (ANN) (Civco, 1993). Each tool has its own advantages and disadvantages. For example, Geomod is designed to simulate only a one-way transition from one land cover category to another land cover category (Pontius, 2005). Again, each method has its own strengths and weaknesses. For example, Markov Chain is better applicable when the trend of land cover changes is known. However, this method lacks spatial dependency and spatial distribution (Balzter, 2013). The Cellular Automata method models the state of each cell in an array depending on the previous state of the cells within a neighbourhood, according to a set transition rules (Santé *et al .,* 2010).

The MLP Neural Network method makes its own decisions about the parameters to be used and how they should be changed to better model the data. It undertakes the classification of remotely sensed imagery through a Multi-Layer Perceptron neural network classifier using the back propagation algorithm. The MLP also performs a non-parametric regression analysis between input variables and one dependent variable with the output containing one output neuron, that is , the predicted memberships (Attinson and Tatnall, 2012). One of its main advantages is that it is distribution-free, that is, no underlying model is assumed for the multivariate distribution of the class-specific data in feature space (Eastman, 2012). Neural networks are non-linear and can be conceived as a complex mathematical function that converts input data (for example, remotely sensed imagery) to a desired output (for example, a land cover classification) (Ahmed, 2011; Atkinson et al., 1997; Eastman, 2012).

NDVI has long been used as a measure of the urbanization impacts *(*Weng and Lu, 2008). Numerous researches of NDVI-LST relationship recorded a negative correlation between them. Weng *et al.* (2007) found that LST has positive correlation with impervious surface but negative with green vegetation land cover class. Other than NDVI, the Normalized Built-Up Index (NDBI) has also been used for analysis of LULC-LST relationship. Unlike NDVI, NDBI has a positive linear regression with LST, meaning that higher LST values occur in built-up areas, rather than non-built-up *(*Li, Me, and Wang, 2009).

2.2.7 Measurement of Land Surface Temperature

Historically urban climate observations were carried out utilizing regular meteorological networks, through ground measurements. Remote sensing approach was not available before the launch of the Landsat 5 satellite in 1982, due to low spatial resolution of other TIR sensors available. These observations differ a lot from those acquired by remote sensing due to the difference in their nature. Previous comparisons have shown that the results of TIR observations are in close agreement with direct measurements *(*Mallick, et al. 2013*)*. Most researchers prefer thermal satellite data, because it has several significant advantages. For example, satellite data allows for the acquisition of data over large areas, while direct measurements provide point measurements. Another important advantage of RS data is its low price and general simplicity of acquiring data, while to cover the whole region of interest with direct measurements will take lots of time and will be extremely expensive. It is also essential, that the data from the sensor cover the region at one time with same conditions. On the contrary, direct measurements are taken at different times and at different conditions, which influences a lot further analysis and interpretation.

However, direct measurement also have a couple of advantages like the ability to take into account the vertical structure of the surface, which is especially important for high-density urban areas(Steward, 2014). Disadvantages of remote sensing are as follows: sensitivity to atmospheric conditions, dependence on surface roughness and land cover type, lack of information about vertical magnitude of LST. Despite these disadvantages, remote sensing remains one of the most reliable sources of .data for urban climatology studies. Researchers have identified UHI using a number of different measures de-

pending on the type of components of comparison made (e.g., spatial, temporal) in their studies. For example, when comparisons are made between two time periods, UHI was identified by measuring LST differences between the periods of an identical location. This method is often applied to measure the impact of urban growth on UHI effect (e.g., temperature differences between pre-urban and post-urban conditions) (Lowry, 1977). Others have identified UHI through measuring rural-urban temperature differences (Lowry, 1997, Karl, Diaz and Kukla, 1988). Therefore, the comparison is made between geographical units rather than between time periods. However, most of these studies are based on observed temperature of places. More recently, researcher started utilizing airborne or satellite remote sensing data to derive UHI based on LST (Gallo *et al.,* 1995, Streutker, 2003). These two types of opportunity (e.g., derivation of surface temperature and monitoring land cover changes), therefore, enabled researchers to investigate the links between land cover changes and LST changes of a given site between two time periods, *i.e.*, the monitoring of UHI effect due to land cover changes (Fabrizi et al., 2010). In the recent past, researchers used the National Oceanic and Atmospheric Administration (NOAA) data to derive LST and consequently to measure UHI for studies conducted at the regional scale (Gallo et al., 1996). However, in recent years, the Landsat Thematic Mapper (TM) and Enhanced Thematic Mapper Plus (ETM+) thermal infrared (TIR) data have often been utilized for smaller scale studies (Rinner and Hussai, 2011;Xiong et al., 2012). Other studies have used mixed type of images. For example, Liu and Zhang (2011) analyzed Landsat TM and ASTER images in order to derive UHI intensity in Hong Kong city, while Enete (2009) analyzed Lansat TM in order to derive UHI intensity in Enugu.

Different types of land cover indices have also been developed in order to investigate the correlations between land cover changes and LST. Amongst the various indices, studies have found that normalized difference vegetation index (NDVI), normalized difference built-up index (NDBI), normalized difference water index (NDWI), and normalized difference bareness index (NDBaI) correlate strongly with LST (Ye,2010;Liu 2011,Essa, Verberren, Vanderkwast, Vande Voorde and Bate, 2012). NDVI is used worldwide to express the density of vegetation, monitor drought, monitor and predict agricultural production, assist in predicting hazardous fire zones, and map desert encroachment (Xiong et al., 2012). The NDVI process creates a single-band dataset that mainly represents healthy biomass. This index output values between −1.0 and 1.0, where any negative values are mainly generated from clouds, water, and snow, and values near zero are mainly generated from rock and bare soil. Very low values of NDVI (0.1 and below) correspond to barren areas of agriculture, rock, sand, or snow. Moderate values represent parks, shrub, and grassland (0.2 to 0.3), while high values indicate temperate and tropical rainforests (0.6 to 0.8) (Environmental system research institute, CA, USA, 2012).

NDWI implies the water content within vegetation and water state of vegetation (Aakriti and Ram, 2015). NDBI is sensitive to built-up area. It has been recently used as an indicator to represent the extent of built-up areas (Zha *et al.,* 2003). NDBaI is useful to classify different barren lands (Zhao and Chen, 2005). These indices are used to classify different land cover types by setting the appropriate threshold values (Zha *et al.,* 2003). The relationship between LST and NDVI has been extensively documented in literature (Kalney and Chai, 2003; Weng and Liang, 2006). The urban thermal environment is re-

lated to the reduction in vegetation coverage (Xiong et al., 2012). NDBI is used for the extraction and mapping of built-up areas (Zha and Chen, 2005). NDWI and NDBaI are being analyzed for delineating water content in vegetation and identifying bareness of soil respectively (Chen et al., 2002, Zhao and Chen, 2002). The intensity of LST is directly related to the rate of urbanization, land use patterns, and building density. LST is related to patterns of land use/cover changes, e.g., the composition of built-up area, vegetation, and water bodies (Chen *et al*., 2002).

In the study conducted by Yu et al. (2014), three different methods were compared for LST extraction from Landsat 8 OLI/TIRS thermal bands which are the single channel (SC) method, the split window (SW) algorithm and the radiative transfer equation-based method. According to their results, radiative transfer equation-based method using band 10 has the highest accuracy while the SC method has the lowest accuracy. In addition, their results show that band 11 has more uncertainty than band 10. Jimenez-Munoz *et al.,* (2014), Rozenstein *et al.* (2014) and Jin *et al.,* (2015) proposed different SW algorithms for LST retrieval using the Landsat 8 TIRS image. In the study performed by Jimenez-Munoz et al., (2014), SC and SW algorithms were proposed for LST retrieval. Algorithms were tested and the obtained results showed that RMSE values are typically less than 1.5 K. Jin *et al.,* (2015) proposed a practical SW algorithm and according to the results, this algorithm provides quite accurate and universal LST retrieval method.

Wang, Berardi and Akbari (2015) developed a new method which is called improved mono-window (IMW) algorithm for LST extraction from Landsat 8 TIRS band 10. They compared this method with SC algorithm for three

main atmosphere profiles and they found IMW algorithm error less than the SC algorithm.

Sekertekin et al. (2016) studied the spatiotemporal variation of UHI in Zonguldak city from 1986 to 2015, using the Landsat 5 TM and Landsat 8 OLI/TIRS imageries. In this study, Mono-Window the International Archives of the Photogrammetry, Remote algorithm was used for estimating the LST values from thermal band 10 of Landsat 8 TIRS. According to the obtained results, the LST values were increased in time for all areas except the city dump. The city dump temperature decreased in 2015, because of the Zonguldak municipality stopped throwing away garbage. It was also observed that the temperatures of built-up areas were increased significantly.

2.2.8 Statistical Analysis of Urban Heat Island.

Regression analyses are statistical tools that have been used extensively in UHI studies. These studies are useful in showing the relationships between different variables, in this case different temperature and NDVI datasets. This section review literature on the application of regression techniques for analysing temperature and NDVI datasets.

According to Lee (1993), linear and multiple regression techniques can be used to perform several statistical tasks on temperature datasets. Lee utilized linear and multiple regressions to compare satellite derived brightness temperature with air and ground surface temperature to determine whether there was a relationship among the parameters in question. Based on the thermal infrared images of Seoul taken in 1986 and 1989, urban areas and heat island

in the Seoul metropolitan area expanded dramatically. The Regression model archived land surface temperatures on the brightness temperatures explain, 72 percent of the variance in this study, making it a useful tool for accessing changing air field in cities. Lee emphasized how the equation verifies that one can estimate and predict ground surface temperatures based on the brightness temperatures.

Also, the approach that Gallo and McNab (1993) utilized was very similar to Lee's method but with different algorithms for analysis. Gallo and McNab (1993) used the vegetation index, satellite derived surface temperatures for their study while performing multiple regression on these parameters. Urban / rural differences for the vegetation index and the remotely sensed land surface temperatures were computed and compared to observed urban/rural differences in minimum air temperature (UHI intensity). The temporal range of the analysis was from June 28 to July 4, 1991 and provided an evaluation of the analysis of data from single dates compared with data from weekly composites along with vegetation index and surface minimum temperatures were sampled from these days (July 1,2, and 3,1991 : clear conditions) and the relationships were examined for each day. The vegetation index was obtained from channels 1 (.62um-- .91um) and (.91um-3.74um) of the AVHRR sensor, both of which were used in various vegetation analyses. These found that the satellite –derived normalized difference vegetation index data (NDVI), sampled over urban and rural areas composed of a variety of land surface environments, were linearly related to the differences in observed urban and rural minimum temperatures when linear regression was performed. The purpose of these comparisons was to evaluate the use of satellite imagery to assess the influence of the urban environment on the UHI effects. The differ-

ence in the NDVI between rural regions appears to be an indicator of the difference in surface properties between the two environments that are responsible for the UHI effect.

In addition, a slightly different statistical approach was used in Florio (et al., 2004) study, which addressed whether combining several different statistical models with satellite data information improved the performance in surface air temperature prediction. Three spatially dependent (Kriging) models were examined along with their non- spatial counterparts (Linear and multiple regressions). Both models predicted temperature very accurately; however, the kriging models had lower errors (average of 0.9 ^{0}C) than the regression models (average of 1.4 degrees C). The purpose of the Florio et al. (2004) study was to evaluate the predictive performance of the statistical approaches that use only the ground level data and no satellite data and to introduce models that utilize the satellite data along with ground level data and evaluate their predictive performance. The results provided an assessment of surface air temperature predictive performance of various statistical models, with and without satellite data, over different imaging conditions. Generally, the integration of satellite temperature data and ground temperature data into one statistical model showed promise as an approach for increasing the precision of air temperature measurement at the surface and can be useful in land surface temperature modelling.

A pixel –by-pixel correlation analysis of Indianapolis, Indiana was conducted by Weng, and Liu and Lu (2007) in which they computed Pearson correlation coefficient between LST's, green vegetation, and impervious surfaces. Three dates of Landsat TM imagery acquired in 1991, 1995, and 2000

were utilized to document the morphological changes in impervious surfaces and vegetation cover and analysed the relationships between the changes and those that occurred in the land surface temperatures. Their results indicated that all land use- land cover types and LST values were negatively correlated.

2.2.9 Gaps in Literature

From the literature reviewed, it is revealed that much of the global lan- use change studies have improved our understanding of the relationship that exist between land-use and land-cover change (LULC) and microclimate (urban heat island). Even though there is an increasing concern regarding global climate change in Nigeria, despite the ongoing research efforts and a greater availability of data, few studies on the effects of land use land cover on land-cover surface temperature have been conducted in major cities in the country. Thus a lot still needs to be done in this area because of the vast size of the country and the rapidity at which the changes are taking place. To the best of my knowledge, in Calabar South Local Government Area and Calabar Municipality (Calabar Metropolis), virtually nothing to our knowledge have been done to correlate the effect of the changing land use to land surface temperature. It is against this background that this study attempts to fill this obvious gap by 'Assessing the impact of land-use / land-cover change on urban heat island pattern in Calabar metropolis.

CHAPTER THREE
STUDY AREA

3.1 Location and Size

Calabar is the capital of Cross River State. It is situated at the Southern part of Cross River State. Calabar is located between longitudes $8^0 17'00''E$ and $8^0 20'00''E$, and latitudes $4^0 50'00''N$ and $5^0 10'00''N$. Calabar metropolis encompasses of Calabar Municipality and Calabar South Local Government Areas and covers an area of about 274.593 Sq km. Calabar is bounded to the north by Odukpani Local Government Area and to the East by Akpabuyo Local Government Area (Figure.4). As depicted in figure 4, Calabar is sandwiched between the Great Kwa River to the East and the Calabar River to the West. The present of urban area is on the eastern bank of the Calabar River its growth to the south is hindered by the mangrove swamps. The map of Nigeria showing Cross River State is presented in Fig.4, while the map of Cross River State showing Calabar Municipality is figure 5.
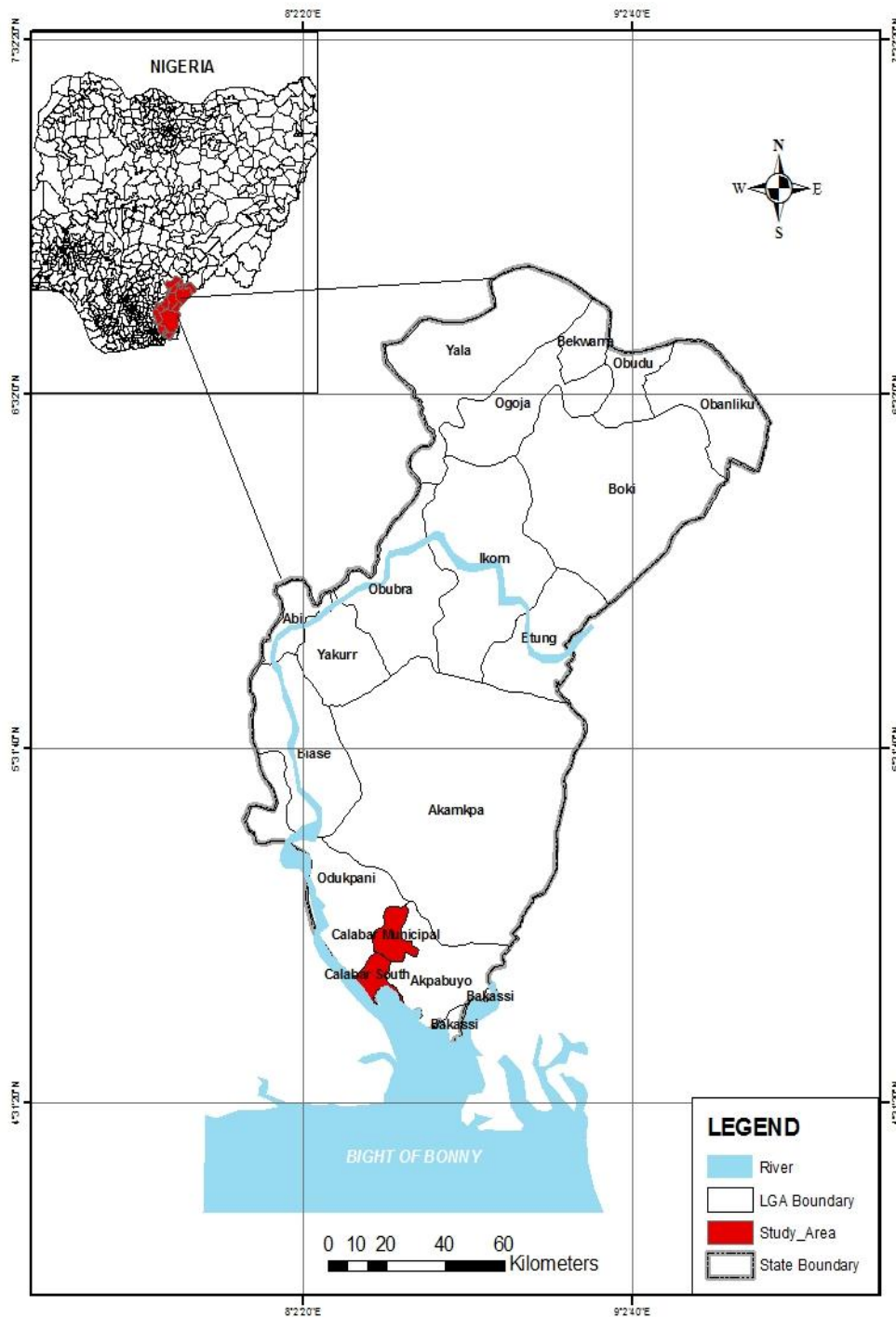
Fig. 4. Cross River State showing Calabar (Study area)
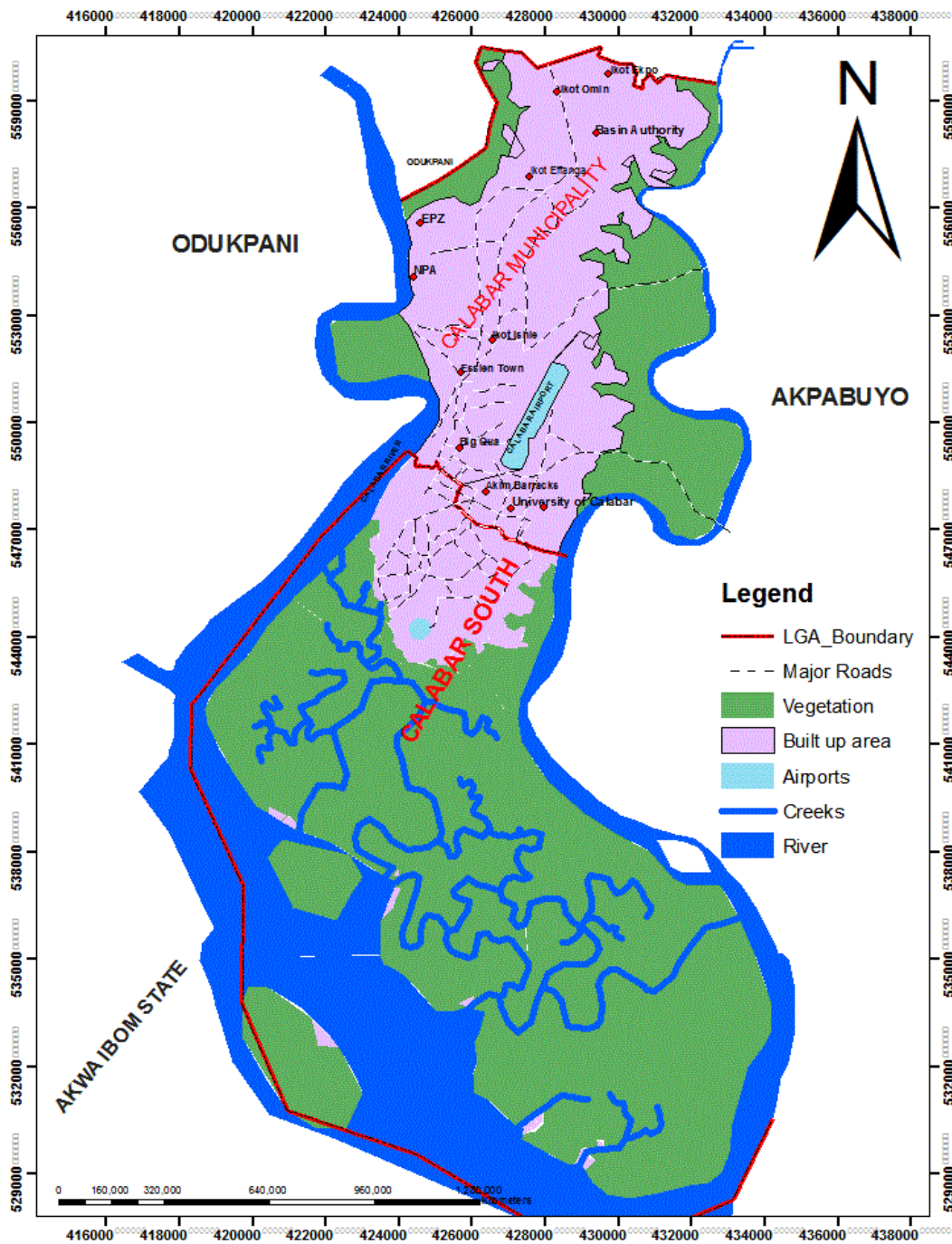 Source: Adopted from Offiong et al., 2012.

Figure 5. Map of the Study Area
Source: Adopted from Offiong et al., 2012

3.2 Climate

Calabar falls within tropical equatorial (Af) climate with high temperature, high relative humidity and abundant annual rainfall (Oguntoyinbo, 1978; Inyang, 1980).The climate of Calabar as well as other contiguous locations in the West African   region is being determined by two major air masses. The Tropical Maritime (mT) and the tropical continental (cT) air masses control the climate with two distinct seasons. mT air prevails and influences its moisture characteristic while the cT air influences the dry season condition due to is desert source across the two air masses at the upper troposphere from east to west. This is called the Equatorial Esterlies (EE). The two air masses meet at the pressure front called Inter Tropical discontinuity (ITD) (Oguntoyinbo, 1978).

The effect of insolation is quite high caused by the sheer factors of its tropical location as well as the activities of urban development which have significantly altered the land cover. Calabar have a double maxima (double peak) rainfall regime with important peaks in July and September depending on the yearly weather cycles. Rainfall duration spans between 9-10 months of the year but is somewhat intermittent during the dry season. Dry season commences from November through February and is heralded by the southward moving air mass from the Saharan-high pressure belt. The dry season weather or the harmattan season produces depression due to the cool-dry temperature and moisture characteristics of the cT air. It transports Aeolian deposits (aveoli) from its source in the Sahara. This incidence produces hazy weather which reduces visibility and also cuts down insolation. Presently, over-grazing and deforestation have caused the impact of harmattan wind to be felt beyond the latitude of Calabar (Inyang, 1980).

Four thermal zones have been identified in Calabar, which has been attributed by Inyang, 1980, to a real differences in population density, incidence of hydrologic/topographic influence on the heat distribution. The main areas include the Mbukpa-Eldgerley complex, the Watt market axis, the central depression (in the area around the State Housing Estate) and the Calabar River Basin.

The mean annual temperature for Calabar was given as 21.6^0C (70^0F), while minimum was 22.7^0C (73^0F). Also, the daily temperature range   was given as 3.8^0C (7^0F). The highest temperature values are recorded in February and March. Relative humidity is high all year round with the lowest value of 76.8 recorded in February and the highest recorded in August with a value of 92 percent (Inyang, 1980)

Calabar has been categorised by Fabgemi and Okulaja (1971) in their climatic classification of Nigeria based on the space correlation technique to be under the zone'A' rainfall category with "wet and moist' conditions, and a monsoonal pattern of rainfall. Thorthwarte and Matter (1955), Papadaski (1996) developed a similar technique where Calabar was identified under the per humid climatic zone with a moisture index of 100.

3.3 Geology

Udo (1970) categorized Calabar and other eastern state in his regional delimitation of Nigeria under the Cross River Basin. This Basin is a trough or depression which extends from the lower Benue plains to the Atlantic shores on the Gulf of Guinea. It is flanked by the eastern Borderland to the east and the Udi/Nsukka ceusta to the west (Ofomata, 1975). It encloses several states such as Cross River, Anambra, Ebonyi, Abia, Imo, Akwa

Ibom and Enugu. The landscape formation of Calabar has been described by Udo (1990) as belonging to the old Benue Basin around the cretaceous period of oceanic transgression in Nigeria. Ofomata (1975) grouped the Calabar formation into two categories. These are the cretaceous sedimentary formation and the Basement complex (igneous) formation. The cretaceous formation is conformal with the complex which appears in the area around Odukpani. The Bende-Ameke formation could also be found through a contagious deposit from Onitsha through Umuahia to Calabar. This formation is a litoral equivalent of the Ijebu formation in western Nigerian (Ofomata, 1975). Predominant soil categories here are of the coastal plain sands.

The city of Calabar as far as relief is concerned is hilly and undulating in most areas. It has a gentle slope which varies in some areas from zero percent to about 20 percent in others. Elevated grounds are predominant in the east with prominently north-south trending orientation. As Inyang (1980) puts it, 'this elevation separates the eastern plateau from the more or less western ridge'. The relief has a characteristically elevated coastal margin in areas around Marina road but lower in areas around Anantigha in Qua River lower valley.

3.4 Vegetation

The exceptional characteristics of high humidity, high rainfall and temperature have resulted to a highly unique, complex and diverse flora and fauna with evergreen tropical rainforest with tall trees and creeping ferns. The flo-

ristic richness is due to high rate of speciation. The vegetation is very rich in both timber and non-timber species. Most of the flora and fauna found in the forest are endemic to the area.

3.5 Population and socio-economic activities

The population of Calabar during the pre-colonial era was estimated at about 10,000. By the census figures of 1963 the population of Calabar was 99,352, and in 1991, it was 328,876, an increase of 3 per cent within 28 years (and percentage total growth of 5.5 from 1987-1997). In 2006, the population of Calabar grew through immigration from the rural areas into Calabar in search of better opportunities. The population growth of Calabar has been followed by the expansion of its physical boundaries. This increase in the physical boundaries implies a corresponding loss of vegetation and land in the area thereby a direct impact on the micro-climate. This fact has been attested to by Ekanem (1980), who asserted that "Calabar has within the span of a decade (1967-1997) been transformed into a booming administrative, commercial, and political nucleus in the state''. Calabar presently, is the economic and political nerve center of Cross River State, and the headquarters of Calabar Municipality and Calabar South Local Government Areas. With its current designation as a tourism destination in West Africa, Calabar has witnessed unprecedented influx of people from within and without its boundaries which has necessitated the building of service structures such as hotels, transportation lines, commercial, industrial and residential areas. The new status of Calabar has also brought industries such as the Tinapa Business and Leisure Resort, the Export Processing Zone (EPZ), Dangote Mills, Unicem Factory, Niger Mills and a host of other business and commercial activities such as banks, hotels and fast food joints

(Atu et al., 2010), . This development is not without repercussions on the natural environment as lands that were formally vegetated, used for agriculture and as habitat for biodiversity are now being used for residential, commercial and industrial purposes to accommodate the growing population and businesses. For instance, Atu et al. (2010), reports that 127.10 ha of agricultural land that was formerly used for cultivation of oil palm are now growing residential houses instead of palm trees and the new secretariat complex is standing on over 50 ha of land formerly used for the cultivation of vegetables. The loss of once vegetated land implies a corresponding alteration of the micro-climate of the area which in turn has great impact on the long term climatic averages of the area, thus, aggravating the UHI effects.

CHAPTER FOUR

RESEARCH METHOD

4.0 Introduction

This chapter focuses on materials and methods that where applied in answering the research questions in order to achieve the aim and objectives of the study.

4.1 Research Design

In order to examine the relationship that exist between land use/ land cover Change and Urban Heat Island (UHI) in Calabar metropolis (Calabar South and Calabar Municipality), the researcher employed experimental research making use of Mono window algorithm technique.

4.2 Data Requirement / Data Need

The variables investigated and derived in this research includes, surface cover, surface temperature and subsequently, urban heat island. To achieve this, data were collected from two different sources for analysis:

i.   Land surface temperature data were downloaded from the NASA website by Metadata ETM+ (Enhance Thematic Mapper Plus) and OLI (Operational Land Imagery for 15 years (2002; 2004-2006; 2008-2010; 2012-2014; 2016)

ii.   Land use maps from 2000-2016

iii. Topographic and administrative map of the study area aided ground Truthing and image classification interpretation.

4.4 Method of Data Collection

In this study, to understand the impact of land use land cover *(LULC)* change on land surface temperature, both primary and secondary data sources were employed. Primary data were generated from the analysis of thermal infrared images (TIR) and Landsat band 6, preliminary survey using GPS, while secondary data were obtained from the Nigeria Meteorological Agency Oshodi Lagos.

4.4.1 Method used for collecting   Land Surface Temperature (LST)

Land surface temperature (LST) is the main factor determining surface radiation and energy exchange (Xiao et al., 2007). Lands surface temperature data was downloaded from NASA's Earth Observing System Data and Information System by Landsat TM for 15years ((2000-2002; 2004-2006; 2008; 2012-2014; 2016).

4.4.2 **Data Description**

4.4.2.1 Landsat data Description

Landsat TM and ETM+ data are widely used in monitoring land surface processes. Landsat visible and near-infrared bands at 30-m resolution are capable of capturing signals of land cover and vegetation properties, while the thermal bands at 60-m resolution are sensitive to surface temperature.

4.4.2.2 Daily ground data

The daily average, maximum and minimum air temperatures were derived from the monthly surface meteorological records submitted by the Nigerian meteorological station obtained from the Agro-Meteorological Station in Calabar. These data were used as quality control and inspection and have

been utilized for validating thermodynamics-based methods for estimating the Ta (Sunet et al., 2005).

4.4.3 Data processing

4.4.3.1 Image and Pre-processing

Landsat 7 ETM+ image, cloud-free were acquired from the NASA web site. A systematically geometric and radiometric correction were performed to the image data using the calibration parameter file (CPF) released by the Earth Resources Observation Systems (EROS) Data Center (EDC), USGS before the satellite image were delivered, and the quality of Landsat image was in 1B level. The Landsat image, including the thermal band, were further rectified to Universal Transverse Mercator coordinate system and were resampled using the nearest neighbor algorithm with a pixel size of 30 by 30 m for all bands and the resultant root mean square error (RMSE) less than 0.5 pixels. The air temperature and moisture data were also collected from the weather stations as references for retrieving land surface temperature from the thermal remote sensing image.

4.4.3.2 Factors Extracted from Classification Images

The urban size, development area and water proportion were extracted directly from the classification images. Here the urban size and development area of Calabar South and Calabar Municipality can be easily calculated from the sum of corresponding land-use/land-cover pixels in the classification images, while the water proportion is the ratio of water area against the total area of urban area (including both land and water areas), was computed using the following equation:

$$P = \frac{S_{water}}{(S_{water}+S_{urban})} \qquad (1)$$

Where P is the water proportion, S_{water} is the pixel area of water; S_{urban} is the pixel area of urban-used land.

4.4.3.3 Retrieving of Land Surface Temperature

To estimate the land surface temperature it comsists of various procedures and steps that have been described by NASA. These procedure range from radiometric calibration and conversion of DN to radiance, up to normalized difference vegetation index, among others which are described below:

The signals received by the thermal sensors were converted to at-sensor radiance (L_λ). Radiance values from the ETM+ thermal band can then be transformed to radiant surface temperature, namely brightness temperature, according to "Eq. (6) using thermal calibration constants supplied by the Landsat Project Science Office (2002):

$$Ts = \frac{K2}{\ln\left(\frac{K1}{L_1} + L_1\right)} \qquad (6)$$

Where T_s is the effective at-satellite temperature in K, K_1 and K_2 are the prelaunch calibration constants (For Landsat 7 ETM+: K_1=666.09 W/(m^2·sr·μm) and K_2=1282.71 K).

The temperature calculated by "Eq. (6) is not the actual LST, but the at-sensor brightness temperature. To obtain a reasonably high quality of LST,

four stages of correction process are required: (1) spectral radiance conversion to at-sensor brightness temperature; (2) correction for atmospheric absorption and re-emission; (3) correction for surface emissivity; and (4) correction for surface roughness (Voogt and Oke, 2003). Traditionally, the retrieval of LST from Landsat TM6/ETM+6 was mainly completed through the method of atmospheric corrections. The principle of atmospheric corrections is to subtract the upward atmospheric thermal radiance and the reflected atmospheric radiance from the observed radiance at satellite level so that the brightness temperature at ground level can be directly computed (Qin, Karnieli and Berliner , 2001; Qin, Li, Zhang, Karnieli and Berliner ,2003). Several programs such as LOWTRAN, MODTRAN and 6S have been designed for the atmospheric corrections, but the atmospheric corrections have proved to be difficult to complete because of many necessary parameters, and this is especially the case when the corrections have to be performed for the image at the time when the satellite passed. Based on the thermal radiance transfer equation, a mono-window algorithm for retrieving LST from thermal band of Landsat TM and ETM+ data were employed for this study and only three parameters were required for the algorithm: emissivity, transmittance and effective mean atmospheric temperature (Qin, Karnieli and Berliner , 2001; Qin, Li, Zhang, Karnieli and Berliner ,2003). The methodology employed for the calculation of the LST maps for this study was based on the the mono-window algorithm. Despite the advantages of high spectral and temporal accessibility to large scale areas, remote sensing data present some limitations, among which cloud cover contamination issue was the most important. For application of landsat, cloud can affect the T_{air} (air temperature) are at least two ways: Erroneous cloud identification can reduce the accuracy of Landsat

LST values, and the presence of clouds can affect the accuracy of the T_{air} estimation and the presence of cloud can greatly reduce the amount of data available in satellite images.The Mono-Window (MW) algorithm is the most commonly used, given that this algorithm removes the atmospheric effect and obtains the LST from the linear or nonlinear combination of the brightness temperatures (Qin, Li, Zhang, Karnieli and Berliner ,2003) and was used to calculate surface temperature in this study. The mono-window algorithm was expressed as follows:

$$T_s = \frac{a6\ (1-C_6-D_6) + [b_6\ (1-C_6-D_6) +C_6+D_6]\ T_6-D_6T_a}{C6} \qquad (7)$$

where T_s is the land surface temperature in K, T_6 is the brightness temperature extracted from 6"Eq. (6) T_a is the effective mean atmospheric temperature in K; a_6 and b_6 are constants with values of $-$ 67.355351 for a_6 and 0.458606 for b_6 when the LST is between 0-70 ^{0}C (Karnieli and Berliner ,2003) C_6 and D_6 can be calculated by the following equations:

$$C_6 = \ E_6\ T_6 \qquad\qquad (8)$$

$$D_6 = (1-T_6)\ [1+ (1-E_6\ T^6] \qquad\qquad (9)$$

where ε_6 is the ground surface emissivity and τ_6 is the atmospheric transmittance. T_a, ε_6, τ_6 are three parameters needed to covert the brightness temperature to LST. Atmospheric transmittance (τ_6) could be estimated according to the near-surface air temperature and the water vapor data from the local me-

teorological observatories because there exists a linear relationship be-
tween τ_6 and water vapor. The effective mean atmospheric temperature (T_a)
was calculated by the linear equations corresponding to the four standard at-
mospheres (10):

T_a=25.9396+0.88045T_0 (For USA1976)   (a)

T_a=17.9769+0.91715T_0 (For tropical)   (b)   10

T_a=16.0110+0.92621T_0 (For mid−latitude summer)   (c)

T_a=19.2704+0.91118T_0 (For mid−latitude winter)   (d)

where T_a is the effective mean atmospheric temperature in K, T_0 is the near-
surface air temperature in K; both of them could be acquired from the local
meteorological observatories. The four standard atmospheres were provided
by atmospheric simulation model LOWTRAN 7 and more detailed informa-
tion about the linear equations could be found in the paper written by Qin *et
al*.(2001). In research, the second equation (Eq. (10b)) will be used.

4.4.3.4 Method to Calculate the HIA

Most previous studies have focused on the spatial distribution or temporal
changes by equally segmenting the urban surface temperatures from thermal
remote sensing images. However, this equally segmenting method is not suit-
able when threshold values are selected arbitrarily, and the results may not
well represent the high-temperature area. In this study, a standard deviation
segmenting method was employed to calculate the HIA from the LST image
for seeking a more suitable threshold value.

With standard deviation segmenting method, both the hot island and cold island can be extracted by determining a threshold from the standard deviation of the surface mean temperature for each city. In order to calculate the HIA, five steps were employed as follows:

i. Step 1. Calculate the mean surface temperatures for the different areas selected and their standard deviations.

ii. Step 2. Use the following equation to calculate the temperature threshold values.

$$T=\alpha\pm\chi*sd \qquad\qquad (11)$$

Where T stands for the temperature threshold value, a is the mean value of the surface temperature for each area, χ (χ = -2.5, -2, -1.5, -1, -0.5, 0.5, 1, 1.5, 2, 2.5, 3) is the times of standard deviation, while sd is simply the standard deviation. Here eleven values were prepared for χ and eleven temperature thresholds was calculated according to the different values of χ ranging from −2.5 to 3 by the interval of 0.5.

iii. Step 3. Divide the surface temperature into eleven scales according to the threshold values calculated in the step 2.

iv. Step 4. Calculate the percentages of urban pixels in different surface temperature scales and their distribution in each area

v. The last step is to calculate the HIA. The threshold of (a + sd) was used to extract the outlines of the hot island and then determine the HIA by calculating the total number of pixels that the temperature is higher than (a + sd). HIA could reflect the spatial extent and the seriousness of SUHI and could be used to quantify the SUHI effect. It

72

should be emphasized that this standard deviation segmenting method was based on the statistic knowledge and was more suitable to extract the hot island compared with the density equally-slicing method.

4.4.4.5 Generating Isotherms   for Calabar

Generating   Isotherms for Calabar metropolis was based on landsat TM imageries that were downloaded from the NASA website. Isotherms based on Landsat TM data for   Calabar metropolis were generated using the Landsat TM band 6 data of January and April (2016), using Quantum GIS software 1.8.0. The temperature data in the form of delimited text was used for the generation of a shape file. Further, the shape file was used for generation of the isotherms using the Polygonize (Raster to Vector) function in the Raster menu.   Temperature ranges were selected for the isotherm generation. Based on these temperature ranges isotherm maps for the study area were generated from the Landsat TM data of January 2002 and 2016 using Quantum GIS software. The steps that were used to generate isotherm map for the study area are given below:

i.   identification of region of interest (ROI) from the layer stacked image,

ii.   Calculation of surface temperature for selected ROI using image processing software ENVI version 4.5,

iii.   Using the ROIs in the stacked image, isotherms are generated using Q-GIS software 1.8,

Classification of the contours in three different classes viz. 1) Class-1: 18˚C - 28˚C, 2) Class-2: 28˚C - 36˚C, 3) Class-3: ≥36˚C. 5.5.1. The isotherms was then divided into several temperature zones for further analysis and were used to identify major urban hot spots across Calabar metropolis.

4.4 STATISTICAL ANALYSIS

To help explain the spatial–temporal relationship between land use land cover (LULC) and land surface temperature (LST), we employed the following statistical approaches: Multiple regression analysis (step wise model) was employed to determine the relative importance of the dependent variables at a confidence level of 95 percent, $p<0.05$. Finally, the Pearson's correlation analysis, was done to determine and test the significant relationship between LST and LULC at 95 percent confidence level.

4.4.1 Pearson's correlation analysis

Land surface temperature (LST) values and their corresponding land use percentage values were extracted in Arch GIS. These data series were processed to determine the relationship between LST and percentage of different land use types using SPSS Statistics. To better understand how LST dynamics associates with land use, correlation strength between LST and the percentage of different land uses for all pixels was available in the attribute table of Landsat grid shape files and for the years 2002 to 2016. The attributes table was exported to excel sheets. To check the linear association between mean LST and percentage of different land uses, Pearson's correlation between land use and mean LST was tested.

4.4.2 **Multiple Regression Analysis**

Based on Su et al. (2010) findings, though correlation indicates the strength of linear association between paired variables, it is unable to show the relative contributions of various land uses to LST. For instance, if one pixel is occupied by both 50 percent water and sparse vegetation, considering the compensating effect of these two land use types on LST value, the land sur-

face temperature value of this pixel will not show the real effect of inland water nor greenhouse farming. In this situation a multiple linear regression model will be applied to understand the influence of built environment (LULC) on urban heat island (LST). The conventional regression model for a study is expressed as:

$$Y = a + \beta x$$

In which **y** (dependent variable) can be the land surface temperature, **x** can represent the percentage cover of land use (independent variables), and **a** is the intercept of the regression model.

In this study all the pixel of LST and NDVI were considered as the independent variable, as LST (UHI) has been found to be strongly determined by vegetation health (Zhang, et al., 2010). Mean yearly LST was considered as the dependent variable and percentage contribution of different land use groups as the independent variable. The regression model revealed the form of linear relationship that best predicts LST from the values of land use percentage. Stepwise regression will be used to predict how the percentages of different land uses affect the mean LST in each pixel. Regression will be repeated for the years (16 years with two years interval). Stepwise is a regression model with sequentially adding or removing variables based on t- statistics of their estimated coefficients (SPSS version 22).

Hypothesis Testing

For the purpose of this study, two types of hypothesis will be considered.

H_O = There is no significant influence of land cover (LC) on the urban heat island (LST)

H_O = There is no significant growth in the annual temperature in Calabar.

T-Test: t – stats > t- table H_O will be rejected and H_1 accepted; t-stats < t- table **with** standard error α = 0.05
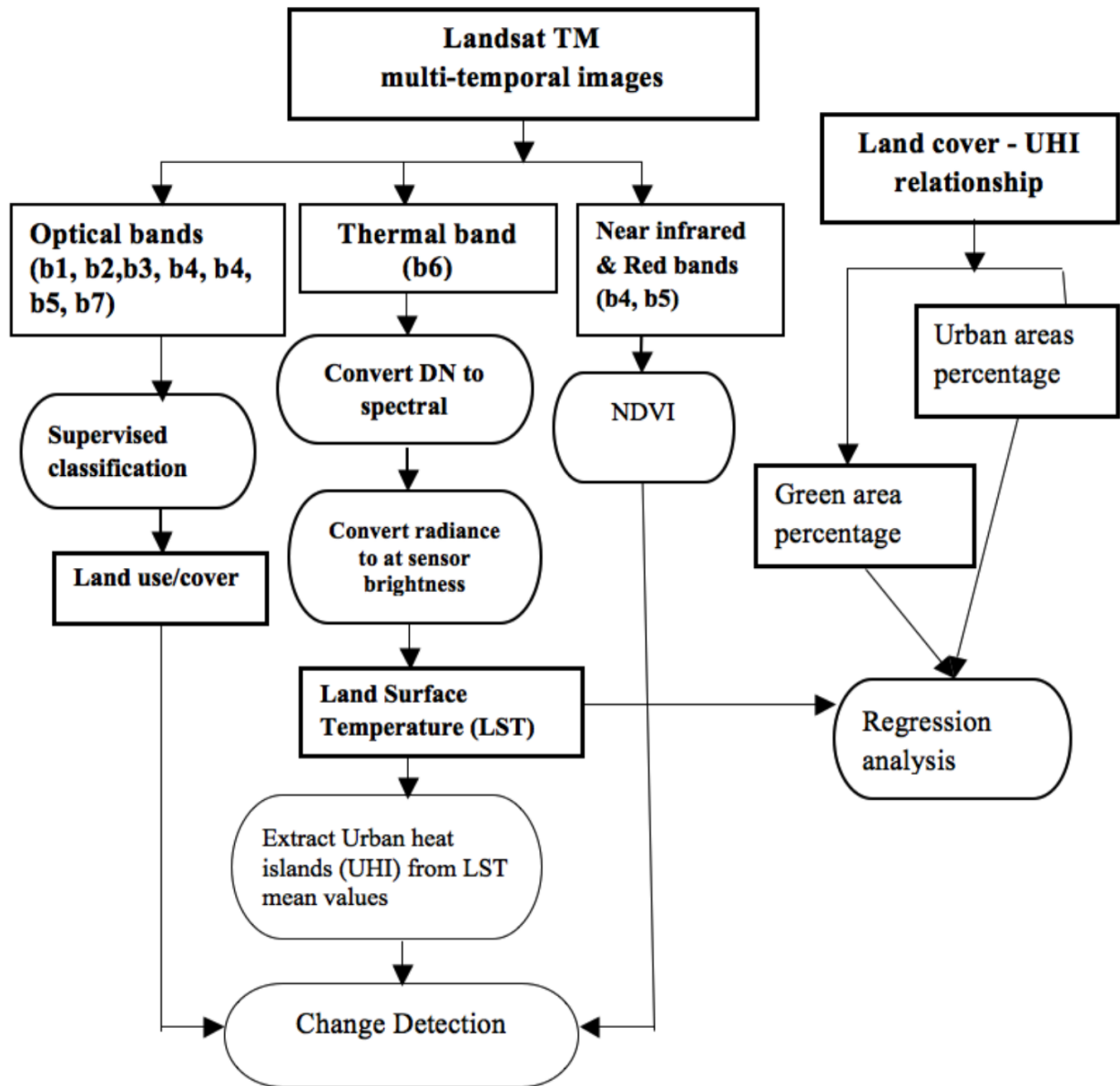

Figure 6: Summary of research design

CHAPTER FIVE
DATA PRESENTATION, ANALYSIS AND DISCUSION OF FINDINGS

5.1 Introduction

This chapter present the results obtained from the field through the use of the research method stated earlier. The analysis was done in a systematic way (following the objectives and hypothesis of the study). The data obtained was analyzed using tables, graphs, charts and maps. The size and area of the land cover changes were calculated and presented in hectares (ha) while LST for the different years were also extracted and presented in degree Celsius. Also, the Aerial photo imageries were processed using the Arc View GIS 9.30 software package. Kappa index of Agreement was used to validate and calculate land cover projection model.

5.2 Results of LULC Accuracy Assessment

The Kappa statistic is generally accepted as a measure of classification accuracy for both the model as well as user of the model of classification (Maingi and Marsh. 2002). Kappa values are characterized as <0 as indicative of no agreements and 0–0.2 as slight, 0.2–0.41 as fair, 0.41–116 0.60 as moderate, 0.60–0.80 as substantial and 0.81–1.0 as almost perfect agreement (Mangi and Marsh, 2002). Accuracy assessment tasks were performed on the 2002, 2006, 2008, 2010, 2012, 2014 and 2016 images. These tasks consisted of an overall classification accuracy, kappa statistics, and error matrix reports. The classification accuracy report calculates the statistics of percentages of accuracy relative to error matrix results. The error matrix report simply compares the historical (reference) values to the assigned class values. Kappa statistics

measure the ability to provide information about a single matrix as well as to compare matrices (Congalton, 1991). Historical reference image were obtained from Google Earth link. Results from the assessment revealed the overall classification accuracy of the images produced almost perfect *Kappa* statistics of 99.60 percent, 99.1 percent, 94.8, 99.9 percent, and 99.6 percent for the2002, 2006, 2008, 2010, 2012, 2014 and the 2016 images, respectively. This is an indication of classification accuracy almost perfect agreement (Appendix 1) (Awuh, 2017).

5.3 RESULT PRESENTATION BASED ON OBJECTIVE ONE *"To Determine LULC Change within Calabar Metropolis between 2002 and 2016"*

5.3.1. Satellite images and LULC classes Analyses

In this sub-section, the details of the LULC classes identified from the classifications imagery was analyzed. It was done by comparing the class composition of the various images to establish whether there is an increases or decreases in the total area occupied by the various LULC types over the periods. The land use was calculated using the LULC profile generation by the SVM algorithm. Cross tabulation was employed to determine quantities of conversions from a particular land cover to another land cover category at a later date (Alphan et al., 2008). The change matrices based on post classification comparison were obtained and are shown in Table 6 and Figure 7 to 13. Though the data was at varying time frame, the result showed that there have been an increasing rate of Landover change within the period of 2002 to 2016 (Figure 7 to 13).

5.3.2 Analysis of LULC classes for 2002 image

Figure 7a presents the results of the LULC class image for 2002. The results for the analysis of the 2002 satellite derived image shows that a great variation exist in the area coverage percent of the different LULC identified in the study area.
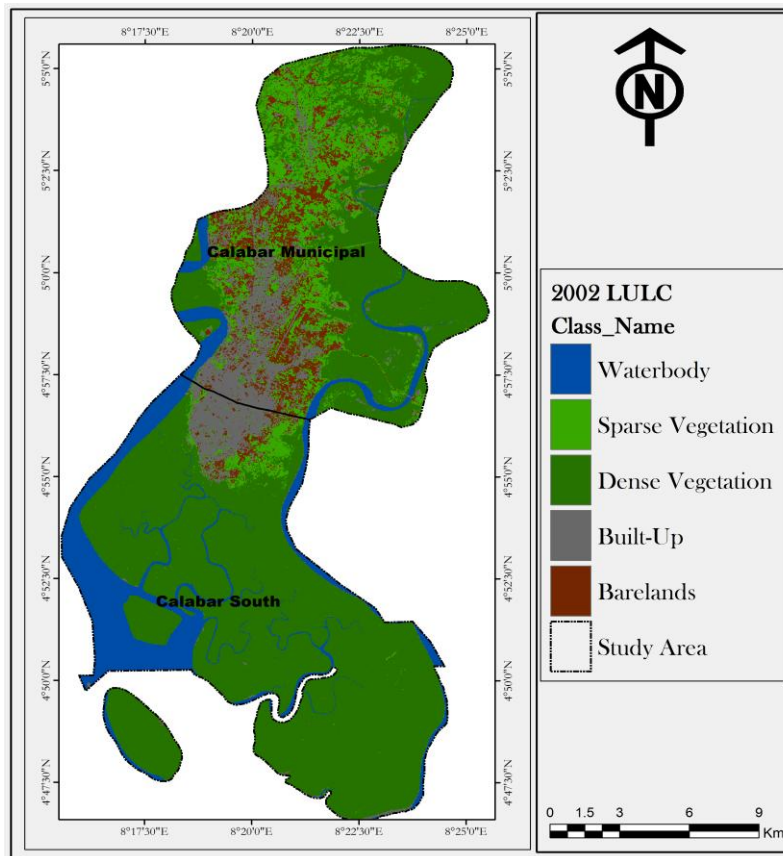

Figure 7a: LULC Map of 2002 Landsat 7 ETM+ image
Source: Authors GIS Analysis

The results of the 2002 classified image reveals that dense vegetation and sparse vegetation LULC class dominated the landscape, with 19861.42 and 3996.47 hectare (ha), representing 61 percent and 12.27 percent of the land area. This was followed by water body covering 3750.3 7 ha (11.52%). Next is the built up area. This covered an area of 2865.19 ha with percentage cov-

erage of 8.80 percent. The LULC class with the lowest percent coverage in 2002 was bareland covering a total area 2084.76 ha (6.40%).
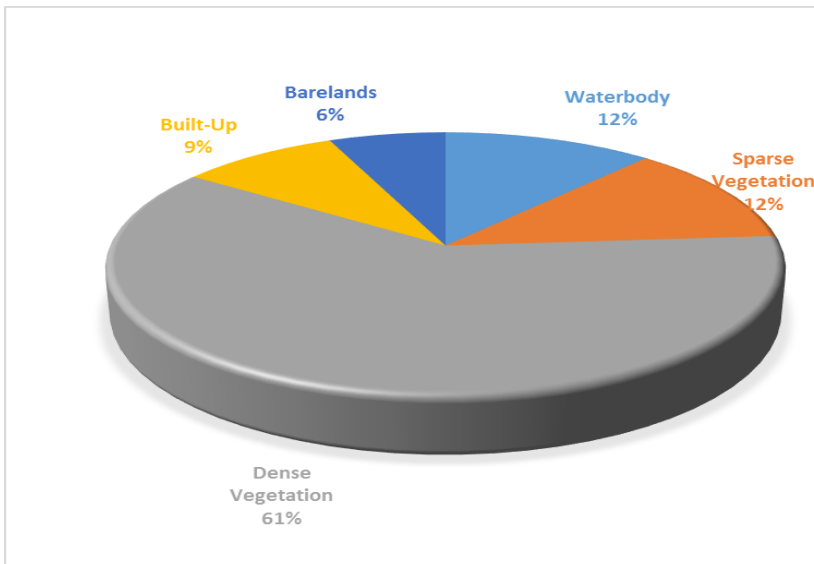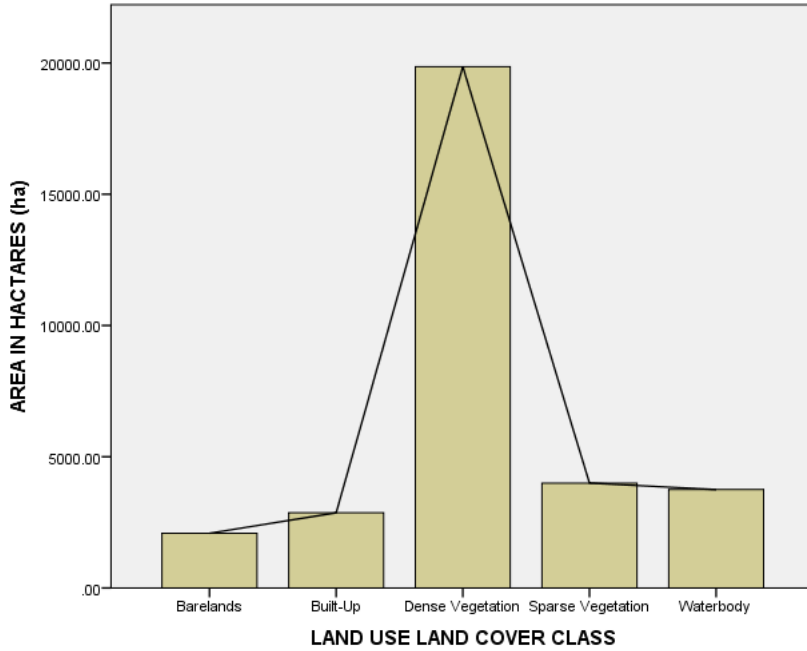

Figure 7b: Pie chart showing Percentage of LULC for 2002
Source: Authors data generated and developed in excel

5.3.3 Analysis of LULC classes for 2006 image

The land use classes in 2006 showed considerable increase in the built up cover with 711.95 ha (3577.14), representing 10.9 percent of the total LULC classes in the area (Table and Figure 8).

Figure8a: LULC Map of 2002 Landsat 7 ETM+ image
Source: Authors GIS Analysis

Based on the result of this study as depicted in figure 8, we also observed a decrease of 2931.71 ha in the area covered by dense vegetation in 2016 compared to the 2002 which covered an area of 52.00 percent. Also, we observed

that the area coverage for barelands decreased by 322.41 ha in 2006 from 2084.76 ha in 2002 to 1762.34 in 2006, covering an area of 5.41 percent.The 322.41 ha of bareland loss between 2002 and 2006 was converted to build up area which accounts to the increase in the built up cover.
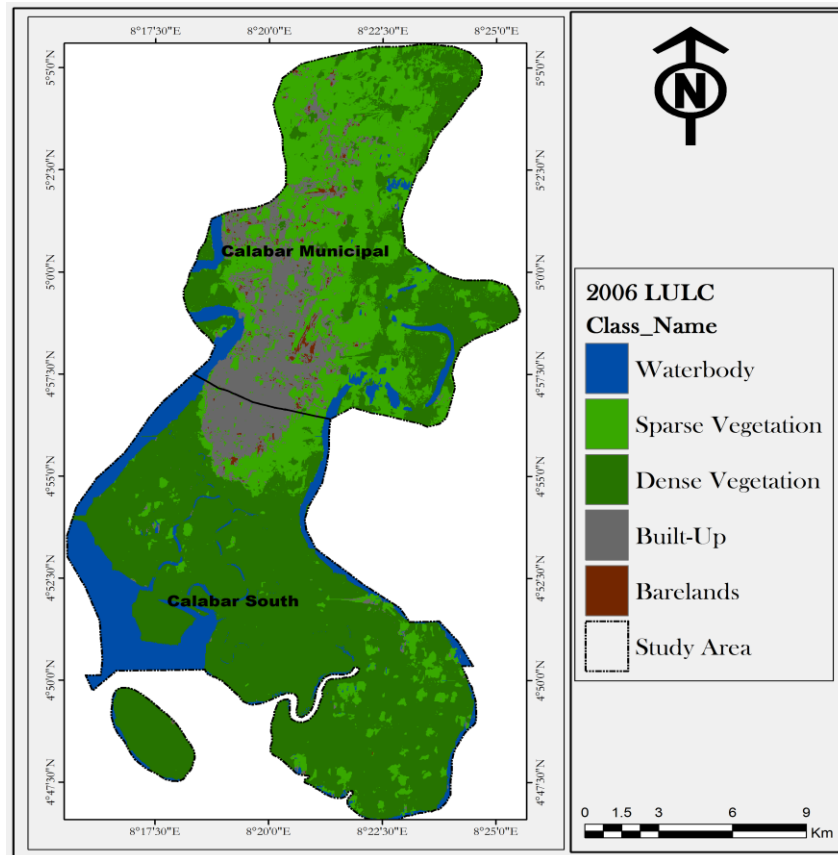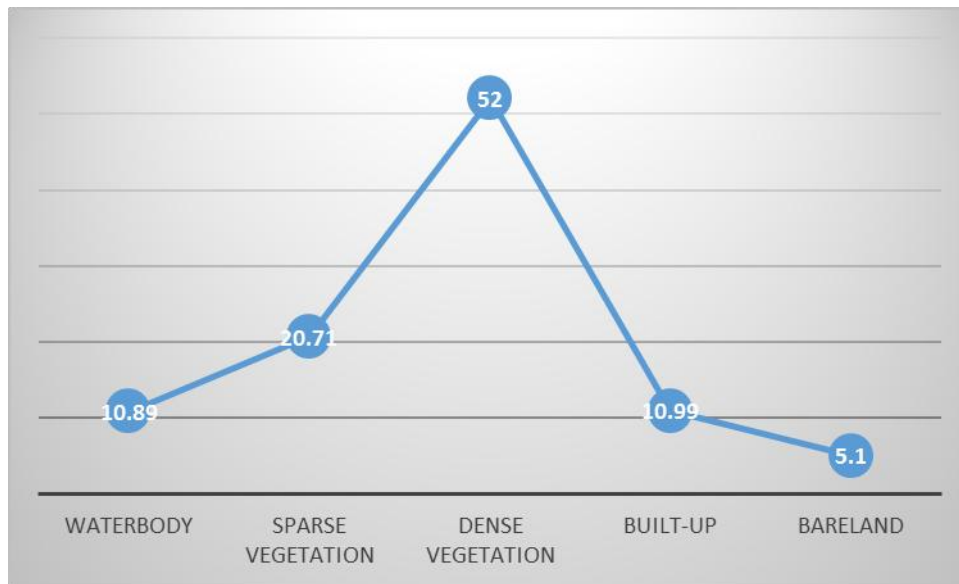

Figure 8b: line graph showing Percentage of LULC for 2006
Source: Authors data generated and developed in excel

Figure 8b displays the percentage of LULC classes in 2006 with dense vegetation having the highest percent cover (52%), this was followed by sparse vegetation with 20.7 percent, built up with 10.99 percent cover. The LULC types with the lowest percent cover in 2006 were water and bareland with 10.89 percent and 5.1 percent respectively with bareland having the least percent cover.

5.3.4 Analysis of LULC classes for 2008 image

The results of this study further revealed that by 2008, the LULC classes have shown considerable change (Figures 9a&b).
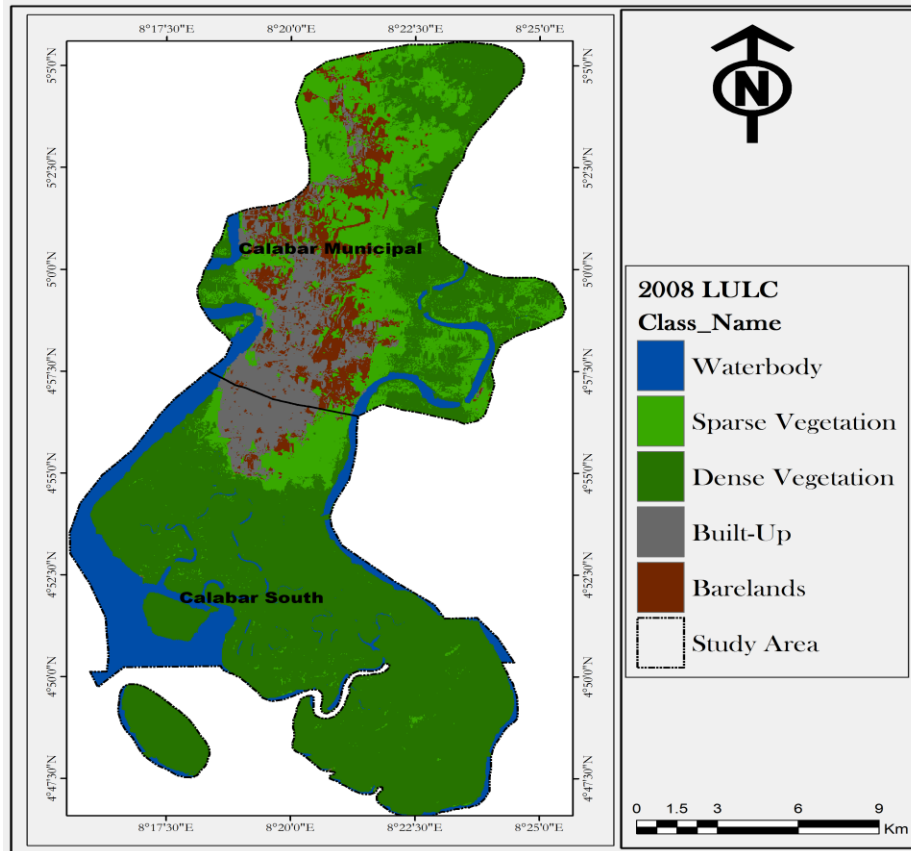
Figure9a: LULC Map of 2008 Landsat 7 ETM+ image
Source: Authors GIS Analysis

As seen in Figure 8a, the total area of dense vegetation cover was 17897.57 ha representing 54.97 percent of the entire Metropolitan LULC. The result revels that there was a decrease in the LULC cover by 1963.85 ha for dense vegetation when compared to the 2002 image (Figure 7a). This deficit in coverage on the dense vegetation led to the increase in certain land areas such as built up area with 3942.37 ha, as well as sparse vegetation, with 5935.43

ha when compared to the 2002 image although the area coverage decreases when compared to the 2006 image, measuring up to about 12.11 percent and 18.23 percent respectively. Bareland LULC class, were identified to be 1035.01 ha representing 3.1 percent of the area coverage. The results of the 2008 image indicates a drastic change in the bareland coverage with a decrease of 1049.75 ha when compared to 2002 image and a decrease of 727.33 ha compared to the 2006 image. Furthermore, water body in that year was 3747.83 ha representing 11.51 percent of the total area. There was an increase in the area coverage of water within this year with a gain of 203.16 ha from 2006 to 2008.

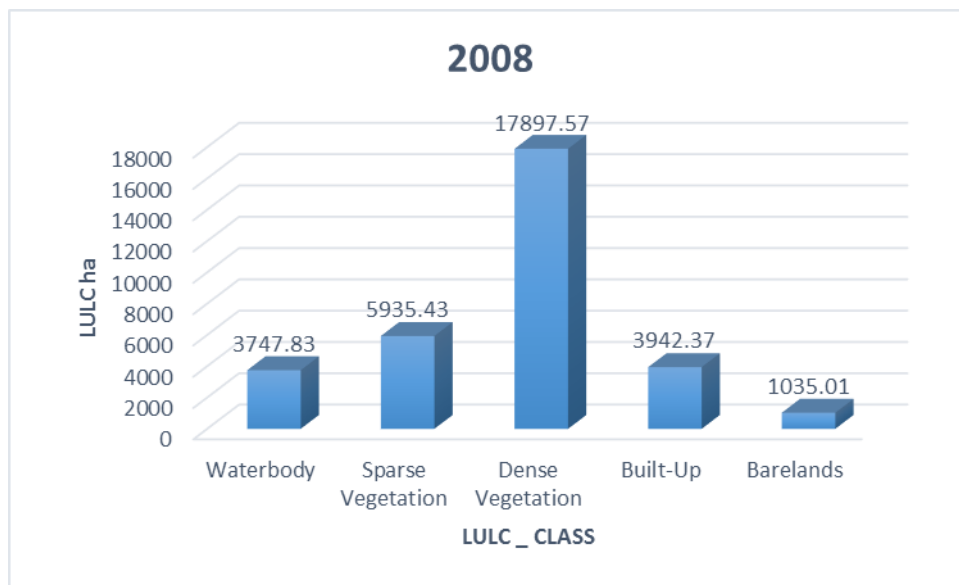*Figure 9.b: Land use land cover classes Area (ha) for 2008*
Source: Authors data generated and developed in excel

Figure 9b displays the area coverage for the different LULC classes identified in 2008. Based on the results of this study, we observed that in 2008 the land use class with the greatest cover was dense vegetation with 54.97 percent cover, followed by sparse vegetation (18.23%), while built –up area and

Barelands had the least cover with 12.11 percent and 3.18 percent respective-ly (Figure8c).
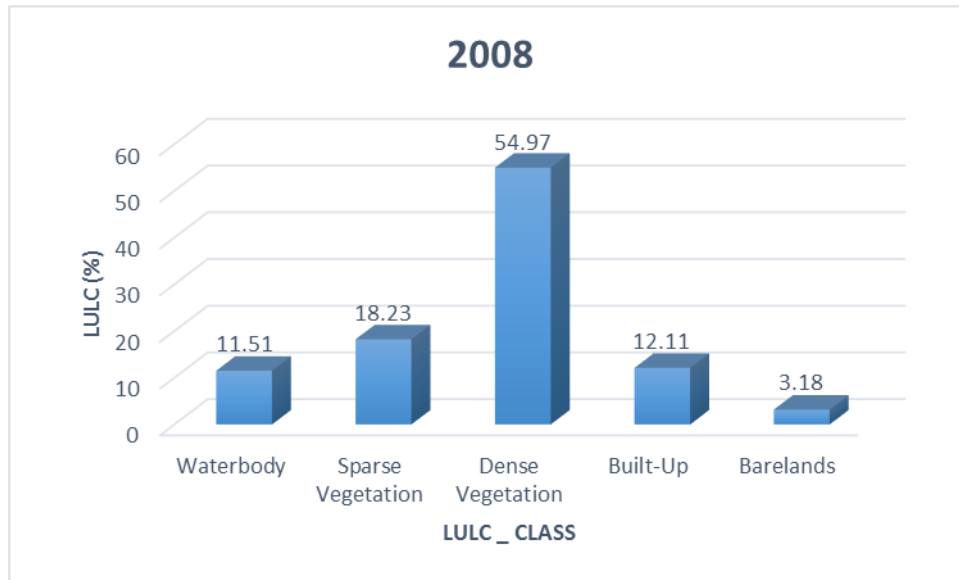
Figure9c: Land use land cover classes Area (ha) for 2008
Source: Authors data generated and developed in excel

5.3.5 Analysis of LULC classes for 2010 image

Figure 10a&b shows that Calabar Metropolis has experienced a substantial level of cover changes in terms of increasing Built up/ bare lands and sparse vegetation. The results revealed that the LULC classes showed some asto-nishing alteration as far as the area coverage of the corresponding land uses was concerned. Dense vegetation cover maintained its high area of coverage with 16560.98 ha, representing 50.87 percent of the total area of land use and covers. Sparse vegetation and built up were also next by area coverage of 6413.92 ha and 4594.32, with 19.70 percent and 14.11 percent respectively. The results further revealed that the area covered by water body was 3468.49 ha representing about (10.65%) of the total area (Figures 10a and b). Al-

though water body showed an increase   by area coverage in other years, the 2010 image indicated a decrease in area.
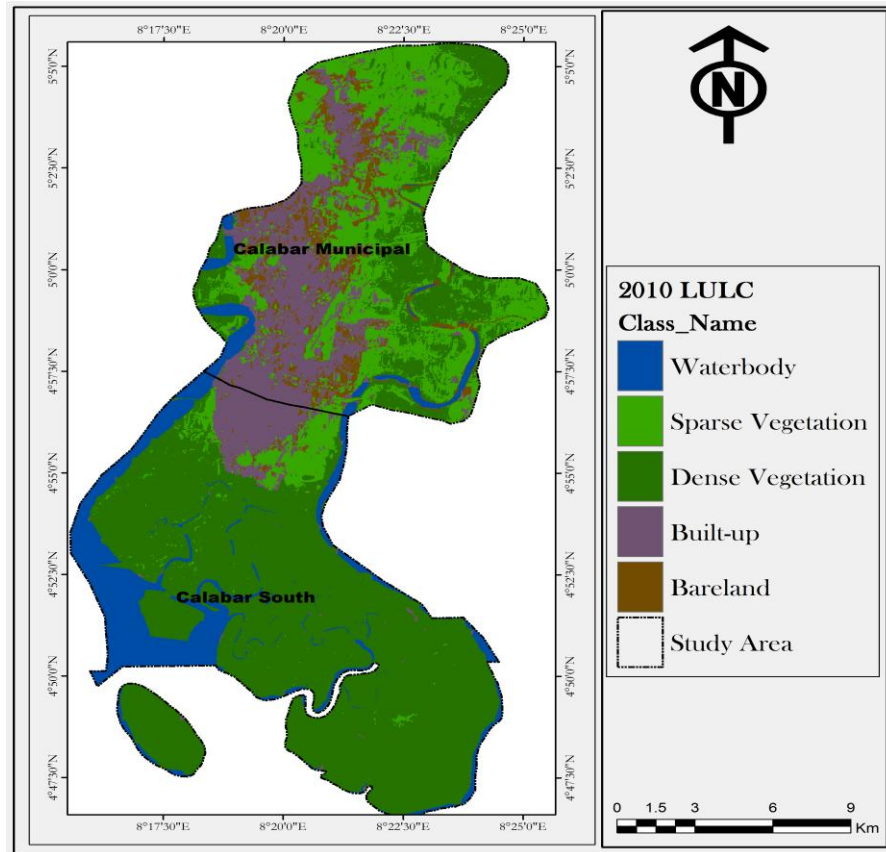
Source: Authors GIS Analysis
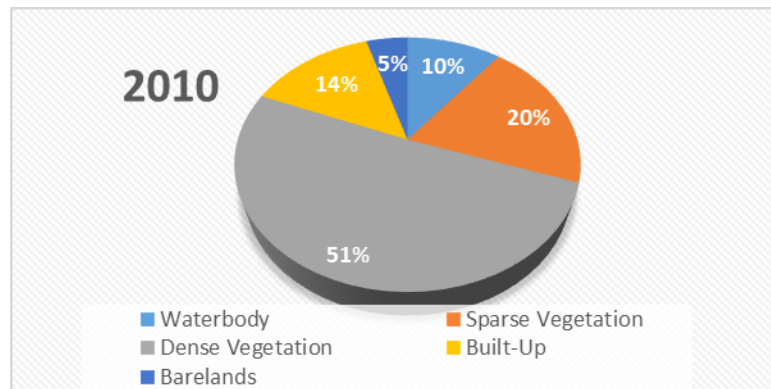
Figure 10b: percentage of land cover types for 2010
    Source: Authors data generated and developed in excel

5.3.5 Analysis of LULC classes for 2012 image

Figure 11 shows the result for the LULC classes for the 2012 image. The results of this study revealed that the built up and bareland classes continued to experience increasing trend compared to the other land use classes although dense vegetation cover continue to maintain its high area of coverage with 17760.39 ha, representing 54.55 percent of the total area of land use and covers. Sparse vegetation was also next by area coverage of 4902.21 with 15.06 percent.
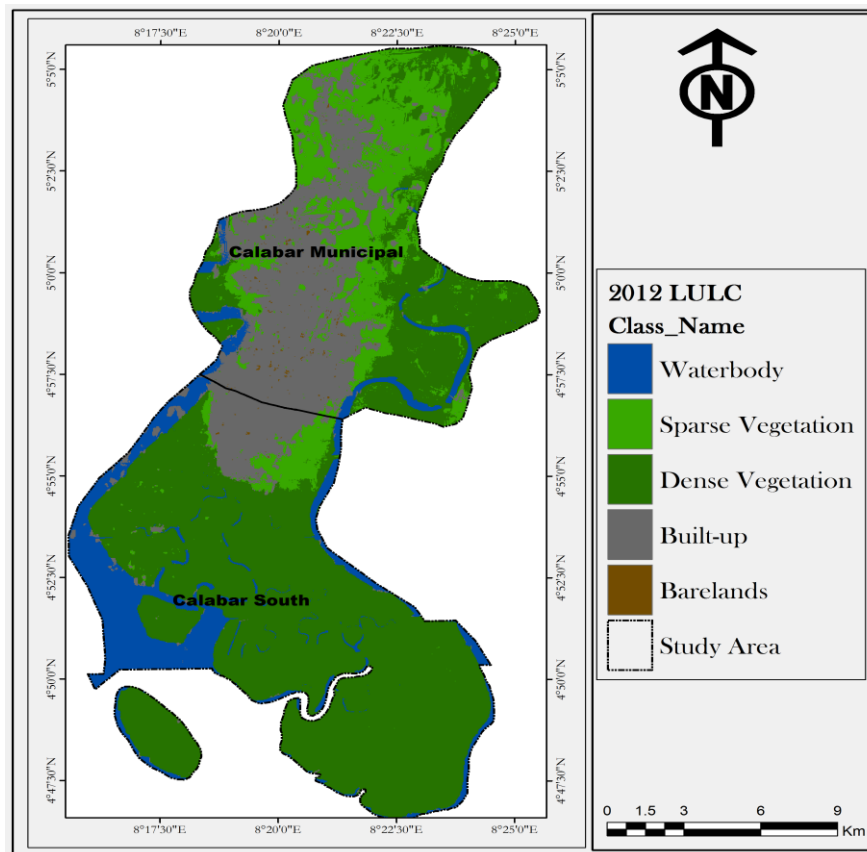
Figure11.a: LULC Map of 2012 Landsat 7 ETM+ image
Source: Authors GIS Analysis

Figure 11b displays the result for the area coverage of the different LULC classes identified in the study area with dense vegetation having the highest area coverage, followed by sparse vegetation with bareland and water body having the least area coverage.

Figure 11.b: Land use land cover classes Area (ha) for 2012
Source: Authors data generated and developed in excel

The results further revealed a very wide margin between dense vegetation and the other LULC identified in the area. Based on the results, the area coverage for the other land uses in 2012 fell below 5000 ha while dense vegetation cover an area of above 1500 ha.

5.3.6 Analysis of LULC classes for 2014 image

The result as derived from the satellite imagery revealed that by 2014, the total area coverage for almost all the land use classes have change completely.

The positive change was noticed in the following LULC classes built up area, barelands, sparse vegetation with 5380.89 ha, 3822.59 ha, 7373.34 ha representing 16.53 percent, 11.74 percent and area coverage, while water body and dense vegetation portrayed a negative change when compared to the base year (2002) (Figure 7a and 12a). The results revealed that despite its negative change, built up area still maintained its high area coverage with 12395.95 ha representing 38.07 percent. Water both showed just a small per-cent increase.
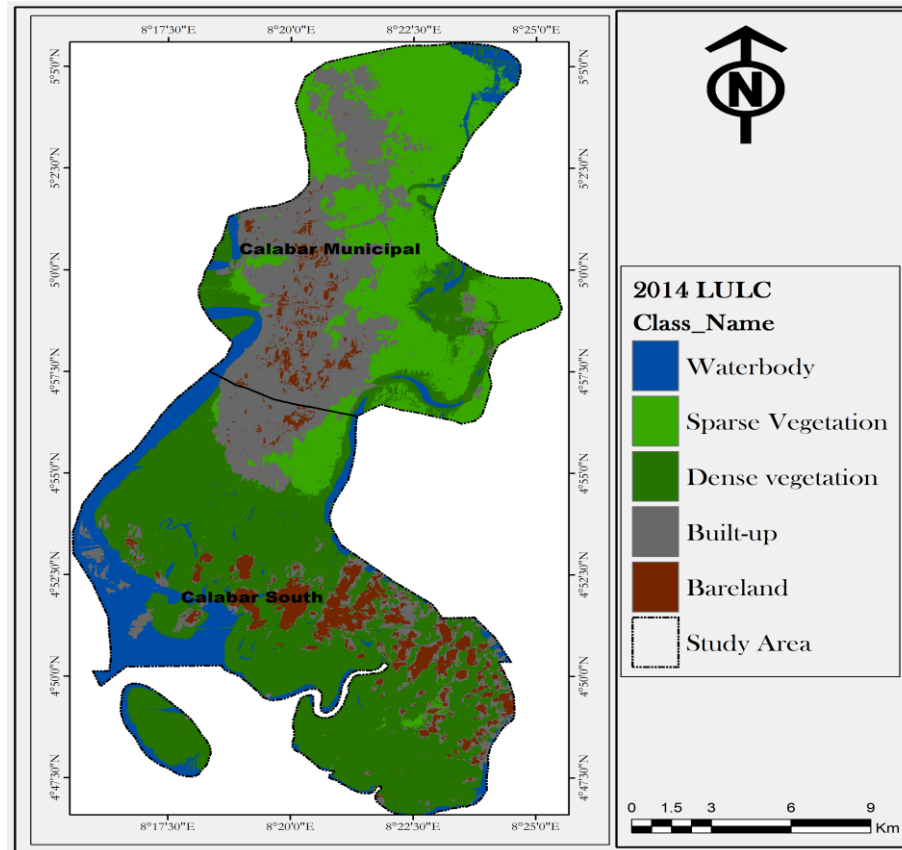
Figure12.a: LULC Map of 2014 Landsat 7 ETM+ image
Source: Authors GIS Analysis

Figure 12b displays the area coverage for the five land use land cover classes identified in the study area.

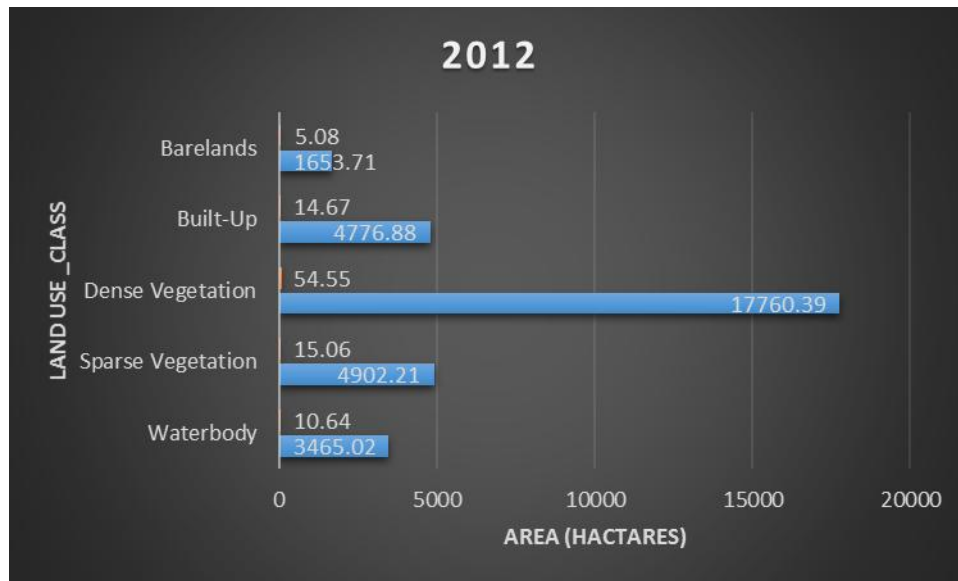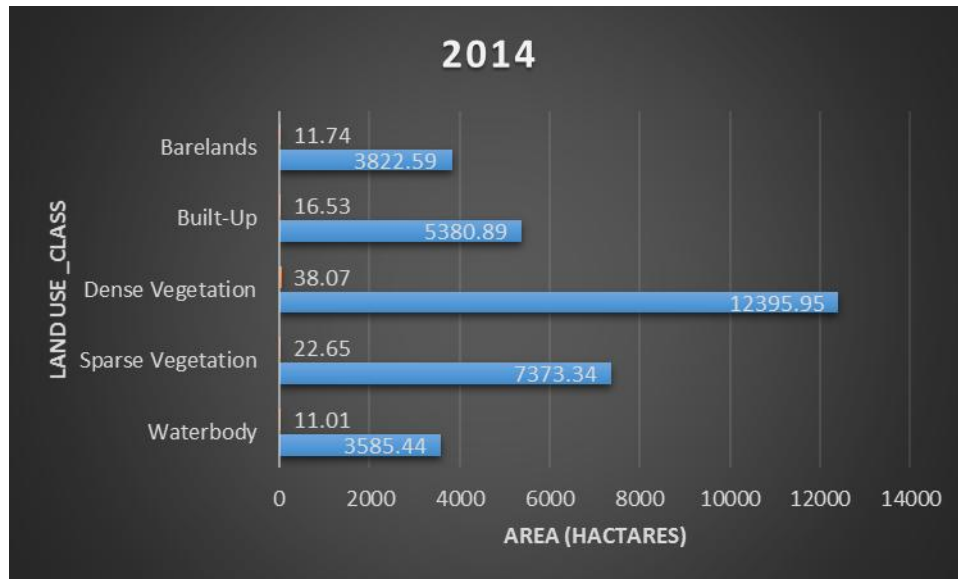*Figure 12.b: Land use land cover classes Area (ha) for 2014*
Source: Authors data generated and developed in excel

Based on our results as depicted in Figure 12b, built up area had the highest area coverage. This was followed by sparse vegetation while water body and barelands had the lowest area coverage. Furthermore, this year recorded the highest percent drop in its dense vegetated cover compared to other years. Sparse vegetation cover witnessed a tremendous increase in its cover compared to 2014 with its area coverage exceeding 6000 ha.

5.3.6 Analysis of LULC classes for 2016 image

By 2016, all the LULC class continue to experience dramatic changes area coverage. This change was twofold (positive and negative) with built up and sparse vegetation and water body having a positive change while dense vege-

tation and bareland showed a negative change in their area coverage. The results further revealed that despite the dramatic negative change in the dense vegetation cover it still maintained its high area of coverage with   16629.85 ha, representing 51.08 percent of the total area of land use and covers.
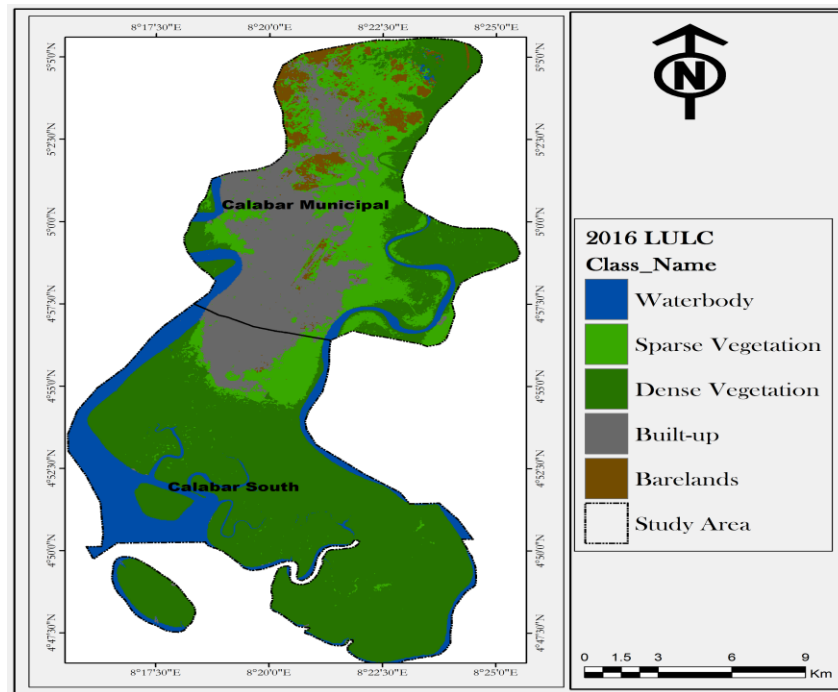
Figure13.a: LULC Map of 2016 Landsat 8 **OLI** *image*
Source: Authors GIS Analysis

Table3: Area coverage (ha) of land cover types for 2016

	2016	
Class_name	Area	%
Waterbody	3934.65	12.08
Sparse Vegetation	5262.53	16.16
Dense Vegetation	16629.85	51.08
Built-Up	5680.81	17.45
Barelands	1050.37	3.23
	32558.21	

Source: Authors data generated and developed in excel

5.6 Change Trends of LULC Classes between 2002 and 2016

Table 4 shows the overall data for the LULC changes trend from 2002 to 2016**.** Throughout this period, there was a corresponding increase in the other land uses particularly built up area, sparse vegetation, as well as water body, up to 2016. The combined data of LULC in terms of area in hectares are displayed in Table4.

Table 4: combined Table of Area Data in Hectares

	2002		2006		2008		2010		2012		2014		2016	
Class_name	Area	%	Area	%	Area	%	Area	%	Area	%	Area	%	Area	%
Waterbody	3750.37	11.52	3544.67	10.89	3747.83	11.51	3468.49	10.65	3465.02	10.64	3585.44	11.01	3934.65	12.08
Sparse Vegetation	3996.47	12.27	6744.36	20.71	5935.43	18.23	6413.92	19.70	4902.21	15.06	7373.34	22.65	5262.53	16.16
Dense Vegetation	19861.42	61.00	16929.7	52.00	17897.57	54.97	16560.98	50.87	17760.39	54.55	12395.95	38.07	16629.85	51.08
Built-Up	2865.19	8.80	3577.14	10.99	3942.37	12.11	4594.32	14.11	4776.88	14.67	5380.89	16.53	5680.81	17.45
Barelands	2084.76	6.40	1762.34	5.41	1035.01	3.18	1520.5	4.67	1653.71	5.08	3822.59	11.74	1050.37	3.23
	32558.21		32558.21		32558.21		32558.21		32558.21		32558.21		32558.21	

Source: Authors data generated and developed in excel

Conversely, between 2002 and 2006, a period of 4 years, we observed that all other land uses reduced in their area converge apart from built up area and sparse vegetation. Between 2002 and 2008, built up, sparse vegetation and water body land uses and covers, increased slightly in growth as the area Figure portrays. Nevertheless, by 2010, built up and sparse vegetation increases in terms of area coverage while dense vegetation, barelands water body also reduced in area (Figure 15a). Furthermore, between 2010 and 2014, Built up bare soils and concrete surfaces reduced; while low to dense forest covers increased appreciably (see analysis of respective area changes).

Figure 15a displays the area coverage in hectares of the different LULC classes for the years understudy. The study revealed dense vegetation to be the land use _ class with the highest area coverage for all the years.
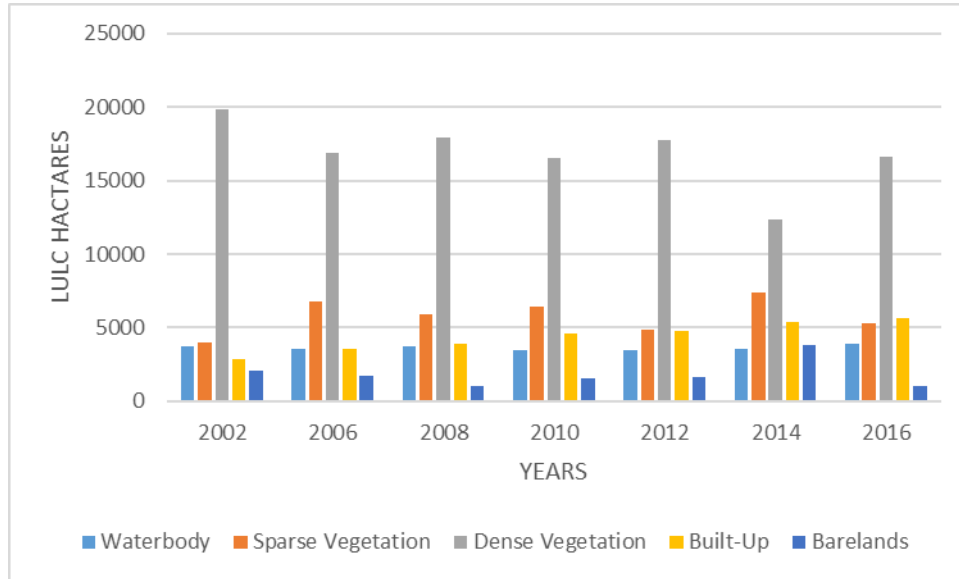
Figure 15a: combined LULC class per year
Source: Authors data generated and developed in excel

5.6 .1 Change Trends of the LULC Classes from 2002 to 2006

Trend analysis of LULC class displays the direction in which the various classes are heading to when compared with the base year which is their corresponding initial years. The results of this study revealed that between 2002 and 2006, dense vegetation and barelands reduced substantially by 2931.72 ha and 322.42 ha, sparse vegetation increased by 2747.89 ha, while built up also increased by 711.95 ha. Water body also receded its shorelines by ha. We also observed that over the four year period dense vegetation was the only land use class that reduced drastically by 205.7 ha (Table 5 and Figure 15b).

Table 5: Change Trends of the LULC Classes from 2002 to 2006

Class_name	Area (ha)	Percent change
Water body	-205.7	-5.48
Sparse Vegetation	2747.89	68.78
Dense Vegetation	-2931.72	-14.76
Built-Up	711.95	24.85
Barelands	-322.42	-15.47

Figure 15b: Change Trends of LULC Classes from 2002 to 2006

Table 5 displays the changing trend in the LULC from 2002 to 2006. The result revealed that within this period water body drop by 5.84 percent in its area coverage, dense vegetation and barelands also decreased by (14.76%) and 15.47 whereas sparse vegetation and built up recorded an increase in

their area coverage by 68.78 percent and 24.85 percent respectively. The highest negative for this time period was observed in the bareland class

5.6.2 Change Trends LULC Classes from 2006 to 2008

Furthermore, the LULC trends from 2006 to 2008 indicates dense vegetation increased by 967.87 ha with 5.72 percent change, while built up also increased by 365.23 ha with 10.21 percent change. We also observed that within this timeframe the area coverage for sparse vegetation and bareland decreased by 11.99 percent and 41.27 percent respectively; whereas water body slightly increase its shores 5.73 percent   (Table 6 figure 15c).

Table 6: Change Trends of the LULC Classes from 2006 to 2008

Class_name	Area (ha)	Percent change
Water body	203.16	5.73
Sparse Vegetation	-808.93	-11.99
Dense Vegetation	967.87	5.72
Built-Up	365.23	10.21
Barelands	-727.33	-41.27

Figure 15c: LULC percent change between 2006 and 2008
Source: Authors data generated and developed in excel

5.6.3 Change Trends of LULC Classes from 2008 to 2010

By 2010 from 2008, the results reals that dense vegetation cover reduced tremendously from the initial increasing trend since 2008, to a substantial decrease by 1336.59 ha. Barelands showed an increase of 485.49 ha, while the water body decreased by 7.4 percent which is 279.34 ha (Table 7and Figure 15d). The result as displayed in Figure 15d also revealed a positive change in the built up cover by 16.53 percent.

Table 6: Change Trends of LULC Classes from 2008 to 2010

Class_name	Area (ha)	Percent change
Water body	279.34	-7.45
Sparse Vegetation	478.49	8.40
Dense Vegetation	-1336.59	-7.47
Built-Up	651.95	16.53
Barelands	485.49	46.91

Source: Authors data generated and developed in excel

Figure 15d: LULC percent change from 2008 to 2010
Source: Authors data generated and developed in excel

5.6.4: Change Trends of LULC Classes from 2010 to 2012

The results further revealed that by 2012 from 2010, sparse vegetation cover reduced tremendously from the initial increasing trend since 2008, to a substantial decrease by 1511.71 ha whereas there was an increase in the dense vegetation cover by 1199.41 ha. Also, Barelands showed an increase by 133.21 ha, while water body decreased by -0.1 percent which is 3.47 ha. The result also revealed a positive change in the built up and bareland cover by 182.56 ha (Table 7and Figure 15e).

Table 7: Change Trends of LULC Classes from 2010 to 2012

Class_name	Area (ha)	Percent change
Water body	-3.47	-0.1
Sparse Vegetation	-1511.71	-23.57
Dense Vegetation	1199.41	7.24
Built-Up	182.56	3.97
Barelands	133.21	8.76

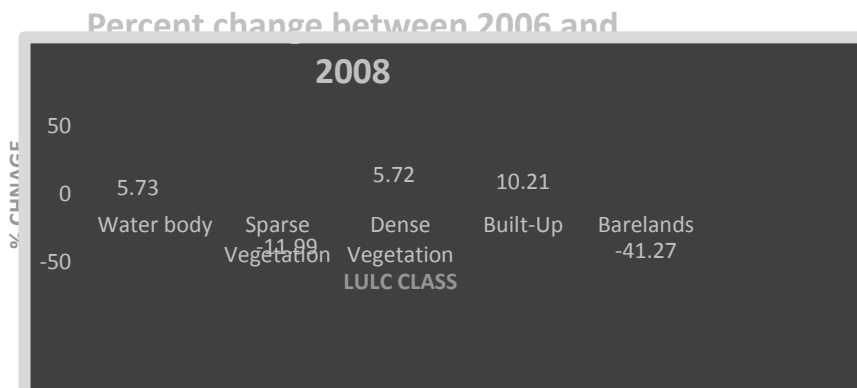*Source: Authors data generated and developed in excel*
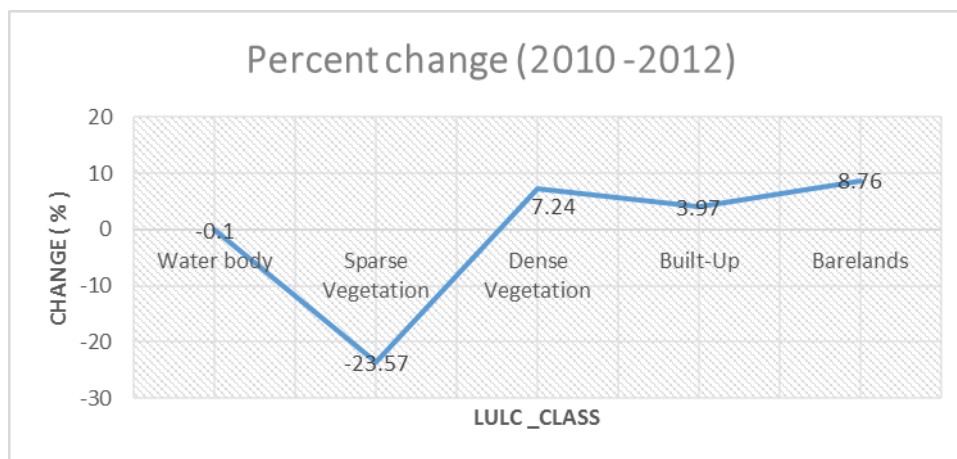
Figure 15d: LULC percent change from 2010 to 2012
Source: Authors data generated and developed in excel

5.6.4b Change Trends of LULC Classes from 2012 to 2014

Furthermore, by 2014 from 2012, there was a drastic increase in the sparse vegetation cover by 50.41 percent whereas built up was rank third in terms of percent increase by 12.64 (604.01 ha). Within this period bareland class increased tremendously by 2168.88 ha (131.15 %) while dense vegetation cover decreased by 5364.44 ha. Also, water body showed an increase by 120.42 (Table 8 and Figure 15e). The result also displayed that all the apart from dense vegetation observed an increasing trend from 2012 to 2014.

Table 8: Change Trends of LULC Classes from 2012 to 2014

Class_name	Area (ha)	Percent change
Water body	120.42	3.48
Sparse Vegetation	2471.13	50.41
Dense Vegetation	-5364.44	-30.20
Built-Up	604.01	12.64
Barelands	2168.88	131.15

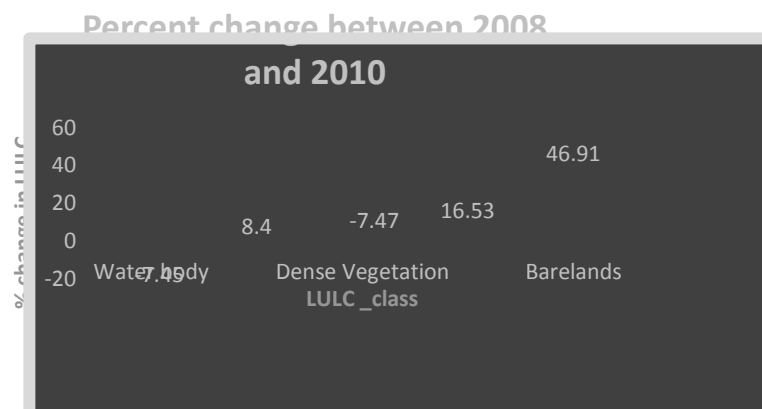*Source: Authors data generated and developed in excel*
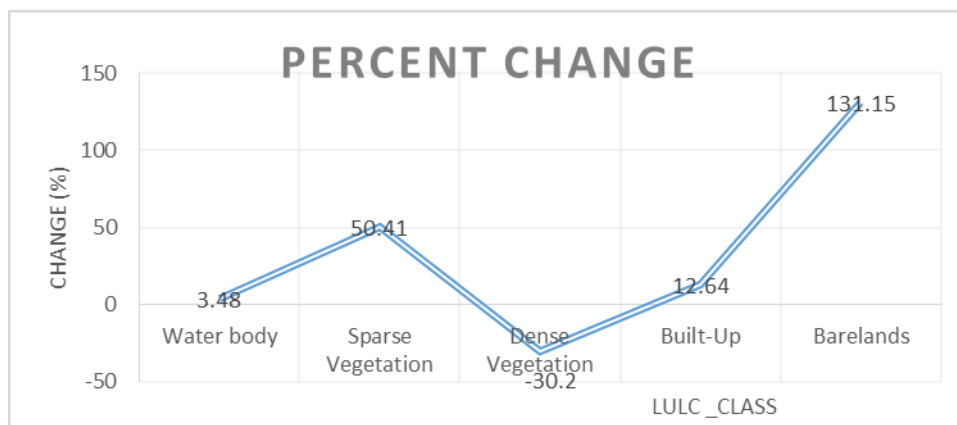
Figure 15e: LULC percent change from 20012 to 2014
Source: Authors data generated and developed in excel

5.6.5 Change Trends of LULC Classes from 2002 to 2016

The LULC classes by the year 2016 have assumed different dimensions of change from the sizes of their previous sizes in comparison to their current sizes (Table 9 and Figure 16) with some having positive change while others had negative change within the study period (2002 to 2016).

Table 9: Change Trends of LULC Classes from 2002 to 2016

Class_name	2002-2006	2006-2008	2008-2010	2010-2012	2012-2014	2014 – 2016
Water body	-205.7	203.16	279.34	-3.47	120.42	349.21
Sparse Ve-getation	2747.89	-808.9	478.49	-1512	2471.1	-2110.8
Dense Vege-tation	-2931.72	967.87	-1337	1199.4	-5364	4233.9
Built-Up	711.95	365.23	651.95	182.56	604.01	299.96
Barelands	-322.42	-727.3	485.49	133.21	2168.9	-2772.2

Source: Authors data generated and developed in excel
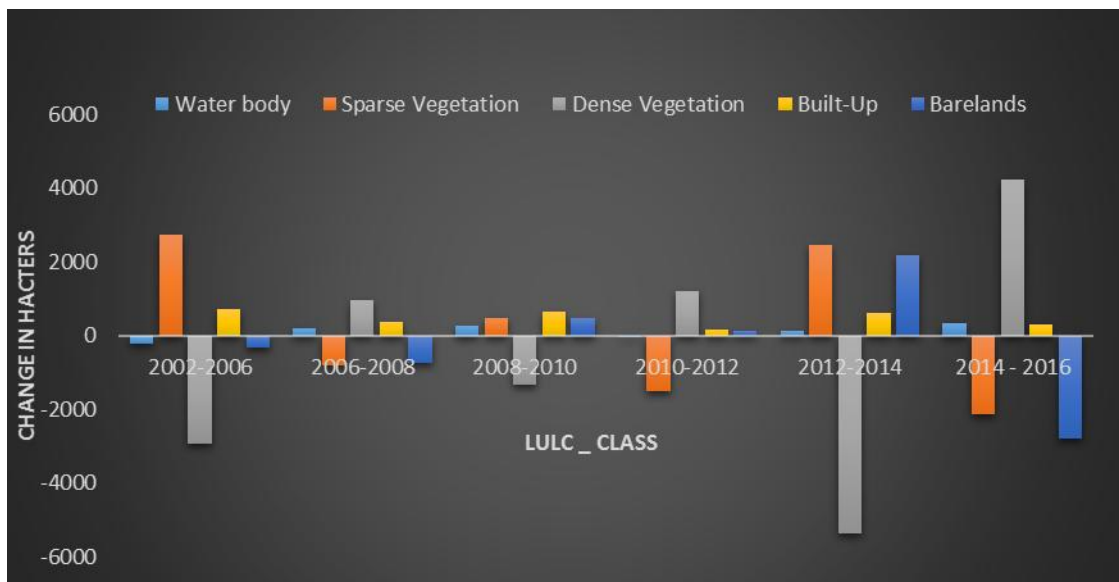
Figure 16: Change Trends of LULC Classes from 2002 to 2016
Source: Authors data generated and developed in excel

Figure 16 and Table 8 displays the changing trend in the LULC for the years understudy. The result as displayed in Figure 16 reveals that during the study period (2002 to 2008, 2008 to 2010, 2010 to 2012, 2012 to 2014 and 2014 to 2016), sparse vegetation experienced a negative trend from 2002 to 2006. By 2008, from 2006 to 2008, there was a gain in the area extent for sparse vegetation which was further loss to other LULC classes by 2010. 2012 showed a slight increase in the dense vegetation cover.

By 2016, a greater proportion of the dense vegetation cover (9.92%) of what was obtained in 2002 was loss to other land use classes. Built up maintained continues increasing trend from 2002 to 2016. Water body also maintained an increasing trend with a slightly negative change from 2010 to 2012. Among all the LULC bareland was the land use class with the second largest

The results further demonstrates that Comparison between the two image (2002 and 2016) shows that the built - up area has increased from 8.8 percent 2002 to 17.45 percent 2016, whereas, densely vegetated area has decreased from being 61 percent in 2002 to 51.08 percent of the total area in 2016 with percentage changes of -9.92 percent respectively . On the other hand water body and barelands are the land use with the smallest area coverage with 0.56 percent increase in the surface area for water body from 2002 to 2016 and a reduction in the area coverage for bareland by 3.17 percent from 2002 to 2016. Built up area on the other hand increased by 8.67 percent (Table 10 and Figure 16).

Table 10: LULC percent cover and change from 2002 to 2016

	2002	2016	% change
Class_name	%	%	
Waterbody	11.52	12.08	0.56
Sparse Vegetation	12.27	16.16	3.89
Dense Vegetation	61	51.08	-9.92
Built-Up	8.8	17.45	8.67
Barelands	6.4	3.23	-3.17

Source: Authors data generated and developed in excel
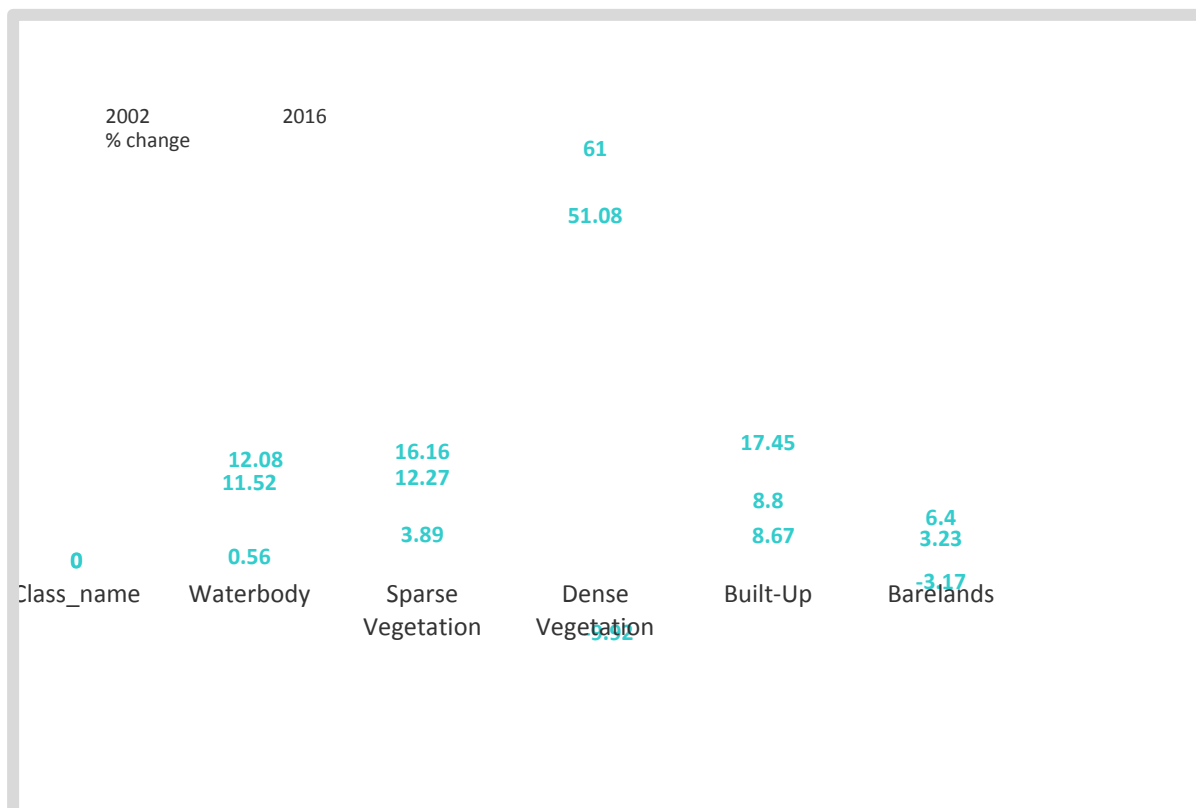
Figure 16:   percentage change in the LULC (2002 to 2016)
Source: Authors data generated and developed in excel

5.7 RESULT PRESENATION OF OBJECTIVE VI "Projection of Future Land Use Land Cover Change (Three Decades)"

A first order Markov analysis was used to develop LULC change matrices for the analysis of the rates of land use type conversions from one land use class type to another type and, between the various years' intervals of analysis. These were the co-transitions occurring between 2001 and 2006 (4yrs.); 2006 and 2008 (2yrs.); 2008 and 2010 (2yrs.) 2010 and 2012 (2yrs); 2012 to 2014(2yrs) well as between 2014 and 2016 (2yrs). The various LULC transitions have been presented in the transition matrices in table 11.

The analysis of the results from the image years between 2002 and 2016 LULC types as were cross-tabulated for their transitional matrix shows that the land use classes transited from one type to another according to some degree of proportions. Table 11, indicates that there are area in hectare of LULC types that remained without any conversions of class. The result revealed that most LULC conversion occurring within this period is the conversion of sparse vegetation into built up with a total conversion area of 2260.10 ha. As seen in Table 11, there was a significant increase in built up, barelands. This was gained from the conversion of sparse vegetation to bareland by 1191.1 ha. Also, 228.23 ha of land was converted from bareland to build- up area while 2260.10 ha of land was converted from sparse vegetation to built-up area. Also, within this period 369.24 ha area that was heavily vegetated became sparsely vegetated .Another transition that occurred was from dense vegetation to bareland and sparse vegetation by 148.41 ha and369.24 ha respectively. The result also revealed that 77.15 ha of dense vegetation was tran-

sited to water body. Less than 1 ha of area occupied by built up cover was transited to water body within this time period

Table 11: Land use class Transition from 2002 to 2016

Class_Name	Area (Hectare)
built-up to built-up	2873.76970535000
bareland to built-up	228.22733313000
sparse vegetation to built-up	2260.10495877000
dense vegetation to built-up	532.05034010800
waterbody to built-up	5.80299404348
builtup to bareland	244.75807478100
bareland to bareland	152.33016858600
sparse vegetation to bareland	1191.11323406000
dense vegetation to bareland	148.40595112400
built-up to sparse vegetation	33.62962588100
bareland to sparse vegetation	7.34913050625
sparse vegetation to sparse vegetation	643.56275427600
dense vegetation to sparse vegetation	369.24252234800
water body to sparse vegetation	0.26487581972
built-up to dense vegetation	64.63211204680
bareland to dense vegetation	7.75721212261
sparse vegetation to dense vegetation	579.78411779300
dense vegetation to dense vegetation	18958.68358030000
water body to dense vegetation	870.38439540800
built-up to water body	0.89109325871
dense vegetation to water body	77.14613103860
water body to water body	3254.35585815000

Source: Authors data generated and developed in excel

From table 9 the result further revealed that the highest rate of transition within this period was from all the other land use / cover type to built-up area with the highest area coverage, this was followed by the transition from dense vegetation to sparse vegetation. Conversion from sparse vegetation to bareland was among the least. During this same period, a proportion of 64.63 ha of Built up, were converted into dense vegetation.
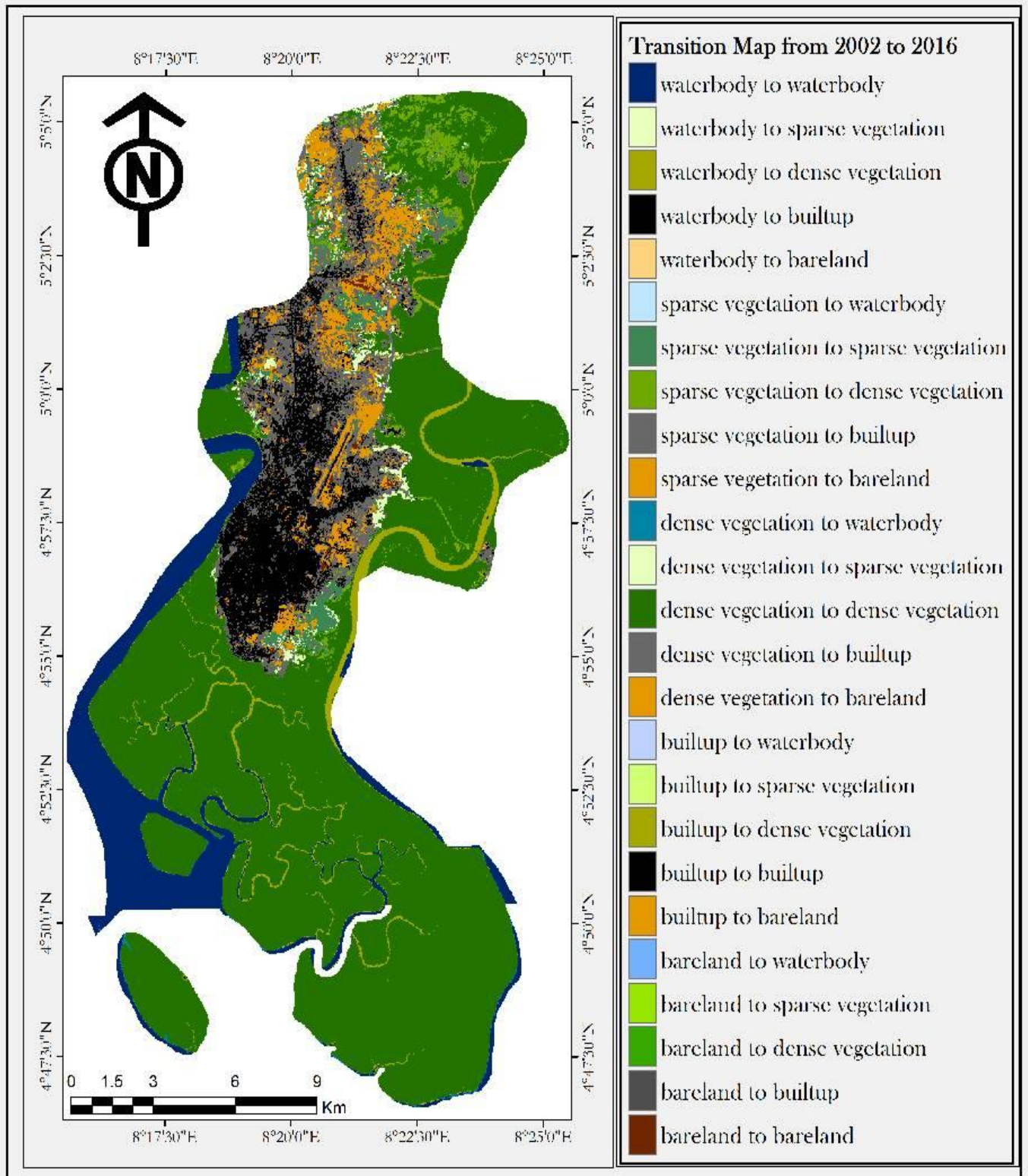
Figure 17: land use transition map from 2002 to 20016 for Calabar Metropolis
Source: Authors GIS Analysis

5.8 RESULT PRESENATION OF OBJECTIVE 6 *"Projection of Future Land Use Land Cover Change (Three Decades)"*

Another objective of this study is to predict the trends of land use change in 2046 (three decades from 2016).The analysis of land cover changes occurring between 2002 and 2016 indicated that throughout Calabar Metropolitan area built – up land have increased by 2515.70 ha or approximately 87.80 percentage (Table 12). Urban area had mostly increased by encroaching on cropland and to a lesser extent on dense vegetation (Figure 18) according to the result of CA –Markov urban growth model.
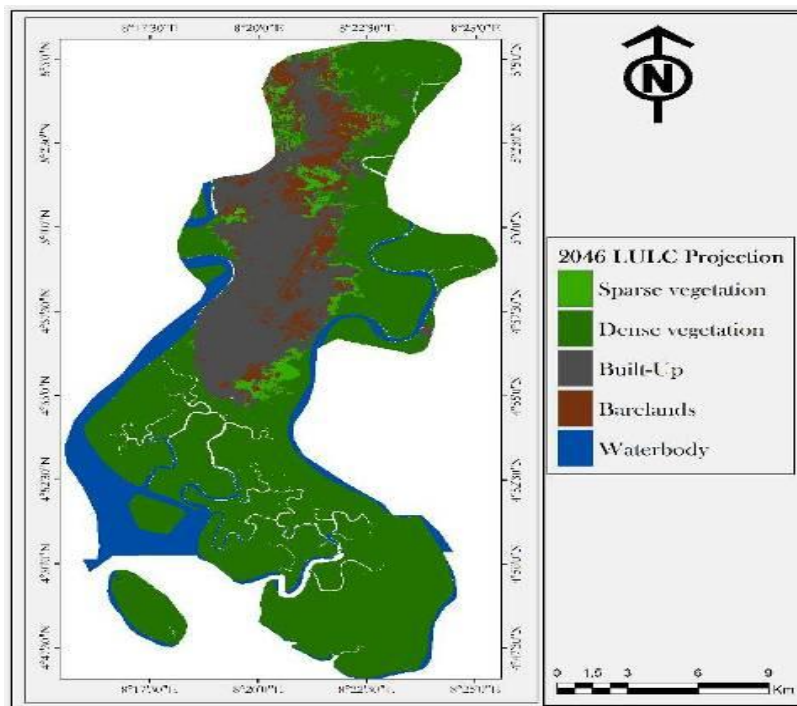
Figure18: Projected land cover classification of the study area in 2046
Source: Authors GIS Analysis

Table 12: land use Probability based on Markov Transition estimation in the period of 2016 -2046

	2016	%	2046	%	% change
Class_name	Area (ha)	Area (%)	Area (ha)	Area	Area (%)
Waterbody	3934.65	12.08	4270.52	13.22	8.54
Sparse Vegeta-tion	5262.53	16.16	1049.93	3.22	-80.0 5
Dense Vegeta-tion	16629.85	51.08	19603.57	60.21	17.88
Built-Up	5380.89	17.45	5916.53	18.17	9.95
Barelands	1050.37	3.25	1717.66	5.28	63.53
	32558.21		32558.21		
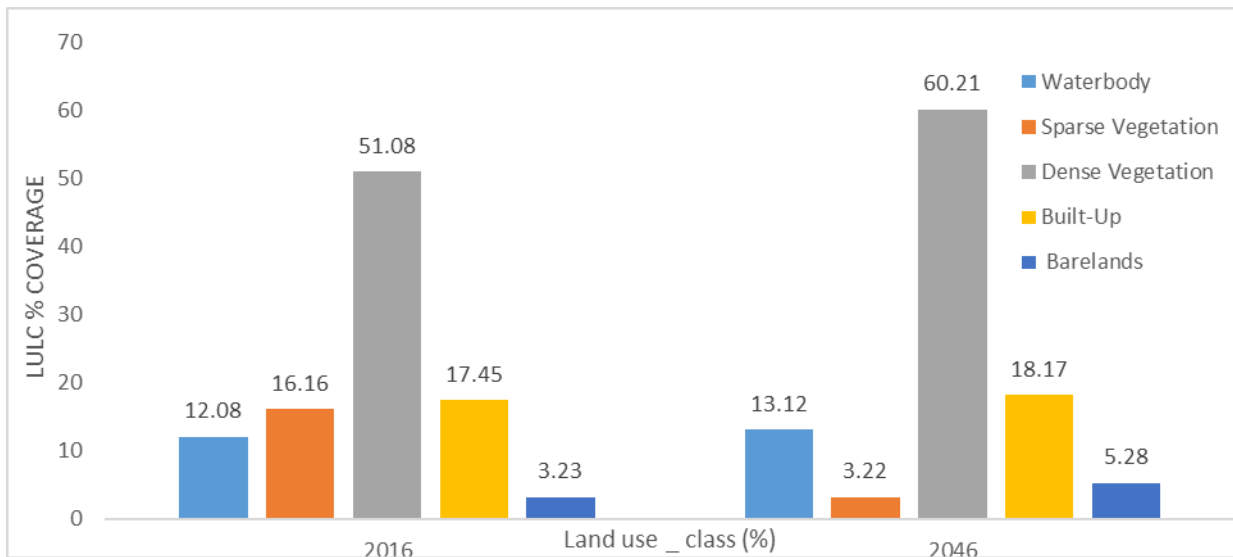
Figure 19: Bar graph showing % of Land use _ class in2016 and projected 2046

Figure 19 displays the projected 2046 LULC status for Calabar Metropolitan Area (Calabar South and Calabar Municipality). The built- up area is expected to increase by 535.64 hectares, approximately 9.95 percentage from 2016 to 2046 (Figure 19 and Table 12). Also, based on the findings of this study, the percentage of dense vegetation is expected to increase as projected

to 60.21percent as compared to 51. 08 percent which was obtained in 2016 (Table 12 and Figure 19) with an increase of 17.88 percent (Figure 20).
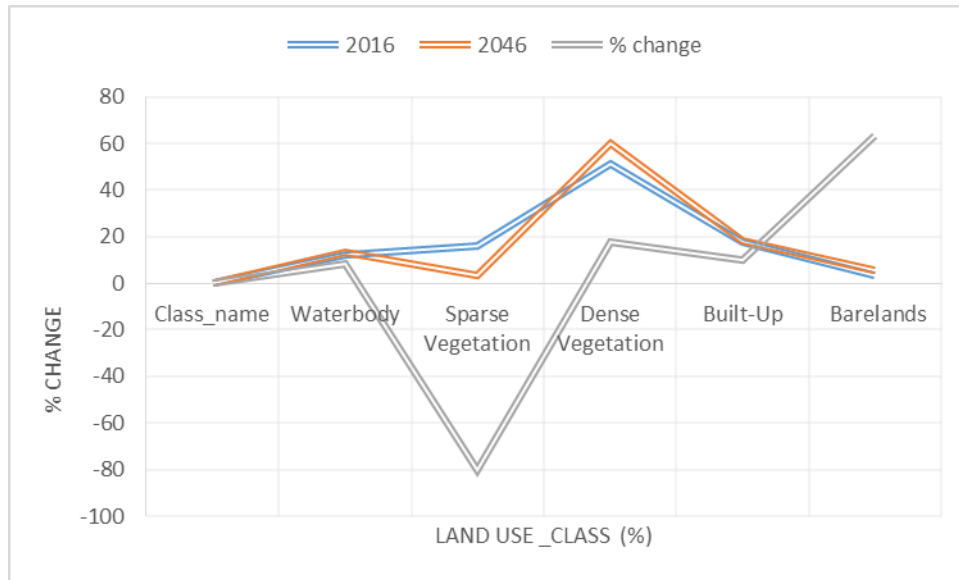
Figure 20: Line graph showing % of Land use _ class in2016, projected 2046 and percent change

Figure 20 shows the projected percentage Change of land use   classes in the study area during 2016 – 2046. Based on the findings of this study as displayed in figure 20, we observed that there is a probability that 80.05 percent of the total area occupied by sparse vegetation (about 4212.63 ha out of the total 5380.89 ha occupied in 2016) as projected will be loss to other land uses thus resulting to a decrease in the area coverage by 2046. Also, 17.88 percent of the area occupied by sparse vegetation will be converted to denser vegetation by 2046 which in turn will result to increase in the area covered by dense vegetation. Furthermore, the percentage of bareland has also been projected to increase by 63.53 percent from 2016 to 2046 while there will be a slight change in the area occupied by water.

5.9 RESULT PRESENATION OF OBJECTIVE 2 *"TO DETERMINE LST IN CALABAR METROPOLIS (2002- 2016)"*

6. 9.1 Spatiotemporal Distribution of LST

Based on the LST retrieval algorithm mentioned earlier, 15yeas land surface temperature maps were generated to measure the magnitude and to quantify LST spatially explicit over the whole study area. In order to display the LST map clearly, the density slice function in ArcGIS was used to distinguish the LST zones by different colors. The UHI over Calabar metropolis were studied from the analysis of Landsat images during the investigated years (2002 to 2016). The results of the LST imagery were classified using standard deviation. Figure 21 to27 and Table displays the LST result for the different land use classes identified in the Study area within the study period.

Table 13: LST change status of Calabar Metropolis (2002 – 2016)

	2002	2006	2008	2010	2012	2014	2016
Class_name	LST (^{O}C)	LST (^{O}C)	LST (^{O}C)	LST (^{O}C)	LST (^{O}C)	LST (^{O}C)	LST (^{O}C)
Waterbody	20.71	18.74	18.92	14.19	21.12	17.64	22.26
Sparse Vegetation	24.27	22.68	23.23	17.71	24.16	21.76	24.80
Dense Vegetation	22.40	20.63	21.13	15.70	22.64	19.70	23.72
Built-Up	31.40	30.13	32.14	24.77	30.25	30.00	29.13
Barelands	27.84	26.60	27.74	21.24	27.20	25.88	26.97

Table 13 shows the descriptive statistics of mean LST for the different LULC class identified in the study as extracted from the satellite derived imagery (Figure 21 to 27), over Calabar Metropolitan area within the seven years period

(2002, 2006, 2008, 2010, 2012, 2014 and 2016) while Figure 21 to 27 shows the distribution of the extracted LST from 2002, 2006, 2008, 2010, 2012, 2014 and 2016 respectively. Figure 21 shows the LST distribution over Calabar Metropolis. The result of this study revealed that LST for 2002 is confined within the range of 14.19 to 31. ^{O}C.
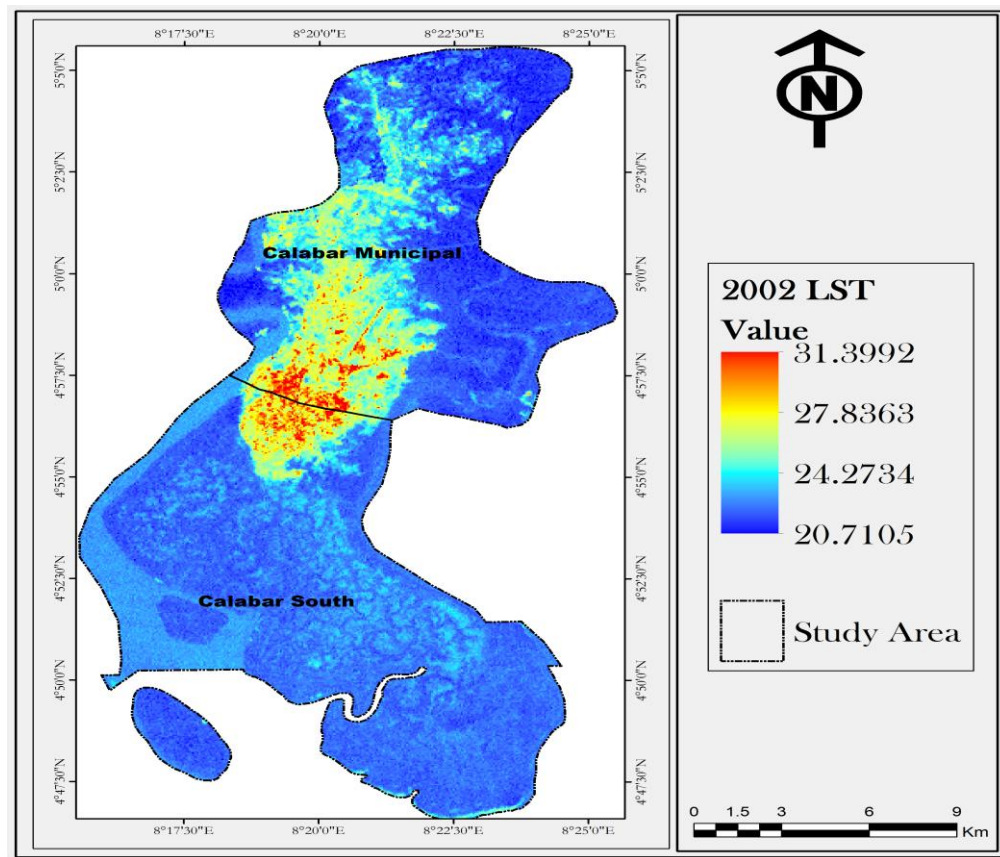
Figure 21: LST Map based on Landsat 7 2002 data
Source: Authors GIS Analysis

Based on the result of this study, in 2002 out of the five land use classes identified (water body, sparse vegetation, dense vegetation, built up area and bareland) the highest mean LST values was observed around the buildup up

area and bareland with mean LST values of 31.40 ^{O}C and 27.84 ^{O}C respectively. The lowest mean LST values was observed around the dense vegetation and water body with a slight difference in their LST values.

 Also, 2006 revealed the LST mean around Calabar Metropolis to be within the range of 18.77 ^{O}C to 30.52 ^{O}C correspondingly (Figure 22).
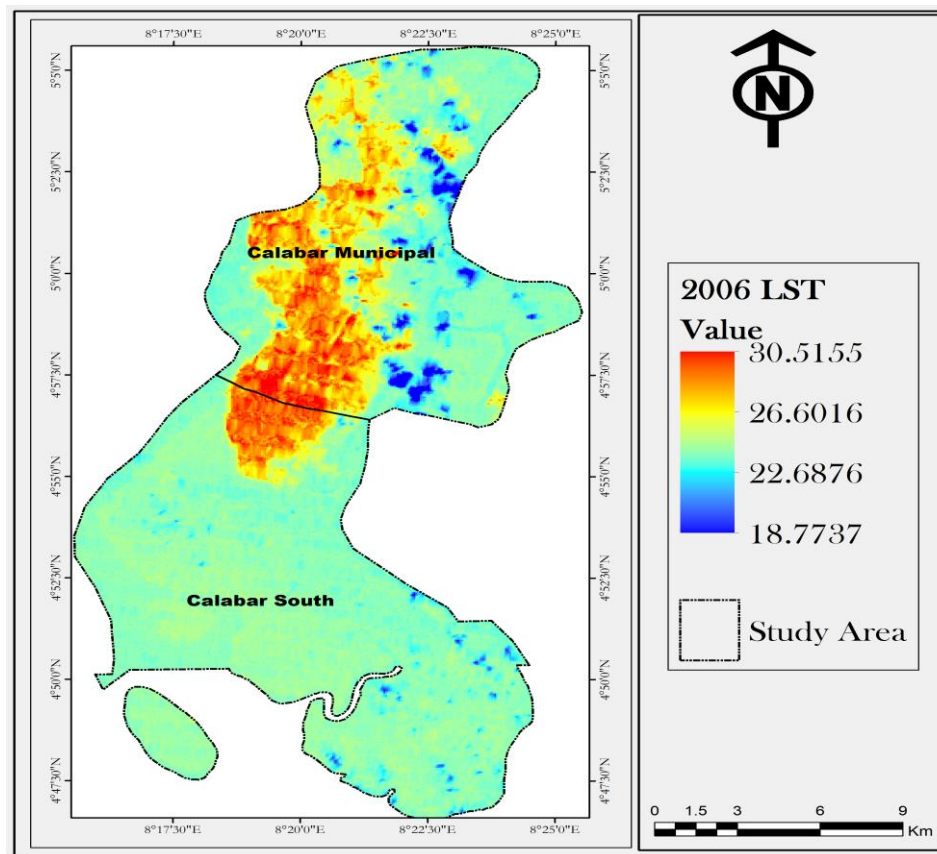
Figure22: LST Map based on Landsat 7 2006 data
Source: Authors GIS Analysis

Based on Figure 18, the highest mean LST in 2006 was displayed around the built up land use class with mean LST value of 30.52 ^{O}C, this was followed by bareland with LST value of 26.6 ^{O}C with water body and dense vegetation with the least LST mean values. Furthermore as seen in Figure 17 and Figure

18, there exist a great variation in the LSTmean values in the selected LULC class for this study with same trend in LST for the different LULC class.
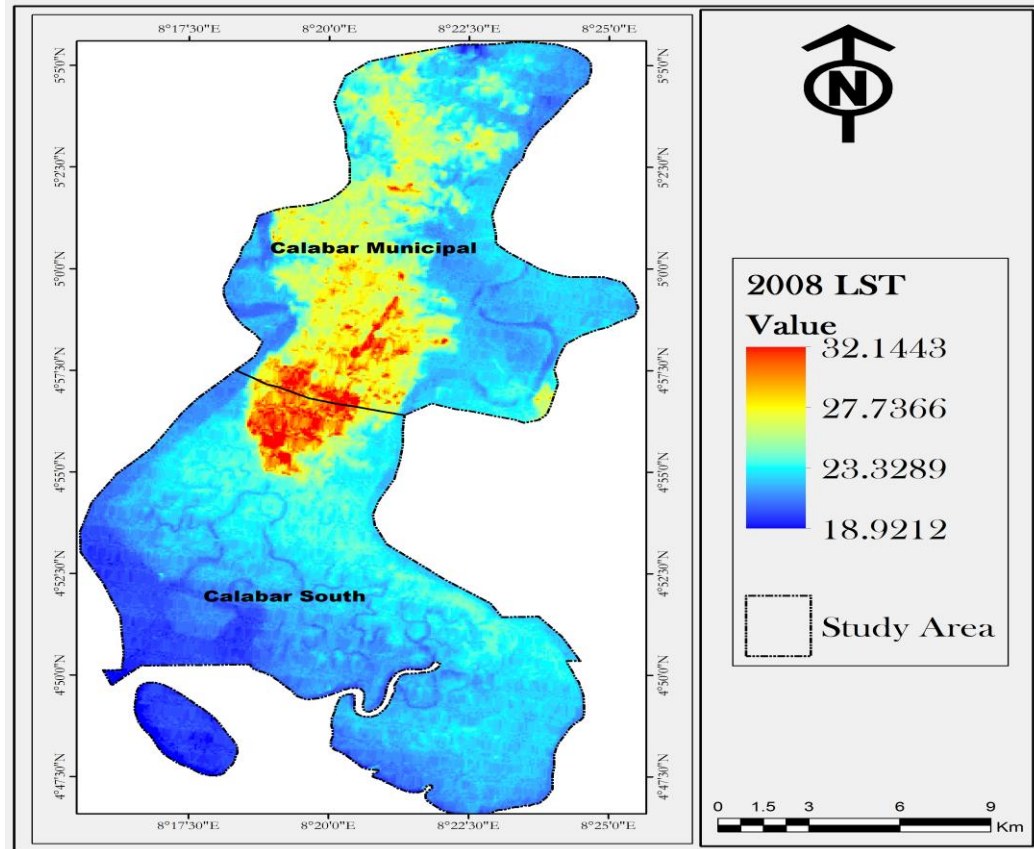
Figure 23: LST Map based on Landsat 7 2008 data
Source: Authors GIS Analysis

Figure 23 shows the mean LST values for the 2008. The result revealed that around Calabar Metropolis, the temperature is confined within the range of 18.92 ^{O}C to 32. 14°C in 2002. The result further revealed that in 2008, the mean LST for built-up LULC class selected for this study was higher than that of 2002 and 2006 correspondingly with mean LST difference of 2.04^{O}C when compared with mean LST value for 2006 and 0.7 ^{O}C when compared with 2002 mean LST value. Furthermore, 2010 recorded the lowest mean

LST (Figure24) in all the LULC class selected for this study when compared with LST values for the other years (2002, 2006, 2008, 2012, 2014 and 2016). Mean LST values for 2010 falls within the range of 14.18^{O}C to 24.77 ^{O}C. Mean LST for built up LULC class for 2010 was 24.77 ^{O}C, while 21.24 ^{O}C was recorded as mean LST for bareland whereas the lowest LST value of 14.18 ^{O}C was recorded around water body . The difference between mean LST value for Built up LULC class in 2010 and the other years was 24.77.
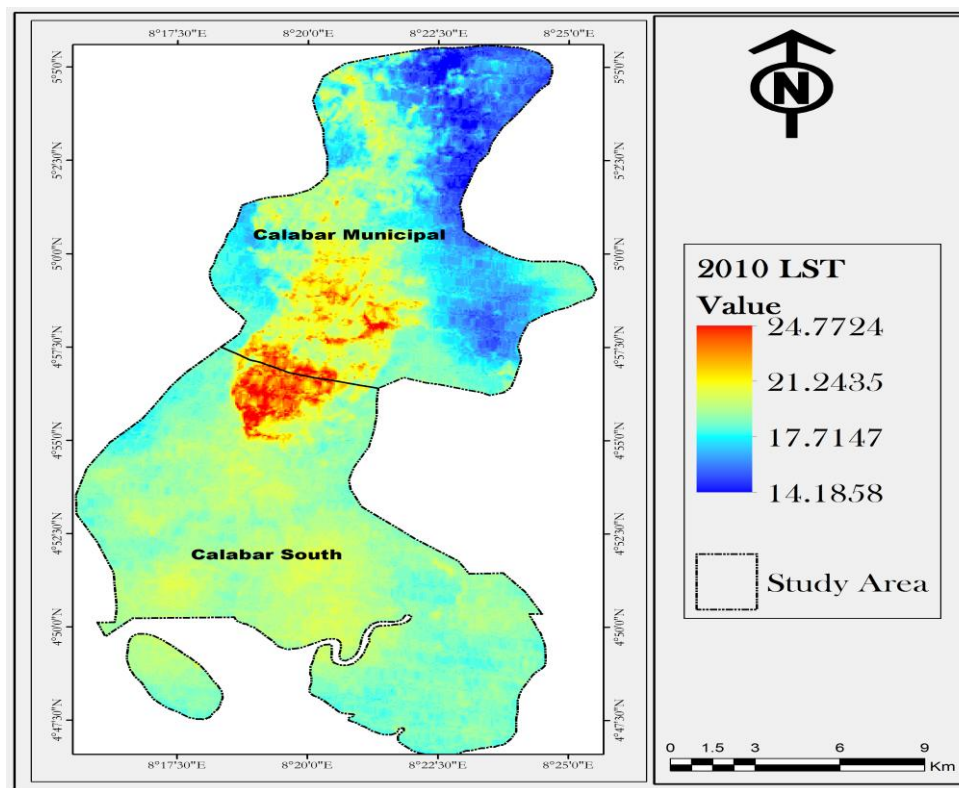
Figure 24: LST Map based on Landsat 7 2008 data
Source: Authors GIS Analysis

Comparing 2010 built up LST value with other years, it was revealed that the value for mean LST for this LULC class was about 4.36^{O}C lesser than the mean of with the lowest LST value in the other years (29.13 ^{O}C) which was observed in 2016. In addition, water body LULC class with lowest LST in

2010 although its LST value was lesser than the values for the other years within same LULC class.
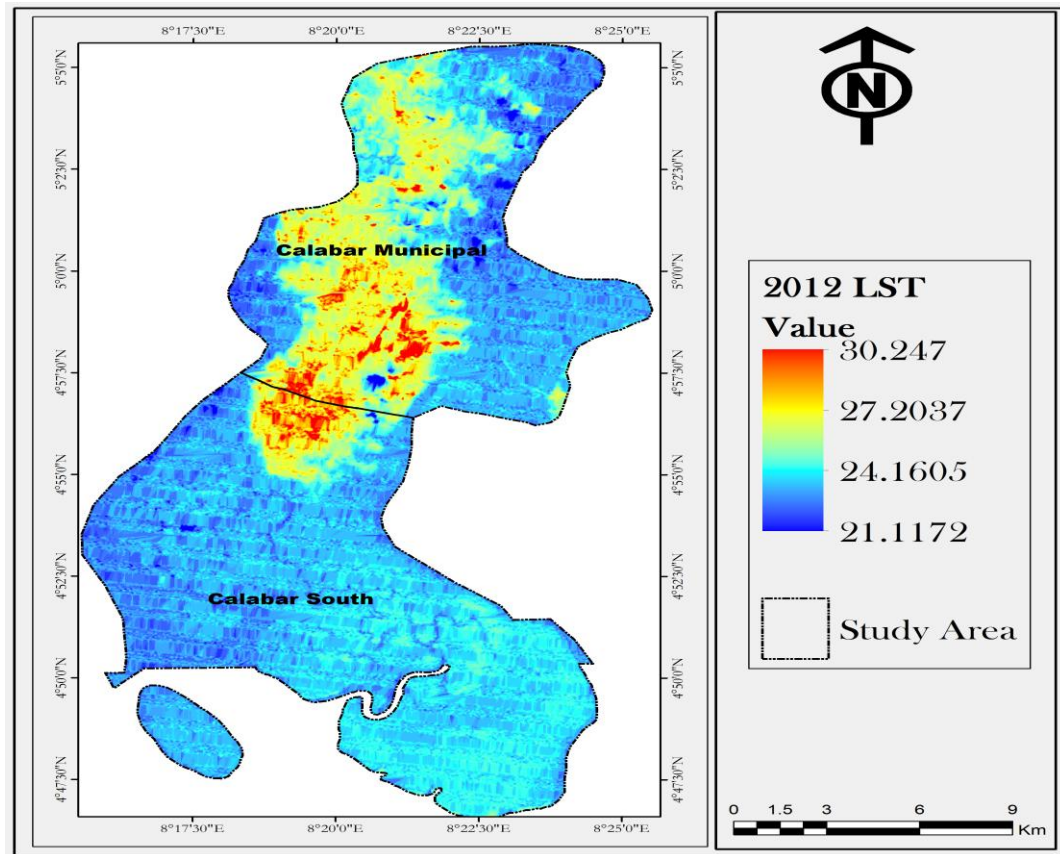
Figure 25: LST Map based on Landsat 7 2010 data
Source: Source: Authors GIS Analysis

Figure 25 divulge the LST for the different LULC class identified within Calabar Metropolis In 2012. The results of this study reveals build up area to be the LULC class with the highest mean LST value (30.25 ^{O}C) for 2012, followed by bareland with mean LST of 27.20^{O}C whereas water body was the LULC class with the lowest LST value. The result further revealed that 2012 mean LST for all the LULC class identified was higher than 2010. The highest mean LST for this year was 30.25 ^{O}C whereas the lowest was 21.12 ^{O}C

compared to 24.77 ^{O}C and 14.18 in 2010. Also, as seen in Figure 20 and 21 mean LST was higher for all LULC class in 2012 compared to 2014 with a slight difference of 0.25^{O}C between built up LULC class, a difference of 1.32 ^{O}C between the bareland LULC classes. In addition, sparsely vegetated areas exhibited mean LST of about 24°C which was higher than 2014 within the same LULC class with mean LST of about 21.76 ^{O}C.
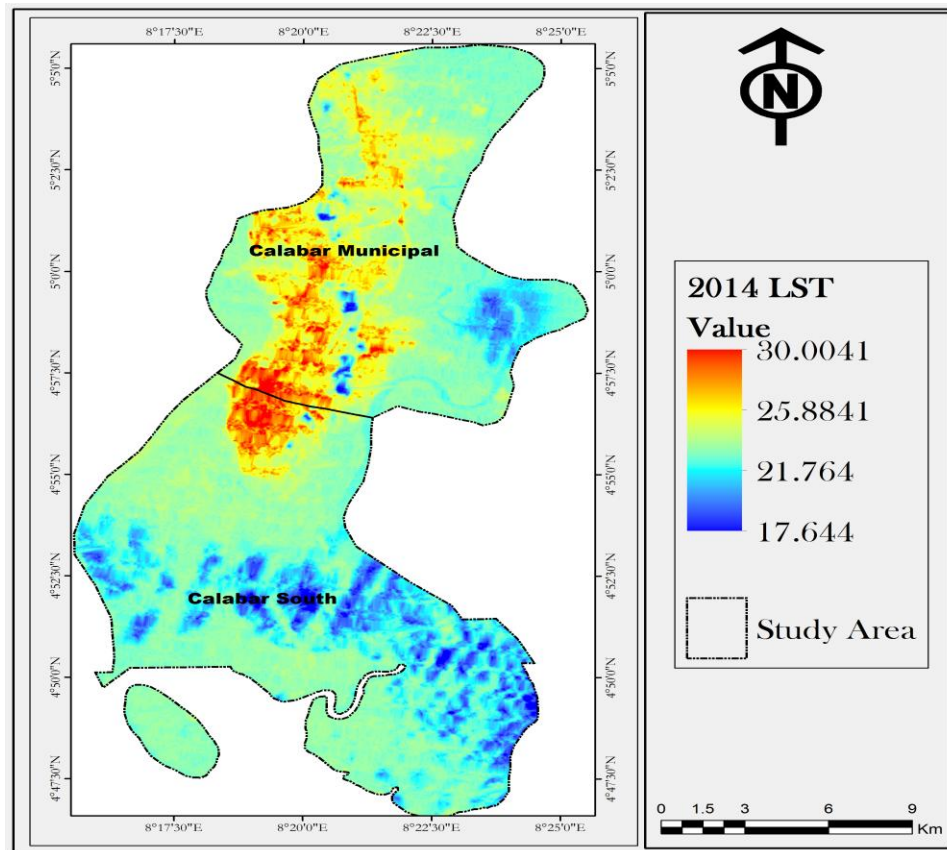
Figure 26: LST Map based on Landsat 7 2014 data
Source: Authors GIS Analysis

The result of this study also reveals the mean LST for the different LULC class identified in 2014 study to fall within the range 17.64 to 30.00 (Figure 27). As seen in Figure 27, LULC class with water body and dense vegetation

shows the lowest LST with water LULC class being the least. The highest LST of about 29.13^{O}C was record around the built up LULC class followed by bareland with 28.97^{O}C.
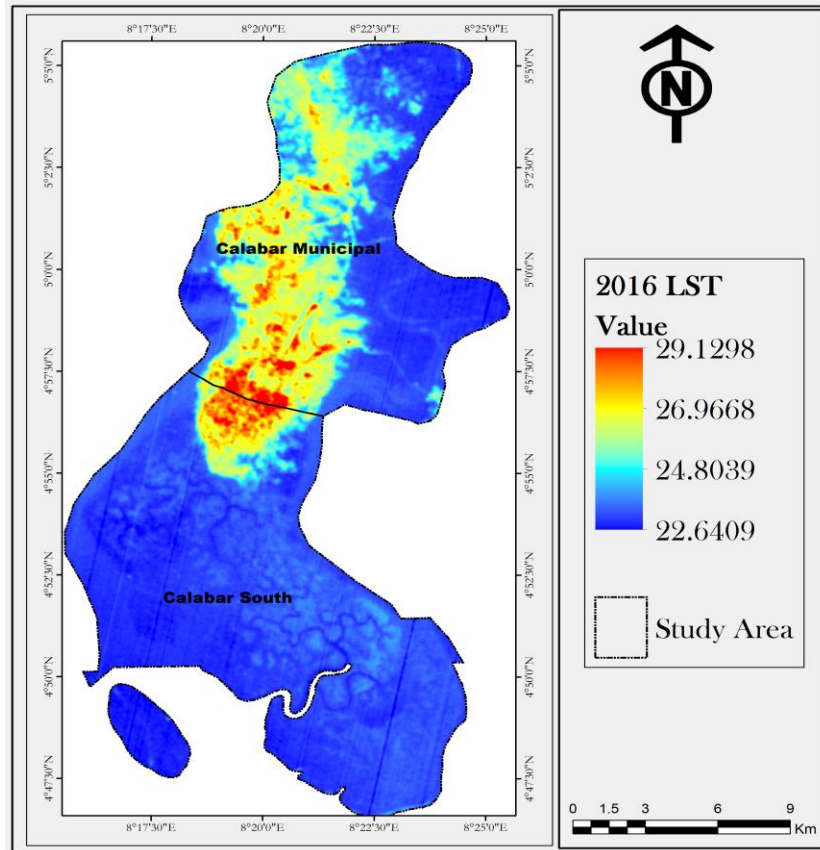
Figure 27: LST Map based on Landsat 8 data
Source: Authors GIS Analysis

5.10 RESULTS BASED ON OBJECTIVE 5 (*to map out UHI Zones within Calabar Metropolis***)**

Isotherm is the line that connects the points on the surface of the Earth that have the same temperature. Isotherms for various zones of Calabar Metropolis were generated using TM data of January 2002 and 2016 using quantum

GIS software. The isotherms were used to identify major hot spots across the city. Figure 28 to 29 clearly depict areas with Hot Island and cold island areas in 2002 and 2006 respectively. Based on the Satellite derived Isotherm map, the present study indicates that areas that were cold islands in 2002 have gradually turn to hot island areas over the years which is not a good sign for ambient living condition. Figure 28 and 29 clearly displays the comparative pattern of different range of temperature in selected areas from 2002 and 2016.

Comparatively, the isotherm maps for 2002 and 2016 (Figure 28 and 29) clearly depicts that a larger proportion of the area shifted to higher temperature zones. In general, during these 7 periods (2002, 2006, 2008, 2010, 2012, 2014, 2017), the hot sports were located around built – up areas , while the cold spots were located around water bodies or part of the area where the natural vegetation cover was barely touched by the urbanization process with minimum temperature at $22\ ^{o}\text{C}$.
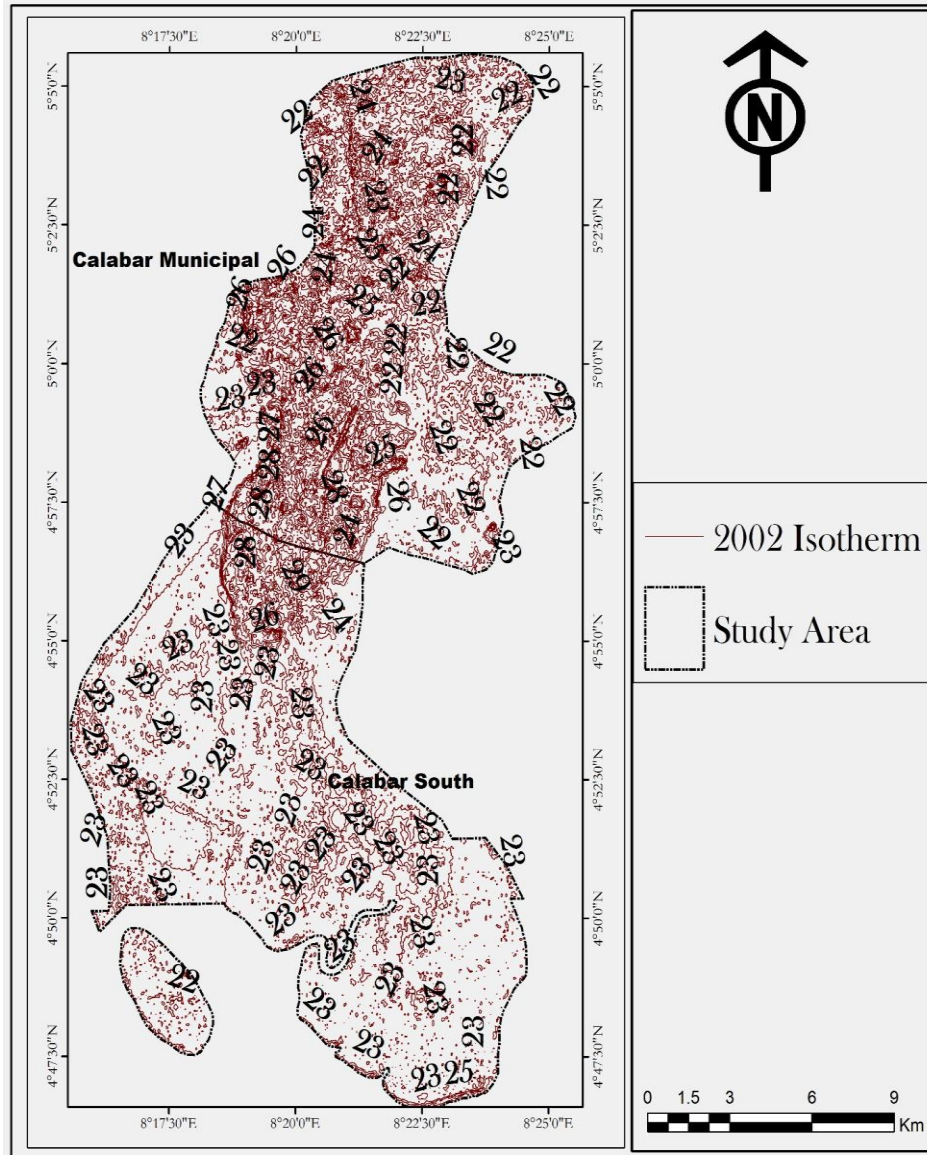
Figure 28: *Isotherm based on Landsat 7 2002 data*
Source: Authors GIS Analysis

Figure 28 illustrates the temperature distribution map of Calabar Metropolis in 2002. In 2002, as revealed in figure 25 LST where as low as 22^OC, no area was found in 2016 with LST below 23 ^{O}C. Water bodies had temperature values of 23^OC in 2002, the value increased to 23.5^OC in 2016.
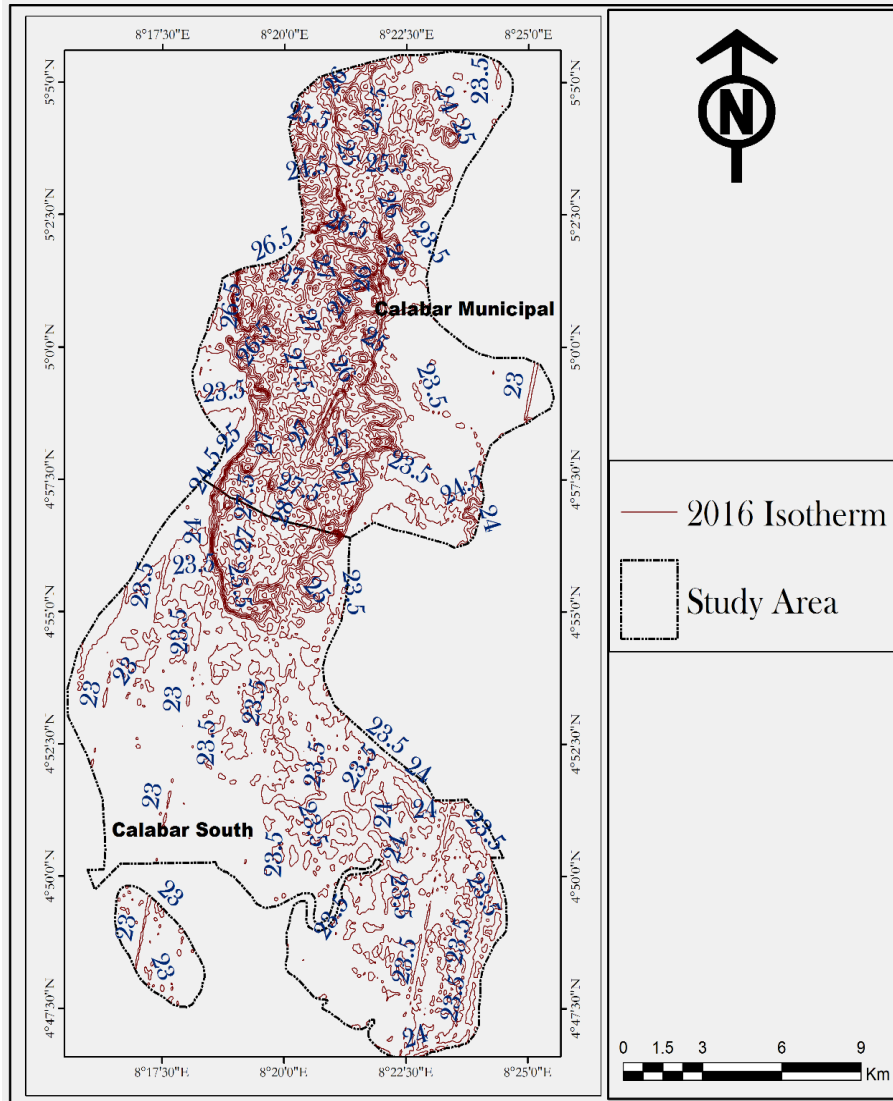
Figure 29: *Isotherm based on Landsat 8, 2016 data*
Source: Authors GIS Analysis

Figure 29 illustrate the temperature distribution map in 2016. During this period, minimum temperature was 23°C. No area was found with LST as low as 22°C which was obtained in 2002.Also, Points taken in the southern part of Calabar metropolis (Calabar South LGA) indicates lower temperature values when compared with points with the same land use in the northern part of Calabar municipality(Figure 29 and Table 14).
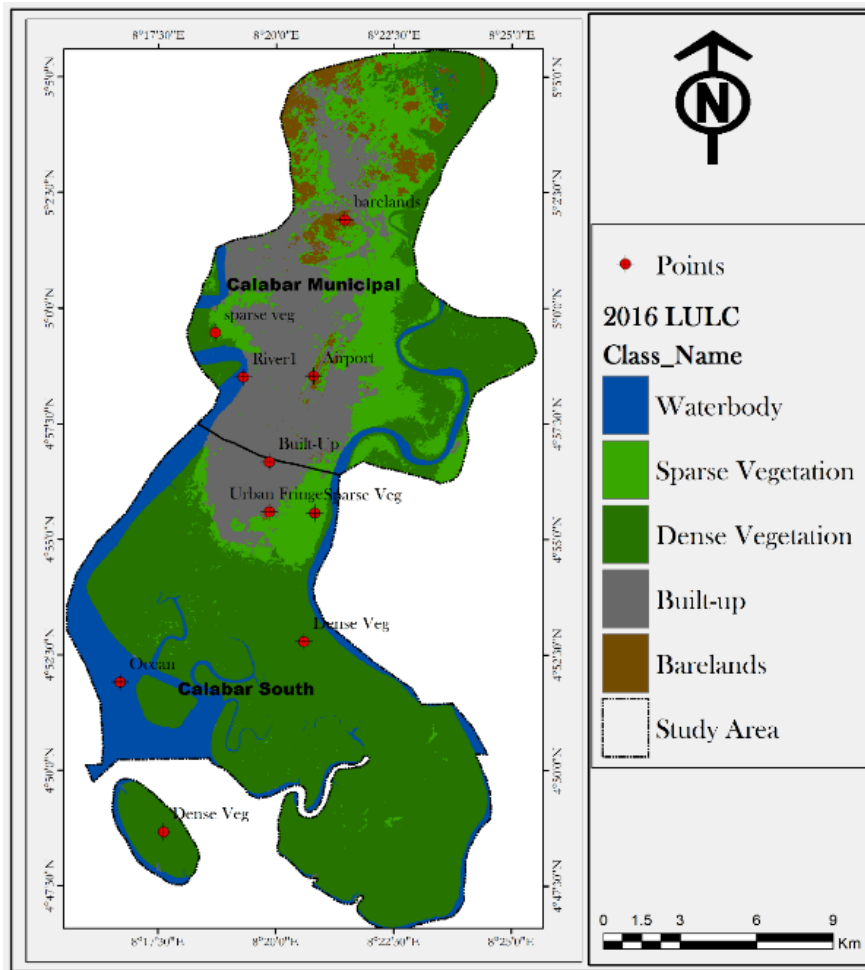
Figure 29: Variation in LST in the selected points and differences
Source: Authors GIS Analysis

Table 14: Variation of Temperature in Selected points at *D*ifferent Time Period (2002/ 2016)

Id	Names	POINT_X	POINT_Y	2002 LST	2016 LST	Differences
1	Built-Up	8.330966	4.944379	28	27.7	-0.3
2	Urban Fringe	8.330984	4.926381	26.4	26.7	0.3
3	Dense Vegetation	8.343248	4.879673	22.8	23.6	0.8
4	Ocean	8.27836	4.865054	2 3	23.3	0.3
`5	Sparse Vegetation	8.347021	4.926014	22.4	23.3	0.9
6	Barelands	8.357609	5.031718	27.6	27.4	-0.2
7	Airport	8.346591	4.975414	27	27.1	0.1
8	Sparse Vegetation	8.311827	4.991079	22.1	23.2	1.1
9	River	8.321771	4.975006	23.5	23.8	0.3
10	Dense Vegetation	8.293687	4.811075	22.3	23.2	0.9

119

After comparing the temperature of different points selected (Figure 29 and table 14) this study emphasis that LST varies depending on the existing land use/ land cover. In general we observed an increasing trend in temperature among the selected points between 2002 and 2016.
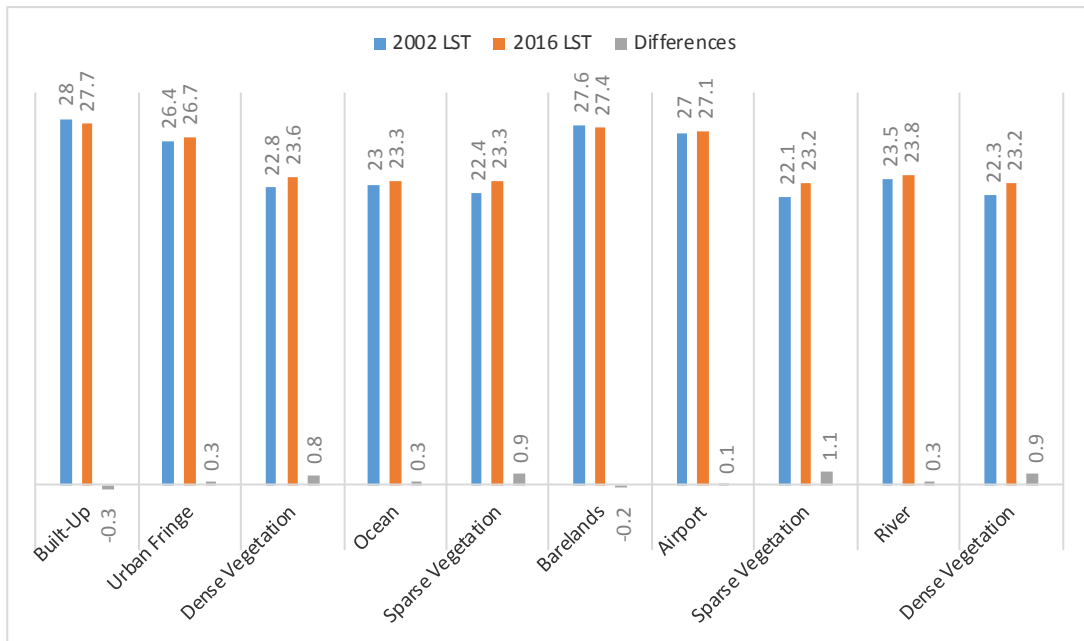
Figure 30: Variation of Temperature in Selected points at Different Time Period (2002/ 2016)

The study also showed that, there exist a great variation in temperature of the selected points on the map. For instance the temperature values for points with sparse vegetation in both local government areas as seen in Figure 28 and 29, in 2002 was 22.4 degree Celsius in Calabar municipality LGA and 21. 1 degree Celsius in Calabar South LGA with a difference of 1.3 degree Celsius. The result of the study also, revealed an increasing trend in the temperature at this particle point when compared with the temperature value in 2016 (Figure 28 clearly depict the variation).

5.11 RESULT PRESENTATION BASED ON HYPOTHESIS ONE *"Relationship between   LULC and LST"*

5.11.1 Descriptive statistics on the relationship between LULC and LST

This section analyzed the relationship between previously determined LST values and LULC classes within Calabar Metropolis as seen in the satellite derived data. The difference in LST among the major land use category (water body, sparse vegetation, dense vegetation and built –up area) were compared in this study (Figure 29 and table 11). Raster layers of LST data with land use fraction data were overlaid in order to analyze the spatial correlation between LST data with Land use fraction. The result revealed that the built-up area was the land use category that significantly linked to high mean and high LST. The study also revealed that the lowest mean LST correspond to areas covered by water bodies, followed by areas over woodland. The sequence indicates that abundant water is helpful in buffering UHIS (Figure 29 and table 11).

Table 15: LULC Types and LST Values

Class	LST Values (^{o}C) 2002	LST Values (^{o}C) 2016	LST Difference between 2002 and 2016
Water body	23.5	23.8	0.3
Sparse Vegetation	22.4	23.3	0.9
Dense Vegetation	22.8	23.6	0.8
Built-Up	28	27.7	-0.3
Barelands	27.6	27.4	-0.2

The LST values as seen in table 11 were increased for almost all areas from 2002 to 2016. This increase ranges between 0.3 $^{\text{O}}$C, 0.9 $^{\text{O}}$C, and 0.8 $^{\text{O}}$C for water body, sparse vegetation and dense vegetation respectively. In contrast, the LST change is negative with -0.2 $^{\text{O}}$C in bare land areas and -0.3 $^{\text{O}}$C between 2002 and 2016.
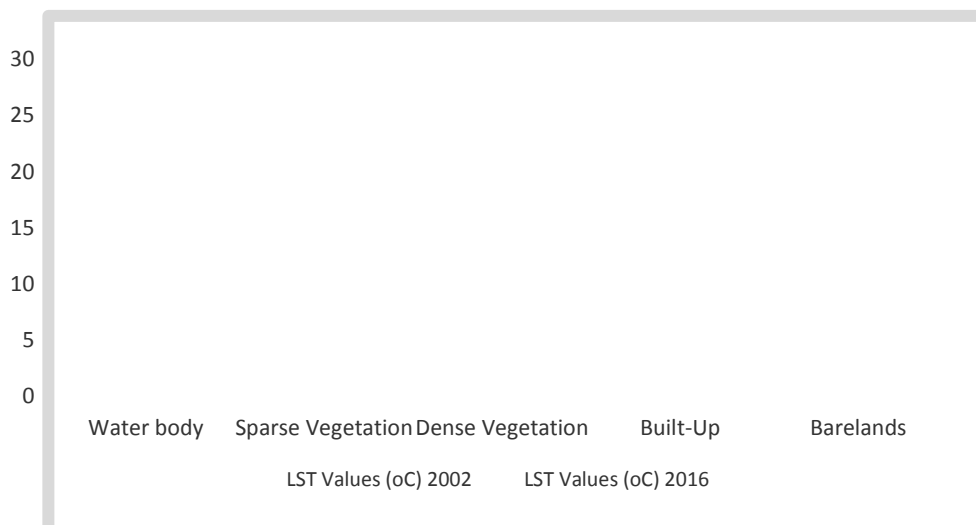
Figure 31: variation of LST in the different LULC types

The relationship between use change and LST was further analyzed as one of the important aspects of anthropogenic (human) influence on nature. The statistical character of LST with corresponding land use fraction change as seen in figure – indicates an increase in built-up area is the factor that contributes to UHIS while water bodies and vegetation were negatively related to LST. It demonstrates that pocket of UHIS were forced to occur by land use change which interfere with surface roughness, evaporation and heat content of the soil (figure – and -). Furthermore due to anthropogenic the cool island effect that were noticed around the northern part of Calabar Municipality with tem-

122

perature of about 22 ^{o}C became weaker as its mean LST increased from 2002 to 2016 (Figure 28 and 29).

5.11.2 Statistical analysis on the relationship between LULC and LST

Simple Correlation analysis was performed to determine the extent of relationships between land surface temperature and changes in land use types. The correlation analysis yielded a correlation coefficient of r = 0.749. This implies that the strength of relationships between the land surface temperatures of Calabar and sets of independent variables of land use types is 0.749. The coefficient of determination, r^2, is given is r^2 = 0.561. The value of coefficient of determination revealed that, out of 100 percent of numerous factors affecting LST of Calabar, 56.1 percent of such variations are explained by the combined variations in the characteristics of the land use types. Most importantly, the reported variations in land use types as determinant factors towards variations in LST in Calabar as reported by the coefficient of determination are attributed to the tendency towards more of the built-up and bare land classes and less of water body, dense vegetation and sparse vegetation. This is made evident by the result of individual correlations of the various classes with the mean LST of Calabar. LST was shown to correlate very highly with built-up and bare lands yielding values of 0.78 and 0.67 respectively while its correlations with other land use types were found to be far below 0.5. However, to determine the precise mathematical form of the relationship between the dependent variable (LST) and sets of independent variables (land use types), a mathematical function was fitted to the sets of variables such that we can use values of the independent variables to predict

changes in LST. The regression equation developed from this relationship is given below as follows:

$$Y = 249.25 - 2.759X_1 - 2.514X_2 - 2.131X_3 - 2.1X_4 - 1.815X_5$$

Where, Y = mean LST for Calabar, X_1 = water body, X_2 = sparse vegetation, X_3 = dense vegetation, X_4 = built-up, X_5 = bare lands

Looking at the inter-correlations of the various land use types in Calabar, a negative relationship was shown to exist between water body and sparse vegetation, built-up and bare lands but positive with dense vegetation. The implication is quite clear; it shows that with a tendency towards more densely vegetated surfaces, the water bodies would be protected from decline. It also showed that the observed change in surface area of water bodies is a result of conversion of dense vegetation to sparse vegetation due to felling of trees for various purposes such as for development (built-up) and agriculture (barelands). For built-up, a strong negative correlation exist between it and dense vegetation. Thus, reported changes in dense vegetation are attributable to urbanization in Calabar.

5.12 Discussion of Major Findings

This section presents the interconnections between the various aspects of the results and their significance for policy and further research. The findings of this study revealed that, the overall condition of the dense cover is decreasing in abundance and resilience. This is revealed by the decreasing NDVI values generated from the maps. These values support the results of increasing trend of LULC transitions from vegetation to other land uses, mostly the built up and barelands and sparse vegetation. Vegetation cover may be slightly in-

creasing in terms of sparse vegetation class. That notwithstanding, dense vegetation are also diminishing in abundance and health in Calabar metropolis. Drastic drop in the dense vegetation cover in 2014 can be attributed to flooding which causes temporal degradation of vegetation cover due to rainfall anomalies which the area experienced in 2012, resulting to sea level rise which led to the transition of over 5000 ha of dense vegetated cover to sparse vegetation and other land uses.

The predominant negative trend in the LULC classes can also be attributed to the expansion, which can be explained by endogenous and exogenous factors such as, population growth through in-migration into the Calabar metropolis. Furthermore, the fact that vegetation, particularly dense covers are diminishing, using the evidence of the LULC classes, as revealed by the findings of this study indicates that, the future changing trends will pose a depleting threat to the overall LULC.

Land use trend between 2002 and 2016 showed that human activities were beginning to take a toll on LULC. Transition that occurred from dense vegetation to sparse vegetation is an indication of environmental degradation. Whereas the increase in the area coverage of sparse vegetation is an indication that extensive land uses have the tendencies to open dense vegetation and degraded sparse vegetation through agricultural activities. The primary cause of these losses was the expansion of urban development. The increase in the   built – up area can be attributed to the rapid urbanization of Calabar Metropolis. Transition from bare to water body can be attributed to see level rise. Although   there is a seemingly moderate growth rate of built-up, bare land cover, efforts must be made to augment vegetation cover in Calabar Metropolis.

This findings supports Weng's et al. results (Indianapolis, Indiana- 2008) that impervious surface not only indicates the degree of urbanization, but also a major contributor to environmental impacts of urbanization. Also the findings of this study as identified in the LULC Transition map, vegetation, (both dense and sparse classes) are not rapidly being replaced by   other LULC classes (built-up, bare land and water). The negative trend in the LULC classes can be attributed to the fact that certain classes had transited into other land use classes. The areas of sparse vegetation have potential tendencies to be converted into other land uses that would lead to the complete removal of the vegetation cover, more rapidly than the rate at which natural forest regrowth could keep pace. From the LULC maps (figure 7 to 13), it is evident that residential activities are spreading in what this study describes as the *funnel-shape growth* of urbanization that result in rural areas expanding into the urban core, along major and minor arterial road routes; obviously, being non-vegetation land uses (Mackenzie, 2009). The high percent coverage of dense vegetation in all the years despite its negative change can be attributed to the presence of mangrove forest which hinders urban development. These fluctuating trends in land use is more in sparse Vegetation

The land surface temperature invariably corresponds to the land-use and land-cover types classified from the seven satellite images. Areas of bare and built-up areas show high reflectance and hence high temperature profiles. These areas, according to Awuh (2014), are the causes of urban islands in high densely-built urban environments. In rural environments, the temperature characteristics are observed to be low in comparison to the urban areas.

This study is in line with the work of Dimoudi and Nikolopoulou (2003) in dense Athens neighborhoods that for every 10 percent increase in percentage of vegetation to highly impervious areas resulted in a decreasing air temperature by 0.8°C. The anthropogenic activities that alter the land cover and exposes it to intense heating is the cause of the differential temperature regimes between the urban core and the rural outgrowth areas. The presence of hot spots can be attributed to the presence of mixed land uses such as; location of historical businesses offices, residential apartment, university of Calabar, the cool island spots were located in parts of the city where the natural vegetation cover was barely touched by the urbanization process. The low mean value in the LST in 2010 compared to the other years can be attributed to the adverse weather condition such as dust haze and fog, which occurred during the period the image for that year was downloaded. This condition was reported by the Nigerian meteorological Agency in their annual report of 2010. This condition affected the visibility (very low horizontal visibility reduced to less than 1000m).

Based on the report from NIMET, during the months of January- March, and November – December 2010, dry north easterly winds prevailed over parts of West Africa as a result of surface pressure built up over the Sahara desert and Sahel region and transporting air borne dust particles southward and reduced horizontal visibility.

CHAPTER 6
SUMMARY OF MAJOR FINDINGS, CONCLUSION AND RECOMMENDATIONS

In this chapter, the major findings obtained are presented based on the hypothesis. Recommendations are made to the government, local people and for further research. A conclusion is also made.

6.1 Summary of Major Findings

By comparing the vegetated and non-vegetated areas of Calabar Metropolis, it can be observed that the built-up areas increased rapidly for all the years. LULCs other than built up slightly increasing at the expense of forest covers. The expansion may be explained by endogenous and exogenous factors such as, population growth through in-migration into the districts. In this period (2002 -2016), built up area covered 2865.19 ha in 2002, 3577.14 ha in 2006, 3942.37 ha in 2008, 4594.32 in 2010, 4776.88 ha in 2012, 5380.89 ha in 2014 and 5680.81 ha in 2016, while the green cover classes (dense vegetated class) covered an area of 19861.42 ha in 2002, 16929.7 ha in 2006, 17897.57 ha in 2008, 16560.98 ha in 2010, 17760.39 ha in 2012, 12395.95 ha in 2014, 16629.85 ha in 2016. On the other hand, areas with sparse vegetation covered 3996.47 ha in 2002, 6744.36 ha in 2006, 5935.43 in 2008, 6413.92 in 2010, 4902.21 in 2012, 7373.34 in 2014 and 5262.53.

In addition, out of 19861.42 ha of the area which was green cover (dense), 1965.51 ha had been converted to urban use by 2016 while the total area coverage for sparse vegetation increased by 1266.06. Mean LST for the different LULC classes identified in 2014 study to fall within the range 17.64 to 30.00.

The highest LST of about 29.13^{O}C was record around the built up LULC class, followed by bareland with 28.97^{O}C.

Comparatively, the isotherm maps for 2002 and 2016 (Figure 28 and 29) clearly depicts that a larger proportion of the area shifted to higher temperature zones. In general, during these 7 periods (2002, 2006, 2008, 2010, 2012, 2014, 2017), the hot spots were located around built – up areas, while the cold spots were located around water bodies or part of the area where the natural vegetation cover was barely touched by the urbanization process with minimum temperature at 22 ^{o}C

The study also showed that, there exist a great variation in temperature of the selected points on the map. For instance the temperature values for points with sparse vegetation in both local government areas as seen in Figure 28 and 29, in 2002 was 22.4 degree Celsius in Calabar municipality LGA   and 21. 1 degree Celsius in Calabar South LGA with a difference of 1.3 degree Celsius.

LST was shown to correlate very highly with built-up and bare lands yielding correlation values of 0.78 and 0.67 respectively while its correlations with other land use types were found to be far below 0.5. The result revealed that the built-up area was the land use category that was significantly linked to high mean and high LST. The study also revealed that the lowest mean LST correspond to areas covered by water bodies, followed by areas over woodland. The sequence indicates that abundant water is helpful in buffering UHIS.

6.2 Conclusion

In this study, a combined approach of remote sensing and GIS was developed for evaluation of land cover change and its impact on surface temperature in Calabar Metropolis. Temporal and spatial dynamics of LST in relation to land cover change was investigated using thermal infrared data of Landsat. The LU/LC thematic maps' overall accuracies were computed above 80 percent. It was observed that, the classification accuracies were increased when all secondary data were used in addition to the original Landsat bands and in this case the classification overall accuracies were computed as 99.60 percent, 99.1 percent, 94.8 percent, 99.9 percent and 99.6 percent for the 2002, 2006, 2008, 2010, 2012, 2014 and the 2016 images, respectively. Built- up and sparse vegetation areas increased, while bareland and dense vegetation reduced significantly within 15-year time interval.

This study has demonstrated that urban heat island climates exist in the urban centers and some surrounding areas in the study area. These heat islands have grown from the 2002 extent to the 2016 size and their spatial extent is getting larger as urbanization intensifies. The results show that the maximum temperature exists in the bare land, stony surfaces and buit-up areas, respectively. The minimum of temperature coincides on the green cover and river classes. Urbanization is the main process of land cover change that can modify the effective variables of land surface temperature (Weng et al., 2004).

6.3 RECOMMENDATIONS

This study in line with the objectives and conclusions, recommend the following for policy and institutional actions; In order to implement mitigation

measures, the government of Calabar should pay more attention to the areas with anomalous high temperature. We noticed the low percentage of green areas inside the city despite the fact that the result of this study showed a negative correlation between dense vegetation and water body.

Effort should be made by the government to increase urban vegetation around the city center and the outliers, building parks and waterfalls which will act as urban sink around the hot spot areas identified. The government of Calabar should embark on reforestation .Vegetation should be introduced extensively and carefully, this will help to provide shading at residential level and building facades or roofs and thus reduce the intensity of the UHI in hot spot areas. Though blockage of air movement should be avoided.

Furthermore, the government should carry out sound urban planning with informed architectural decisions. Example of urban planning decision may include: the location / allocation of industrial building and workshops outside the city core center. Example of some architecture solution may include the use of solar reflective roofing materials, placement of deciduous shade trees near south and west walls of short and middle height buildings, use of reflective pavement material.

Finally, Town Planners should enforce land use regulations towards the protection and sustenance of prime agricultural and forest land covers, as physical development cannot be avoided entirely. The removal of the vegetal cover exposes the land surface to insolation expressed in reflectance that signifies the heating or cooling surface systems. Vegetation cover should be protected to reduce potential future urban heat islands around the urban fringe transits through a peri-urban heating system.

6.4 Suggested Area for Further Research

A study on Air Pollution Tolerant Index on Plant Species   is recommended in Calabar in order to identify the plant species that can strive in the area.

6.5 Contribution to knowledge

The correlation between land use land cover effects on land surface temperature with satellite remote sensing in Calabar Metropolis, is an addition of a layer of knowledge and a methodological contribution. Secondly, the study has demonstrated that it is possible to study the relationship between land use land cover change and urban heat island pattern using remote sensing and GIS. This is a theoretical contribution to knowledge. Thirdly, the production of a projected land use land cover map for 2046 (that is, three decades from 2016); land use and land surface temperature maps for 2002, 2006, 2008, 2010, 2012, 2014, and 2016; Isotherm maps for 2002 and 2016   into the land surface temperature studies as surrogates of urban heat island (UHI) analyses is original and hence, an addition and theoretical contribution to the existing knowledge.

REFERENCES

Aakriti, G., Ram, B., Sign, c. (2015). Analysis of urban heat island (UHI) in Relation to Normalized Difference Vegetation index (NDVI): A comparative study of Delli & Mumbai. *Journal of Environments*.2, 125,138.

Abegunde, L., Adedeji, O. (2015). Impact of Land use Change on Surface Temperature in Ibadan, Nigeria: *World Academy of Science Engineering & Technology International Journal of Environmental Chemical, Ecological, Geological and Geophysical Engineering* Vol: 9, No: 3.

Abdulhamed, A. I., Nduka, I.C, B.A., Sawa, and A.K. (2016). An Analysis of the Urban Canopy Heat Island (UCHI) of Kano Metropolis during the Warm/Wet Season: Usman Geography Department, Ahmadu Bello University, *Zaria Journal of Environment and Earth Science*, ISSN 2225-0948 (Online) Vol.5, No.13, 2015 166.

Abutaleb, K., Ngie, A., Darwish, A., Ahmed, M., Arafat, S. and Ahmed, F. (2015). Assessment of Urban Heat Island Using Remotely Sensed Imagery over Greater Cairo, Egypt. *Advances in Remote Sensing*, **4**, 35-47.http://dx.doi.org/10.4236/ars.2015.41004

Adebayo, Y.R. (1985). The Microclimatic Characteristics within the urban Canopy of Ibadan: *Ph.D. Thesis, University of Ibadan.*

Ademiluyi, I. A., Okude, A. S. & Akanni, C. O. (2008). An appraisal of Land-use and Land-cover mapping in Nigeria: *African Journal of Agricultural Research*, 3 (9), 581 – 586.

Adeoluwa P. A. (2015). Assessment of Daytime Surface Urban Heat Island in Onitsha, Nigeria: International Conference & 29th Annual General Meeting of the Nigerian Meteorological Society, 23rd – 26th November, 2015, Sokoto, Nigeria., At Usman Danfodiiyo University, Sokoto, Nigeria, Volume: 29 DOI: 10.13140/RG.2.1.5117.5765 ·

Adegoke B., Ogwumike, O. O. (2002): Prevalence of leg length discrepancy among Secondary school children in Ibadan North Local Government Area of Oyo State: *Journal of Physical Education and Research* Vol. VII (11): 84-852.

Adinna, E.N., Enete, I.C, and Okolie, A.T. (2009). Assessment of UHI and possible adaptations in Enugu urban using Landsat-ETM: *Journal of Geography and Regional Planning, 2:* 030- 036.

Akbari, H., Pomerantz, M. & Taha, H. (2001). Cool Surfaces and Shade Trees to Reduce Energy Use and Improve Air Quality in Urban Areas: *Solar Energy*, 70(3), 295-310.

Appiah, D.O., Bugri, J.T and Forkuo E.K. (2016). Land use conversion probabi - lity in a Peri-Urban District of Ghana. *Chinese Journal of Urban and Environmental Studies* Vol. (3):1-21.

Alberti, M. (2009). Advances in Urban Ecology: New York City, NY: *Springer Sciences + Business Media, LLC.*

Ali-Toudert, F., & Mayer, H. (2007). Effects of asymmetry, galleries, Overhanging facades and vegetation on thermal comfort in urban street canyons. *Solar Energy Applied Ecology, 4*:27-34

Allegrini, J., Dorer, V., & Carmeliet, J. (2015). Influence of morphologies on the microclimate in urban neighbourhoods. *Journal of Wind Engineering and IndustrialAerodynamics*,*144*,108–117.doi.org/10.1016/j.jweia.2015.03.024

Amed, B. (2011). Urban Land Cover Change Detection Analysis and Modeling Spatio-Temporal Growth Dynamics Using Remote Sensing and GIS Techniques: A Case Study of Dhaka, Bangladesh. Masters Thesis, Erasmus Mundus Program, Universiade Nova De Lisboa(UUL), Institude Superior De Estatistica E Gestao De Informaca (ISEGI) l, Lisbon, Portugal.

American Meteorological Society. (2015, May 11). *Climate System.* Retrieved From http://glossary.ametsoc.org/wiki/Climate_system

Anderson, J.R., Hardy, E.E., Roach, J.T. &Winter, R.E. (1976). A Land Use & Land Cover Classification System for Use with Remote Sense Data: *Geological Survey Professional Paper* 961, Washington. United States Government Printing office.

Areola, O. (1977). Aerial photo-interpretation of land types and terrain Conditions in the Lagos coastal region, Nigeria. *Geographical Journal*, 20 (1), 70-84.

ArcGISC10Help; (2012). Environmental Systems Research Institute: Re lands,CA,USA.Avialable.Online:http://help.arcgis.com/en/arcgisdesktop/10.0/help/ (accessed on 15december 2016).

Aslan, N., Koc-San, D. (2016). Analysis of Relationship between UHI effects & land use/land cover types using Landsat 7ETM+ and land sat 8OLIImages: International Archives of the photogrammetric, *remote sensing and spatial information sciences*. Vol.XLI-B8.doi:10, 5194-XLI-1381321.

Atkinson, P.M., Tatnall, A.R.L. (2012). Introduction Neural networks in Remote *Sensing: Int. J. Remote Sens*, *18*, 699–709.

Atkinson, P.M., Tatnal, A.R.L. (1997). Introduction Neural Networks in Remote Sensing: *Int.J.Remote Sens,* 18,699-709.31:251-257.

Atu, J. E. Offiong, R.A., Eni, D.I., Eja, E.I., Esien, O.E. (2012). The Effects of Urban Sprawl on Peripheral Agricultural Lands in Calabar: *Nigeria International Review of Social Sciences and Humanities* Vol.2, No2 (2012), PP.68-76.

Attua, M. A. (2003). Land covers Change Impact on the Abundance and Composition of Flora in the Densu Basin. *West African Journal.*

Awuh, M.E., Amawa, S.G. (2017). Urban Heat Island Coping /Adaptative Strategies in Douala Metropolis Cameroon: *Journal of Geography Meteorology and Environment Studies* Vol. (2).

Balster, H. M. (2013). Chain Models for Vegetation Dynamics, Ecology Model 2000, 126,139-154: *Remote Sens*, 55997.

Bayan, H., Alhawiti, Diana, M. (2016). Using landsat-8data to explore the Correlation between urban heat island and urban land uses: *International Journal of Research in Engineering and Technology*.2319-1163/23217308.

Becker, F. and Z.-L. Li, (1990). Towards a local split window method over Land Surface. *Int. J.mRemote Sens*, 3, 17–33.

Bernard, T. Tyubee1, Raymond, N. C. Anyadike (2015). Investigating the Effect of Land Use/Land Cover on Urban Surface Temperature in Makurdi, Nigeria: ICUC9 – 9th International Conference on urban Climate jointly with 12th symposium on the Urban Environment

Bhang K.J., Park S.S. (2009). Evaluation of the Surface Temperature Variation with Surface Settings on the Urban Heat Island in Seoul, Korea, Using Landsat-7 ETM+ and SPO*T*: *Geoscience and Remote Sensing Letters,* 2009 .

Bisong, F. E. (2007). Land use and deforestation in the rainforest of South-Eastern Nigeria (1972-2001): *Nigerian Geographical Journal*, 5 (1), 19 − 28.

Bisong, F. E., Animashaun, A. & Andrew-Essien, E. (2007). Participatory Land-use planning for community based forest management in South-eastern Nigeria: *LWATI: A Journal of Contemporary Research.* 4, 329 − 347.

Brandsman, T. and Walters, D. (2012). Measurement and Statistical Modelling of the Urban Heat Island of the City of Utrecht (the Netherlands). *Journal of Applied Meteorology and Climatology*, 51(6), 1046-1060. doi: 10.1175/jamc-d-11-0206.

Brown, A.G., Nambiar, E.K.S, & Cossalter, C. (1997). Plantations for the Tropics; Their Role Extent and Nature in E.K.S. Nambiarand. G. Brown (Editors). Management of Soil, Nutrients and Water in Tropical Plantation Forests. ACIAR, Canberra, PP.1-23.

Britter, R. E., & Hanna, S. R. (2003). Flow and Dispersion in Urban Areas. *Annual Review of Fluid Mechanics, 35*, 469-496.

Buechley, R.W, Van Bruggen, J. and Trippi, L. E. (1972): "Heat Island /Death Island" Environmental Research, Vol. 5. pp. 85 − 92.

Cao, X. M., Bao, A. M., et al. (2008). Land surface temperature in response to Landuse /cover change based on remote sensing data in Sangong River: In W. Gao & H. Wang (Eds.), *Remote Sensing and Modeling of Ecosystems for Sustainability*, 7083.

Chaobin, Y.X, He, F.Y, Lingxue, Y. K, Jiuchum, Y, Liping, C and Shuwen, Z (2017). Maping the influence of land use/ land cover changes on urban heat island effect. A case study of Changchun, China: *Sustainability 9*, 312

Chen, Y., Wand .J., Li, X. (2002). A Study on Urban Thermal Field in summer on Satellite Remote Sensing*: Remote Sens. Land Resource*.4, 55-59.

Civco, D.L. (1993). Artificial Neutral Network for Land –Cover Classification and Mapping.*Int.J.Geogr.Inf.Sci.7*, 173-186.

Clarke, J.F (1972): "Some Effects of the urban Structures on Heat Mortality". Environmental Research 5, pp. 93 – 104.

Coseo, P. (2013). How Factors of Land Cover, Building Configuration, and Adjacent Heat Sources and Sinks Differentially Contribute to Urban Heat Islands in Eight Chicago Neighborhoods. Manuscript in preparation.

Cross River State Forestry Commission (1988, 1990, 2000, 2001 and 2003). *Annual report.* Calabar: Forestry Commission.

Dimoudi, A., & Nikolopoulou, M. (2003).Vegetation in the Urban Envi ronment Micro Climatic Analysis and Benefits .Energy and Building 35, 69-76.

Djen, C.S., Jingchun, Z., &Lin, W. (1994).Solar Radiation and Surface Temperature in Shanghai City and their Relationship to Urban Heat Island Intensity. Atmospheric Environment, 28(12), 2119-2127.

Dozier J., Warren S.G. Effect of viewing angle on the infrared brightness temperature of snow. *Water Resources. Res*. 1982; 18:1424–1434.

Eastman, J.R. IDRIS, (2012). Selva Manual; Clark University: Worcester, MA, USA.

Effat, H.A., & Hassan, O.A.K. (2014). Change detection of UHI and some related parameters using multi-temporal Landsat images; a case study for Cairo city, Egypt. *Urban Climate, 10*, pp. 171-188.

Efiong-Fuller, E. O. (2008). Land use mapping: a system approach. Unpublished lecture note, University of Calabar, p. 8-9.

Efe, S.I. (2002). Aspect of Indoor Microclimates Characteristics in Nigeria Cities: The Warri Experience. *Environmental Analar*, **8**, 906-916.

Ekanem, I.I. (1980). The Demography of Calabar, in: P E. B. (eds) Calabar and Environs, Geographic studies. Abstract and papers: 23rd Annual conference of the Nigerian Geographical Association Calabar, Nigeria: NGA (LOC).pp 23- 47

Ekpenyong, R. E. (2008). Analysis of findings from the AkwaIbom State Land-use/land-cover change early warning system: *Nigerian Journal of Geography and the Environment, 1, 68 – 76.*

Ema, k., Nengah, I. S., Widiatmaka, J. (2016). Satellite-Based Land Surface Temperature Estimation of Bogor Municipality, Indonesia. *Indonesian Journal of Electrical Engineering and Computer Science, 2,221-228.* DOI: 10.11591/ijeecs.

Enete, I.C, Awuh, M.E and Amawa .S. (20014).Assessment of Health Re lated Impacts of urban heat island (UHI) in Douala Metropolis, Cameroon: *International Journal of Environmental protection and policy*. 2(1):35-40.

Enete, I.C, Awuh, M.E and Ikekpeazu, F.O. (2014). Assessment of urban heat island (UHI) situation in Douala Metropolis Cameroon: *Journal of Geography and Earth Sciences.*2 (1):35-40.

Enete, I.C. (2009). Assessment of urban heat island and possible adaptation in Enugu, Using Landsat/ETM. *Pakistan Journal of social sciences* .1(1):26-31.

EPA, (2009). Heat Island Compendium: Urban Heat Island Basics. Available Online at: http://www.epa.gov/heatislands/heat-island pdf (Accessed January 3rd, 2016).

EPAb. (2012).Urban Heat Island Mitigation. Retrieved, from http://www.epa,gov/hiri/mitigation/index.htm.

EPA (2014). Reducing Urban Heat Islands: Compendium of Strategies. In, *06/documents/basicscompendium.pdf* (14 April 2016). *https://www.epa.gov/sites/production/files/2014*

Essa, W., Verberren, B., Van der Kwast, J., VandeVoorde, T. Bate Laan.O. (2012). Evaluation of the Dis Trad Thermal Sharpening Meteorology for Urban areas.*Int.J.Appl.EarthObs.Geoinf*.19, 163-172.

Evans. (1992). Plantation Forestry in the Tropics: 2nd Edition. Claredon Prex, Oxford.

Fabrizi, R., Bonafoni, S., Biondi, R. (2010).Satellite and Ground-Based Sensors for the Urban Heat Island Analysis in the City of Rome. *Remote Sens*.2, 1400-1414.

Feizizadeh, B., & Blaschke, T. (2013). Examining UHI Relations to Land Use and Air Pollution: Multiple End member Spectral Mixture Analysis for Thermal Remote Sensing. *Ieee Journal of Selected Topics in Applied Earth Observations and Remote Sensing, 6*, pp. 1749-1756.

FORMECU, (1996). Preliminary report on the assessment of land use and vegetation changes in Nigeria between *1978 – 1993/95.* Submitted by Geometrics International Inc., Ontario, Canada.

Foley, J. A., Chad M., Navin R., and David Z. (2005). Our share of the Planetary pie: *Proceedings of National Academy science*.104 (31):570-573.

FSNAU, (2010). Understanding the Normalized Difference Vegetation Index. Available at: http://www.fsnau.org/ (accessed 15 December 2010).

Fu, G., Shen, Z., Zhang, X., Shi, P., Zhang, Y., and Wu, J. (2011). Estimating air temperature of an alpine meadow on the Northern Tibetan Plateau using MODIS land surface temperature: *Acta Ecol. Sin*., 31, 8–13, doi:10.1016/j.

Fung T., Siu W. (2000).Environmental quality and its changes, and analysis using NDVI. Int. J. Remote Sens.21:1011–1024.

Gallo, K.P., McNab, A.L., Karl, T.R; Brown, J.F., Tarpley, J.O. & Hood, J.J. (1993). The Use of NOAA AVHRR Data for Assessment of the UHI Effects: *Journal of Applied Meteorology,* 32,899-908.

Gallo, K.P., Tarpley, J.D. and McNab, A.L. (1995). Assessment of urban heat island: a satellite perspective. *Atmospheric Research*, 37, pp. 37-43.

Gallo K.P., Tarpley, J.D. (1996). The comparison of vegetation index and surface temperature composites of urban heat-island analysis. *Int. J. Remote Sens.* 17:3071–3076.

Gartland, L. (2008). Heat Island: Understanding and Mitigating Heat in Urban Areas: Sterling, Virginia. Earth scan.

Gaylan, R., and Faqe, I. (2017). Urban Land Use Land Cover Changes and Their Effect on Land Surface Temperature, Case Study Using Dohuk City in the Kurdistan Region of Iraq: *climate, 5*(1), 13; doi: 10.3390/cli5010013

Gillespie, A.R., Rokugawa S., Matsunaga, T., Cothern, J.S., Hook S.J., Kahle A.B. (1998). A temperature and emissivity separation algorithm for advanced space borne thermal emission and reflection radiometer (ASTER) images: *IEEE Trans*. *Geosci. Remote Sens*. 36:1113–1126.

Golden, J.S., & Kalaish, K.E. (2006). Mesoscale and Microscale Evaluation of Surface Pavement Impacts on the Urban Heat Island Effects *International Journal of pavement Engineering,* 7(1), 37-52.139.

Hartemink, A. E., Veldkamp, T. and Bai, Z. (2008). Land Cover Change & Soil Fertility Decline in Tropical Regions: *Turk J Agric For*, 32:195-213

He, F.; Liu, J.Y.; Zhuang, D.F.; Zhang, W.; Liu, M.L (2007). Assessing the effect of Landuse/landover change on the change of urban heat island intensity. *J. Theor. Appl. Climatol. 90*, 217–226.

Hough, M. (2004). Cities and Natural Processes. New York: Routledge.

Hu, Y.S., & Jia, G.S. (2010). Influence of land use change on UHI derived from multi-sensor data: *International Journal of Climatology, 30*, pp. 1382-13.

Idoko, M. A., Bisong, F. E., Bisong, J. N. & Okon, I. E. (2008). Application of geo-information for evaluation of land use change: a case study of Federal Capital Territory, Abuja: In Bisong, F. E. (Ed.), Geography and the millennium development goals: translating vision into reality (444-448). *Calabar: Index Books Publishers*.

Imhoff, M.L., Zhang, P., Woife, R.E., & Bounoua, L. (2010). Remote sensing of Urban Heat Island Effect across Biomas in the Continental USA.*A Remote Sensing of Environment,* 114,504-513.

IPCC. (2007). Climate Change Impacts, adaptation and vulnerability. Fourth Assessment Report. *Cambridge University Press*, New York.

Inyang, P. E. B. (1980) Calabar Environs: geographical studies, published by *Department of geography, University of Calabar*, Pp.12 and 63.

Jenerrete, G., Darrel, S. L., Harlor, Anthony. B., Nancy, J. Larissa, L. and William L., (2007). Regional Relationships between Surface Temperature, Vegetation and Human Settlement in rapidly urbanized Ecosystem Land Scape Ecol., 22, pp.353.365.

Jiang, Y., Fu, p., and Weng, Q. (2015). Downscaling GOES land surface temperature for assessing heat wave health risks, *IEEE Geoscience and Remote Sensing Letter*s, 12(8), 1605-1609.

Jiménez-Muñoz, J. C. and J. A. Sobrino. 2008, *IEEE Geoscience and Remote Sensing Letters,* Vol. 5, No. 4, pp. 806-809.

Jimenez-Munoz, J.C., Sobrino, J.A., Skokovic, D., Mattar, C., & Cristobal, J. (2014). Land Surface Temperature Retrieval Methods from Landsat-8 Thermal Infrared Sensor Data: *Ieee Geoscience and Remote Sensing Letters, 11*, pp. 1840-1843.

Jin, M.J., Li, J.M., Wang, C.L., & Shang, R.L. (2015). A Practical Split-window Algorithm for Retrieving Land Surface Temperature from Landsat-8 Data and a Case Study of an Urban Area in China. *Remote Sensing, 7*, pp. 4371-4390.

Juliana, A.A., Lee, C. Catherine. M. (2016) .Quantifying Daytime and Night time urban heat island in Birmingham, UK. A comparism of Satellite Derived land surface temperature and High Resolution Air Temperature observation. *Remote sensing* .doi: 10.3390/rs8020153.

Julius, O.O., Oyewole, A. I. (2016). Analysis of Akure Urban Land Use Change Detection from Remote Imagery Perspective. *Urban studies Research* Available. at: *http*://dx.doi.org/10.1155/2016/4673019

Kalnay, E., Cai, M. (2003). Impact of Urbanization and Land Use Change on Climate: *Nature*, 423, 528-531.

Karl, T.R., Diaz, H.F., Kukla, G. (1988).Urbanization: Its Detection& Effect in the United States. *Climate Record. J. Clim*. 1, 1099-1123.

Kantzioura, A., Kosmopoulos, (2012). Urban surface temperature and micro climate measurements in Thessaloniki: *Energy and Buildings*, 44(0), 63-72. doi: 10.1016/j.enbuild.2011.10.019.

Keramitsoglou, I., Kiranoudis, C.T. et al. (2011). Identification & Analysis of urban surface temperature patterns in Greater Athens, Greece, using MODIS imagery: *Remote Sensing of Environment* 115(12): 3080-3090.

Kilibarda, M., Hengl, T., Heuvelink, G. B. M., Gräler, B., Pebesma, E., Perˇcec Tadiˊc, M., and Bajat, B. (2014). Spatio-temporal interpolation of daily temperatures for global land areas at 1 km resolution*: J. Geophys. Res.-Atmos.*, 119, 2294–2313, doi: 10.1002/2013JD020803
.

Klysik, k, K., & Fortuniak, K. (1999). Temporal and Spatial Characteristics of the Urban Heat of Lodz, Poland. *Atmospheric Environment*, 33, 38885-3895.

Lambin, E. F, (1997a). Modelling and Monitoring Land-Cover Change Processes in Tropical Regions. *Progress in Physical Geography*. 21, 375-393.

Lambin, E.F.,Turner, B. L., Geist, H. J., Agbola, S., Angelseri, T.,Brace, J. W., Coomes, O., Dirzo, R., Fischer, G., Folke, C., George, P. S. , Homewood, K., Imbernon, J., Leemans, R., Li, X., Moran, E. F., Mortimore, M., Ramakrislinan, P. S., Richards, J, F., Skanes, H., Steffen, W., Stone, G. D., Svedin, U., Veldkamp, T., Vogel, C. and Xu, J. (2001). The Causes of Landuse and Land-cover Change -Moving beyond the Myths Global Environmental Change. Human and Policy Dimensions. 11: 261-269.

Lambin, E. F., Geist, H. J., & Lepers, E. (2003). Dynamics of land-use and Land-cover change in tropical regions. *Annual Review of Environment and Resources* 28:205-241.

Landsat Project Science Office (2002) Landsat 7 science data user's hand book. Goddard Space Flight Center: US.

Lays S Usman. (2013). "The Dynamic of land Cover Change in Abuja City Federal Capital territory, Nigeria" *Confluence Journal of Environmental Studies* Vol.

Lee, H**.** (1993). An application of NOAA AVHRR thermal data to the study of urban heat islands. *Atmospheric Environment, 27B*, 1-13.

Lepers, E.,Lambin, E. F.,Janetos, A. C., DeFries, R., Achard, F., Ramankutty, N. and Scholes, R.J. (2005). A Synthesis of Information on Rapid Land-cover Change for the Period 1981-2000. Bioscience. 55: 115-124.

Li, J., Wang, X R.., Wang, X J., Ma, W., & Zhang, H. (2009). Remote sensing evaluation of urban heat island and its spatial pattern of the Shanghai metropolitan area, China. *Ecological Complexity*, 30, 1-8.

Lin, X., Pielke Sr., R. A., Mahmood, R., Fiebrich, C. A., and Aiken, R. (2016). Observational evidence of temperature trends at two levels in the surface layer: *Atmos. Chem. Phys*., 16, 827–841, doi: 10.5194/acp-16-827-2016, 2016.

Lin, S. P., Moore, N. J., Messina, J. P., DeVisser, M. H., and Wu, J. P. (2016). Evaluation of estimating daily maximum and minimum air temperature with MODIS data in east Africa, *Int. J. Appl. Earth Obs*., 18, 128–140, doi:10.1016/j.jag.2012.01.004.

Liu, L., Zhang, Y. (2011). Urban Heat Island Analysis Using the Landsat TM Data and ASTER Data. A Case Study in Hong Kong*, Remote Sens*.3, 1535-1552.

Liao, L., Zhang, L., and Bengtsson, L. (2005). Analyzing Dynamic Change of Vegetation Cover of Desert Oasis Based on Remote Sensing Data in Hexi Region. In: Guodong, C., Zhidong, L., and Bengtsson, L., eds., *Proceedings of the International Symposium on Sustainable Water Resources Management and Oasis-hydrosphere-desert Interaction in Arid Regions*. 279-295.

Lo, C.P., Quattrochi, D. A. (2003). Land Use and Land-Cover Change, UHI Phenomenon and Health Implications. A Remote Sensing Approach. Photogramm.Eng.*Remote Sens*.69, 1053-1063.

Lowry, W.P. (1977). Empirical Estimation of Urban Effects on Climate: A Problem Analysis.*J.Apple.Meteor*.16, 129-135.

Lutz, W., Sanderson, and Scherebor, S. (2001). The End of the World Population Growth. Nature .412:543-545.

Mallick, J., Rahman, A., & Singh, C.K., 2013. Modeling urban heat islands in heterogeneous land surface and its correlation with impervious surface area by using night-time ASTER satellite data in highly urbanizing city, Delhi-India. *Advances in Space Research, 52*, pp. 639-655.

Maingi, J.K., Marsh S.E. (2002). An Accuracy Assessment of 1992 Landsat-MSS Derived Land cover for the Upper San Pedro Watershed (U.S./Mexico); United States Environmental Protection Agency: Washington, DC, USA, 2002; 29p.

Mackenzie, J. (2009). Land-Use/Land Cover Transitions in Delaware, 2002–2007. PhD Thesis, College of Agriculture & Natural Resources. University of Delaware, Newark, DE, USA, p. 7.

MC CONNELL, V. & WALLS, M. (2005). The Value of Open Space: Evidence from Studies of Nonmarket Benefits, Washington, Resources for the Future

Memon, R. A., & Leung, D. Y. C. (2010). Impacts of environmental factors on urban heating. *Journal of Environmental Sciences, 22*(12), 1903-1909.

Memon, R. A., Leung, D. Y. C., & Liu, C. (2009). An investigation of urban heat island intensity (UHII) as an indicator of urban heating. *Atmospheric Research, 94*, 491-500.

National Population Commission, Federal Republic of Nigeria Official Ga zette 24: (96), Federal Government of Nigeria, (2007).

National Population Commission (2006). Nigeria's Population Census 2006.

Nasrallah, H. A., Brazel A J and Balling R. C. (1990). Analysis of the Ku wait City urban heat island. *Int. J Climatol.* 10, 401-405.

Nduka, I.C., Abdulhamed A.I. (2011). Classifying Urban Climate Field sites by "Thermal Climate Zones" the Case of Onitsha Metropolis. *Research Journal of Environmental and Earth Sciences* 3(2), pp. 75-80.

NASA LP DAAC, USGS EROS Center, Sioux Falls, SD, (2012). MODIS Land Products Quality Assurance Tutorial: Part-1 available at "http://earthobservatory.nasa.gov/GlobalMaps/view.php?d1

Neteler, M. (2010). Estimating Daily Land Surface Temperatures in Moun tainous Environments by Reconstructed MODIS LST Data. Remote Sensing Journal.

Newsom, 2006. USP 534, Data Analysis1, Post Hoc Tests. Available at: www.upa.pdx.edu/IOA/newsom/da1/ho_posthoc.doc.

Nigeria Climate Review Bulletin (2010).

NWS. Heat Wave (2009, November 29). A Major Summer Killer, Retrieved From http:www.Noaawater,gov/themes/heat.php

Ofomata, G.E. K. (1975). Soil Erosion. In: Nigeria in maps: Eastern States, Ofomata, G.E.K. (Ed). *Ethiopie Publishing House, Benin City, Nigeria*, pp. 41-42.

Oguntoyinbo, J.S. (1970). Reflection Coefficient of Natural vegetation, Crops and urban Surfaces in Nigeria: Quart. J. Royal Meteorological Society.

Oguntoyinbo, J.S.C. (1973) Aspects of Urban Micro-Climate: The Case Study of Ibadan: In Sada, P.O. and Oguntoyinbo, J.S., Eds., Urbanization Processes and Problems in Nigeria, University of Ibadan, Ibadan, 131-140.

Oguntoyinbo J.S. (1978) A Geography of Nigerian Development. Ibadan Heinemann.

Ojo, S.O. (1981). Land-use Energy Balance Relationships and the planning Implications in Metropolitan Lagos: Occasional Paper No. 1.Department of geography, University of Lagos, Nigeria.

Oke, T.R., Yap, D. and Maxwell, G.B. (1972). Comparison of urban/rural Cooling rates at night. *Proceedings Int. Symp. On Environment and Second Conf. on Biometeor. American Meteorological Society*, Boston, pp17-21.

Oke, T.R. (1975). The distinction between canopy & boundary-layer urban heat islands. *Atmosphere* 268-277.

Oke, T.R. (1982). The energetic basis of the urban heat island. *Quarterly Journal of Royal Meteorological Society, 108,* 1-24.

Oke, T.R. (1984). Towards a prescription for the greater use of climatic Principles in settlement planning. *Energy and Buildings* 7, 1-10.

Oke, T.R. (1987). Boundary Layer Climates. 2nd edition. Routledge.

Oke, T.R. (1988). Street design and urban canopy layer climate. *Energy & Buildings* 11, 103-113.

Oke, T.R. (2004). Initial guidance to obtain representative meteorological Observations at urban sites: Instrument and Observing Methods, Report No. 81. WMO/TD No. 1250.

Oke, T.R. (2006). Towards better scientific communication in urban climate *Theoretical and Applied Climatology* 84, 179-190.

Okude, A. S. (2006). *Landcover change along the Lagos coastal area.* Ph.D. Dissertation, Department of Geography, University of Ibadan, Nigeria, p. 93-95.

Opeyemi Z. (2014). Potential Application of Change in Urban Green Space as an Indicator of Urban Environmental Quality Change. *Universal Journal of Geoscience.* 2. 222-228. 10.13189/ujg.2014.020705.

Oyler, J. W., Dobrowski, S. Z., Holden, Z. A., and Running, S. W.(2016). Remotely Sensed Land Skin Temperature as a Spatial Predictor of Air Temperature across the Conterminous United States, J. *Appl. Meteorol. Clim.*, 55, 1441–1457, doi:10.1175/JAMC-D-15-0276.1,

Oyler, J. W., Ballantyne, A., Jencso, K., Sweet, M., and Running, S. (2015). Creating a topoclimatic daily air temperature dataset for the conterminous United States using homogenized station data and remotely sensed land skin temperature, Int. J. Climatol., 35,2258–2279 .

Omojola, A. (1997). Landuse and landcover inventory and change assessment in a semi-arid region in Nigeria using remote sensing and GIS Techniques. Ph.D. Thesis, University of Lagos, Nigeria, p. 113-115.

Omogbai, B.E. (1985). Aspects of urban Climate of Benin City. M.Sc. Thesis, University of Ibadan.

O'Neill, M. S., Zanobetti, A., & Schwartz, J. (2007). Disparities by race in heat-related mortality in four U.S. cities: The role of air conditioning prevalence. *Journal of Urban Health, 82*(2).

Opeyemi, A. and Zubair, W. (2011). potential Application of change in urban green space as an indicator of urban Environmental quality change: *Universal Journal of Geoscience 2(7)*:222-2282014.DOI: 10131891ujg.

Parmentier, B., McGill, B. J., Wilson, A. M., Regetz, J., Jetz, W., Guralnick, R., Tuanmu, M. N., and Schildhauer, M. (2015). Using multi-timescale methods and satellite-derived land surface temperature for

the interpolation of daily maximum air temperature in Oregon, *Int. J. Climatol*., 35, 3862–3878.

Papadakis J (1996). Climate of the world and their agricultural potentialities: Buenos Aires.pp.1-48.

Perini, K., & Magliocco, A. (2014). Effects of vegetation, urban density, building height, and atmospheric conditions on local temperatures and thermal comfort: *Urban Forestry & Urban Greening*, *13*(3), 495–506. "http://doi.org/10.1016/j.ufug.2014.03.003

Pijanowski, B.C., Brown, D.G., Manik, G., Shellito, B. (2002).Using Neural Nets and GIS to Forecast Land Use Changes: A Land Transformation Models. Comput. Environ. Urban Syst. 26,553-575.

Pitman A. J., Avila F. B., Abramowitz G., Wang Y. P., Phipps S. J., de Noblet- Ducoudre N. (2011). Importance of background climate in determining impact of land cover change on regional climate. *J. Geophys. Res.*

Pontius, R.G., Jr., Spencer, J. (2005).Uncertainty in Extrapolations of Predictive Land Change Models. Environ.Plan.B, 32,211-230.

Rafferty, J.P. (2011). Climate and climate change. Britannica Educational Publishing, New York, 345p.

Qin Z., Karnieli A., Berliner P. (2001). A mono-algorithm for retrieving land surface temperature from Landsat TM data and its application to the Israel-Egypt border region: *Int. J. Remote Sens*.18:583–594.

Qin Z., Li W., Zhang M., Karnieli A., Berliner P. (2003). Estimation of the essential atmospheric parameters of mono-window algorithm for land surface temperature retrieval from Landsat TM6: *Remote Sens. Land Res.2:37–43.*

Ramankutty, N., Heller, E., Rhemtulla, J. (2002b). Prevailing myths about agricultural abandonment and forest regrowth in the United States: Annals of the Association of American Geographers. 100: 502–512

Rinner, C., Hussain, M. (2011). Toronto's Urban Heat Island .Exploring the Relationship between Land Use and Surface Temperature: *Remote Sens, 3,* 1251-1265.

Rizwan, A. M., Dennis, Y. C., & Liu, C. (2008). A review of the generation, determination and mitigation of urban heat island. *Journal of Environmental Sciences, 20*, 120-128.

Rizwan, Ahmed Memon, Leung YC Dennis, and Chunho Liu. 2008b. "A review on the generation, determination and mitigation of Urban Heat Island." *Journal of Environmental Sciences* no. 20 (1):120-128

Rozenstein, O., Qin, Z.H., Derimian, Y., & Karnieli, A., 2014. Derivation of Land Surface Temperature for Landsat-8 TIRS Using a Split Window Algorithm. *Sensors, 14*, pp. 5768-5780.

Santamouris, M., Kapsis, O., Livada, I., Pavlou, C. & Assimakopoulos, M.N. (2007). On the Relation between the Energy and Social Characteristics of the Residential Sector: *Energy and Buildings*. 39, 893-905.

Santé, I., Garcia, A.M., Miranda, Crecents, R. (2010).Cellular Automata Models for the Simulation of Real –World Urban Processes: A Review and Analysis , Land Use urban Plan. 96,108-122.

Sekertekin, A., Kutoglu, S.H., & Kaya, S. (2016). Evaluation of spatiotemporal variability in Land Surface Temperature: A case study of Zonguldak, Turkey.:*Environmental monitoring and assessment, 188*, pp. 1-15.

SEOS, 2010. Remote Sensing and GIS in Agriculture. Available online at: http://www.seosproject.eu/modules/agriculture/agriculture-c01-s01.html (accessed 14 December 2016).

Snyder W.C., Wan Z., Zhang Y., Feng Y.Z. (1998).Classification-based emissivity for land surface temperature measurement from space. *Int. J. Remote Sens.* 1998; 19:2753–2774.

SPSS Inc. Released 2008. SPSS Statistics for Windows, Version 17.0. Chicago: SPSS Inc.

Steeneveld, G. J., Koopmans, S., et al. (2011). Quantifying urban heat island effects and human comfort for cities of variable size and urban morphology in the Netherlands. Journal of Geophysical Research-Atmospheres, 116. Doi: 10.1029/2011jd015988.

Stewart, I. D., Oke, T. R., & Krayenhoff, E. S. (2014). Evaluation of the "local climate zone" scheme using temperature observations and model simulations. *International Journal of Climatology*, *34*(4), doi.org/10.1002/joc.3746

Streutker, D.R. (2003). A remote Sensing Study of the Urban Heat Island of Houston, Texas: *Remote Sensing Environment*, 85,282-289.

Stone, B., Jr. (2012). The City and the Coming Climate: Climate in the Places we Live, New York, NY: *Cambridge University Press.*

Su, W., Gu, C., and Yang, G., (2010). Assessing the impact of land use/ land cover on urban heat island pattern in Nanjing city, China. Journal of Urban Planning and Development, 136, 365-372.

Suzana, A, Biswajeet, P., Usman, S. l., Saleb, A. (2016). Spatial assessment of land surface temperature and land use/land cover in Langkawi Island. Earth and environment sciences .dio: 10, 1088/1755-13711/012064.

Svensson, M. K. (2004). Sky view factor analysis – implications for urban air temperature differences. *Meteorological Applications, 11*, 201-211.

Taha, H. (1997).Urban Climate and Heat Islands: Albedo, Evaporation, and Anthropogenic Heat. Energy and Buildings .25, 99-103

Tam, K.C., Lim, H.S., MatJafri, M.Z., and Abdullah, K. (2010). Landsat data to evaluate urban expansion and determine land use/land cover change in Penang Island, Malaysia. *Environmental Earth Sciences*, 60, 1509-1521.

Thornthwaite, C.W. Mather, J.R (1955): Water balance publication in Climatology. Drexel Ins. of Tech., 8(1).

Udo, R. K (1970) Geographical Regions of Nigeria. Heinemann. *London and University of California Press,* 232 pages.

Udo, R. K (1990) Land Use Policy and Land Ownership in Nigeria. Ebie Akwa Ventures, Lagos, 167 pages.

Umah, M. U. & Satish, J.K. (2016). Spatial and Temporal Changes of Urban Heat Island in Kano Metropolis, Nigeria: *International journal of research in engineering science and technologies (IJRESTs)*, Vol.1 No 2.

United Nations (2012). Global Land-Use Analysis.

United Nations Department of Economic and Social Affairs. (2015). *World Urbanization Prospects: 2014 Revision*. New York. Retrieved from "http://esa.un.org/unpd/wup/FinalReport/WUP2014-   Report.pdf" http://esa.un.org/unpd/wup/FinalReport/WUP2014- Report.pdf.

Vancutsem, C., Ceccato, P., Dinku, T., and Connor, S. J. (2010). Evaluation of MODIS land surface temperature data to estimate air temperature in different ecosystems over *Africa, Remote Sens. Environ*., 114, 449–465, doi:10.1016/j.rse.2009.10.002

Van de Griend, A. A., Owe, M. (1993). On the relationship between thermal emissivity and the normalized different vegetation index for natural surfaces. *International Journal of Remote Sensing.* 14:1119–1131

Valor E., Caselles V. (1996). Mapping land surface emissivity from NDVI: Application to European, African, and South American reas. *Remote Sens.Environ.*57:167–184.

.

Verheye, H, W. (2004). Land Use, Land Cover and Soil Sciences. Encyclopedia of Life Support Systems (EOLSS).

Verburg, A.P.H., & Castelia, J.C. (2004). Landscape Level Analysis of the Spatial and Temporal Complexity of Land- Use Change, Ecosystems and Land Use Change Geophysical Monograph Series 153:217-230.

Vooght, J.A and Oke, T.R. (2003). Thermal Remote Sensing of Urban Areas. *Remote Sensing of Environmental 86*: 370-3884.

Voogt, J.A. (2004). Urban Heat Island: Hotter Cities. Action Bioscience, Northport.   Available   at http://www.actionbioscience.org/environment/voogt.htm

Wan, Z. (2014). New refinements and validation of the collection-6 MODIS land-surface temperature/emissivity product. *Remote Sens. Environ*.140: 36–45.

Wang, Y., Berardi, U., & Akbari, H. (2015). Comparing the effects of Urban Heat Island Mitigation.

Wang, F., Qin, Z.H., Song, C.Y., Tu, L.L., Karnieli, A., & Zhao, S.H., (2015). An Improved Mono-Window Algorithm for Land Surface Temperature Retrieval from Landsat 8 Thermal Infrared Sensor Data. *Remote Sensing, 7*, pp. 4268-4289.

Weirer, J. and Herring, D., 2010. Measuring Vegetation (NDVI & EVI). Observatory). Available http://earthobservatory.nasa.gov

Weng Q., Yang S. (2004). Managing the adverse thermal effects of urban development in a densely populated Chinese city. J. Environ. Manage.70:145–156

Weng, Q., H. Liu, and D. Lu. 2007. "Assessing the effects of land use and land cover patterns on thermal conditions using landscape metrics in city of Indianapolis, United States." *Urban Ecosystems* no. 10 (2):203-219.

Weng, Q. (2008) Thermal Infrared Remote Sensing for Urban Climate and Environmental Studies: Methods, applications, and trends. ISPRS J. Photogramm. Remote Sens. 2008, 64, 335–344.

Weng, Q. (2014). Modeling diurnal land temperature cycles over Los Angeles using downscaled GOES imagery. *ISPRS Journal of Photogrammetry and Remote Sensing*, 97, 78-88

Wilby, R. L. (2003). Past and projected trends in London's urban heat island: Weather, 58(7), 251-260.

Xu, Y., Knudby, A., & Ho, H.C. (2014). Estimating daily maximum air temperature from MODIS in British Columbia, Canada: *Int. J. Remote Sens.,* 35, 8108–8121, doi: 10.1080/01431161.
.
Zhou, W., G. Huang, and Cadenasso M.L. (2011). "Does spatial configuretion matter? Understanding the effects of land cover pattern on land surface temperature in urban landscapes." *Landscape and Urban Planning* no. 102 (1):54-63.

Xiao, H. and Weng, Q. (2007). The impact of land use and land cover Changes on and surface temperature in a karst area of *China. Journal of Environmental Management*, 85(1), 245-257, doi:10.1016/j.jenvman.2006.07.016.

Xiong, Y.; Huang, S.; Chen, F.; Ye, H.; Wang, C.; Zhu, C. (2012).The Impacts of rapid urbanization on the thermal environment: A remote sensing study of Guangzhou, South China. Remote Sens. 4, 2033–2056.

Yasuyo, M. Y., Shandas V, Ferwati S, Sailor D. (2016). Daytime Variation of Urban Heat Islands: The Case Study of Doha, Qatar. Climate. 4(2):32.

Yu, X.L., Guo, X.L., & Wu, Z.C. (2014). Land Surface Temperature Retrieval from Landsat 8 TIRS-Comparison between Radiative Transfers Equation-Based Method, Split Window Algorithm and Single Channel Method. *Remote Sensing, 6*, pp. 9829-9852.

Zha, Y., Gao, J., & Ni, S. (2003). Use of normalized difference built-up index in automatically mapping urban areas from TM imagery. *International Journal of Remote Sensing, 24*(3), 583-594.

Zhang, X.X.; Wu, P.F.; Chen, B. (2010). Relationship between vegetation Greenness and urban heat island effect in Beijing City of China: *Procedia Environ*. Sci. 2, 1438–1450.

Zhao, H. M., & Chen, X. L. (2005). Use of normalized difference bareness index in quickly mapping bare areas from TM/ETM*: Geoscience and Remote Sensing Symposium, 3*(25–29), 1666−1668.

APPENDIX 1

Kappa Coefficient of Agreement of the LULC image from 2002 to 2016

Error Matrix Analysis of 2002TRAINING (columns: truth) against 2002MINDST (rows: mapped)

	1	2	3	4	5	Total	ErrorC
1	98	3	0	0	0	**101**	**0.029703**
2	0	52	0	0	0	**52**	**0**
3	0	0	84	0	0	**84**	**0**
4	0	0	0	191	0	**191**	**0**
5	0	0	0	0	2204	**2204**	**0**
Total	98	55	84	191	2204	2632	
Error0	0	0.054545	0	0	0		**0.001140**

ErrorO = Errors of Omission (expressed as proportions)
ErrorC = Errors of Commission (expressed as proportions)

90% Confidence Interval = +/- 0.001082 (0.000058 - 0.002222)
95% Confidence Interval = +/- 0.001289 (0 - 0.002429)
99% Confidence Interval = +/- 0.001697 (0 - 0.002837)

KAPPA INDEX OF AGREEMENT (KIA)

Using 2002MINDST as the reference image

Category	KIA
1	0.969148
2	1.000000
3	1.000000
4	1.000000
5	1.000000

Category	KIA
1	1.000000
2	0.944355
3	1.000000
4	1.000000
5	1.000000

2002TRAINING

Overall Kappa = 0.996078

Kappa Coefficient of Agreement of the LULC image for 2006

Error Matrix Analysis of 2006TRAINING (columns: truth) against 2006MINDST (rows: mapped)

	1	2	3	4	5	Total	ErrorC
1	784	0	0	0	0	**784**	**0**
2	0	45	0	0	0	**45**	**0**
3	0	0	135	0	0	**135**	**0**
4	0	0	0	3381	0	**3381**	**0**
5	0	0	0	50	6787	**6837**	**0.007313**
Total	**784**	**45**	**135**	**3431**	**6787**	**11182**	
Error0	**0**	**0**	**0**	**0.014573**	**0**		**0.004471**

ErrorO = Errors of Omission (expressed as proportions)
ErrorC = Errors of Commission (expressed as proportions)

90% Confidence Interval = +/- 0.001038 (0.003434 - 0.005509)
95% Confidence Interval = +/- 0.001237 (0.003235 - 0.005708)
99% Confidence Interval = +/- 0.001628 (0.002844 - 0.006099)

KAPPA INDEX OF AGREEMENT (KIA)

Using 2006MINDST as the reference image

Category	KIA
1	1.000000
2	1.000000
3	1.000000
4	0.979111
5	1.000000

Category	KIA
1	1.000000
2	1.000000
3	1.000000
4	1.000000
5	0.981393

2006TRAINING

Overall Kappa = 0.991580

Error Matrix Analysis of 2008TRAINING (columns : truth) against 2008MAX (rows : mapped)

	1	2	3	4	5	Total	ErrorC
1	3946	0	0	0	0	**3946**	0
2	0	116	0	0	0	**116**	0
3	0	0	500	0	0	**500**	0
4	0	0	0	3186	0	**3186**	0
5	0	0	0	0	10843	**10843**	0
Total	**3946**	**116**	**500**	**3186**	**10843**	**18591**	
Error0	**0**	**0**	**0**	**0**	**0**		**0**

ErrorO = Errors of Omission (expressed as proportions)
ErrorC = Errors of Commission (expressed as proportions)

90% Confidence Interval = +/- 0 (0 - 0)
95% Confidence Interval = +/- 0 (0 - 0)
99% Confidence Interval = +/- 0 (0 - 0)

KAPPA INDEX OF AGREEMENT (KIA)

Using 2008MAX as the reference image

Category	KIA
1	1.000000
2	1.000000
3	1.000000
4	1.000000
5	1.000000

Category	KIA
1	1.000000
2	1.000000
3	1.000000
4	1.000000
5	1.000000

2008 TRAINING Overall Kappa = 1

Error Matrix Analysis of 2010TRAINING (columns: truth) against 2010MINDIST (rows: mapped)

	1	2	3	4	5	Total	ErrorC
1	98	10	0	0	0	108	0.092593
2	0	143	0	0	0	143	0
3	0	0	143	0	0	143	0
4	0	0	0	1591	197	1788	0.110179
5	0	0	0	0	62896	62896	0
Total	98	153	143	1591	63093	65078	
Error0	0	0.065359	0	0	0.003122		0.003181

ErrorO = Errors of Omission (expressed as proportions)
ErrorC = Errors of Commission (expressed as proportions)

90% Confidence Interval = +/- 0.000363 (0.002818 - 0.003544)
95% Confidence Interval = +/- 0.000433 (0.002748 - 0.003613)
99% Confidence Interval = +/- 0.000569 (0.002611 - 0.003750)

KAPPA INDEX OF AGREEMENT (KIA)

Using 2010MINDIST as the reference image

Category	KIA
1	1.000000
2	0.934497
3	1.000000
4	1.000000
5	0.906875

Category	KIA
1	0.907268
2	1.000000
3	1.000000
4	0.887060
5	1.000000

2010TRAINING

Overall Kappa = 0.948963

Error Matrix Analysis of 2012TRAINING (columns: truth) against 2012MINDST2 (rows: mapped)

	1	**2**	**3**	**4**	**5**	**Total**	**ErrorC**
1	251	18	0	0	12	**281**	**0.106762**
2	0	76	0	0	12	**88**	**0.136364**
3	0	0	116	0	0	**116**	**0**
4	0	0	0	30808	2	**30810**	**0.000065**
5	0	0	0	0	514486	**514486**	**0**
Total	251	94	116	30808	514512	**545781**	
Error0	**0**	**0.191489**	**0**	**0**	**0.000051**		**0.000081**

ErrorO = Errors of Omission (expressed as proportions)
ErrorC = Errors of Commission (expressed as proportions)

90% Confidence Interval = +/- 0.000020 (0.000061 - 0.000101)
95% Confidence Interval = +/- 0.000024 (0.000057 - 0.000104)
99% Confidence Interval = +/- 0.000031 (0.000049 - 0.000112)

KAPPA INDEX OF AGREEMENT (KIA)

Using 2012MINDST2 as the reference image

Category	KIA
1	0.893189
2	0.863613
3	1.000000
4	0.999931
5	1.000000

2012TRAINING

Category	KIA
1	1.000000
2	0.808480
3	1.000000
4	1.000000
5	0.999119

Overall Kappa = 0.999255

Error Matrix Analysis of 2014TRAINING (columns: truth) against 2014MINDST (rows: mapped)

	1	2	3	4	5	Total	ErrorC
1	2083	0	0	0	5	**2088**	**0.002395**
2	0	89	0	0	2	**91**	**0.021978**
3	0	0	308	0	0	**308**	**0**
4	0	0	0	20065	0	**20065**	**0**
5	0	0	0	0	75727	**75727**	**0**
Total	**2083**	**89**	**308**	**20065**	**75734**	**98279**	
Error0	**0**	**0**	**0**	**0**	**0.000092**		**0.000071**

ErrorO = Errors of Omission (expressed as proportions)
ErrorC = Errors of Commission (expressed as proportions)

90% Confidence Interval = +/- 0.000044 (0.000027 - 0.000116)
95% Confidence Interval = +/- 0.000053 (0.000018 - 0.000124)
99% Confidence Interval = +/- 0.000069 (0.000002 - 0.000141)

KAPPA INDEX OF AGREEMENT (KIA)

Using 2014MINDST as the reference image ...

2014TRAINING

Category	KIA
1	1.000000
2	1.000000
3	1.000000
4	1.000000
5	0.999597

Overall Kappa = 0.999804

Error Matrix Analysis of 2016TRAINING (columns: truth) against 2016MINDIST (rows: mapped)

	1	2	3	4	5	Total	ErrorC
1	514	0	0	0	0	**514**	**0**
2	1	104	0	0	0	**105**	**0.009524**
3	0	0	127	0	0	**127**	**0**
4	0	0	0	17603	111	**17714**	**0.006266**
5	0	0	0	0	62782	**62782**	**0**
Total	**515**	**104**	**127**	**17603**	**62893**	**81242**	
Error0	**0.001942**	**0**	**0**	**0**	**0.001765**		**0.001379**

ErrorO = Errors of Omission (expressed as proportions)
ErrorC = Errors of Commission (expressed as proportions)

90% Confidence Interval = +/- 0.000214 (0.001164 - 0.001593)
95% Confidence Interval = +/- 0.000255 (0.001123 - 0.001634)
99% Confidence Interval = +/- 0.000336 (0.001043 - 0.001714)

KAPPA INDEX OF AGREEMENT (KIA)

Using 2016MINDIST as the reference image...

Category	KIA
1	0.998046
2	1.000000
3	1.000000
4	1.000000
5	0.992233

2016TRAINING

Category	KIA
1	1.000000
2	0.990464
3	1.000000
4	0.992000
5	1.000000

Overall Kappa = 0.996111

APPENDIX 2

Multiple Linear Regression Results

Model Summary

Model	R	R Square	Adjusted R Square	Std. Error of the Estimate	Change Statistics				
					R Square Change	F Change	df1	df2	Sig. F Change
1	.749[a]	.561	-1.636	3.8488	.561	.255	5	1	.895

a. Predictors: (Constant), Barelands, Built-Up, Water body, Sparse Vegetation, Dense Vegetation

ANOVA[a]

Model		Sum of Squares	Df	Mean Square	F	Sig.
1	Regression	18.906	5	3.781	.255	.895[b]
	Residual	14.814	1	14.814		
	Total	33.720	6			

a. Dependent Variable: LST

b. Predictors: (Constant), Barelands, Built-Up, Waterbody, Sparse Vegetation, Dense Vegetation

163

Coefficients[a]

Model		Unstandardized Coefficients		Standardized Coefficients	t	Sig.	95.0% Confidence Interval for B	
		B	Std. Error	Beta			Lower Bound	Upper Bound
1	(Constant)	249.254	426.047		.585	.663	-5164.186	5662.694
	Waterbody	-2.759	8.757	-.622	-.315	.806	-114.030	108.512
	Sparse Vegetation	-2.514	3.949	-4.034	-.637	.639	-52.686	47.658
	Dense Vegetation	-2.131	3.721	-6.324	-.573	.669	-49.415	45.152
	Built-Up	-2.100	3.838	-2.699	-.547	.681	-50.863	46.663
	Barelands	-1.815	3.467	-2.333	-.524	.693	-45.862	42.232

a. Dependent Variable: LST

Correlations

		Water-body	Sparse Vegetation	Dense Vegetation	Built-Up	Barelands	LST
Waterbody	Pearson Correlation	1	-.620	.507	-.278	-.482	.552
	Sig. (2-tailed)		.137	.246	.546	.273	.198
	N	7	7	7	7	7	7
Sparse Vegetation	Pearson Correlation	-.620	1	-.829*	.382	.483	-.562
	Sig. (2-tailed)	.137		.021	.398	.273	.189
	N	7	7	7	7	7	7
Dense Vegetation	Pearson Correlation	.507	-.829*	1	-.726	-.719	.344
	Sig. (2-tailed)	.246	.021		.064	.069	.450
	N	7	7	7	7	7	7
Built-Up	Pearson Correlation	-.278	.382	-.726	1	.282	-.132
	Sig. (2-tailed)	.546	.398	.064		.540	.779
	N	7	7	7	7	7	7
Barelands	Pearson Correlation	-.482	.483	-.719	.282	1	-.196
	Sig. (2-tailed)	.273	.273	.069	.540		.673
	N	7	7	7	7	7	7
LST	Pearson Correlation	.552	-.562	.344	-.132	-.196	1
	Sig. (2-tailed)	.198	.189	.450	.779	.673	
	N	7	7	7	7	7	7

*. Correlation is significant at the 0.05 level (2-tailed).

Y = 24.712315 - 0.392915 X   r = -0.047458

Regression Parameters:

X axis: 2016lulc
Y axis: 2016lst

Coeff. of Det.	=	0.23 %
Std. Dev. of X	=	1.012190
Std. Dev. of Y	=	8.380192
S.E. of Estimate	=	8.370750
Std. Error of Beta	=	0.007644
t Stat for r or Beta	=	-51.402216
t Stat for Beta <> 1	=	-182.224838
Sample Size (n)	=	1170498
Apparent df	=	1170496

low frequency   high frequency